A Progress Report

on

A Comprehensive Kinetic Model of Ethylene and Acetylene Oxidation at High Temperatures

for

Work carried out under a contract from the trustees of Princeton University

as a part of a research program on

Optimization of a Comprehensive Detailed Chemical Kinetic Model for Simulating High-Speed Propulsion

An AFOSR New World Vista Program

Submitted to

Department of Mechanical and Aerospace Engineering
Princeton University
(Professor C. K. Law)

Prepared by

Hai Wang, Assistant Professor

and

Alexander Laskin, Postdoctoral Research Associate

Department of Mechanical Engineering
University of Delaware
Newark, DE 19716

Table of Contents

List of Tables

List of Figures

1. Introduction

The objective of the present study is to develop a comprehensive kinetic model for the combustion of a wide variety of practical fuels. The starting point of such a model is naturally the combustion mechanism of the major intermediates of all hydrocarbon combustion, namely ethylene and acetylene. This is because the initial reaction during the combustion of higher-alkane and alkene compounds are dominated by the β-scission process, which leads to the production of ethylene. While a substantial amount of ethylene is oxidized to C_1 species and formaldehyde, acetylene may form as a result of pyrolytic reactions of ethylene. For stoichiometric to fuel rich flames, acetylene is the dominate intermediate.

A reliable fundamental model should not only be self-consistent and physically justifiable, it should also be predictive for a variety of combustion problems, ranging from ignition, laminar flame propagation, to major and minor species concentrations in flames. There have been several comprehensive kinetic models reported in the literature for the combustion of acetylene and/or ethylene (e.g., Warnatz 1981; Miller *et al.*, 1982; Westbrook and Dryer, 1984; Dagaut *et al.*, 1990). A variety of combustion properties have been successfully predicted by these models. However, recent progresses in the fundamental reaction kinetics and noticeably in the reaction kinetics of the vinyl radical have brought with significant changes to the kinetic rates and pathways during the oxidation of acetylene and ethylene. In addition to the kinetics of the vinyl radical, comprehensive reviews of the kinetic data relevant to acetylene and ethylene combustion are also available and continuously being updated (e.g., Tsang and Hampson, 1986; Baulch *et al.*, 1992, 1994; Frenklach *et al.*, 1995). These factors, along with the critical importance of the acetylene and ethylene chemistry in high-hydrocarbon combustion, warrant a re-examination of the kinetic mechanisms of acetylene and ethylene combustion.

In the present study, we (a) undertook a critical review of the fundamental data of ethylene and acetylene combustion, (b) compiled a detailed kinetic model through a critical review of

relevant kinetic data and through quantum mechanical/RRKM calculations, and (c) performed extensive verification tests of the model against the compiled combustion data. Here, we shall report the results obtained from this phase of study.

2. Critical Survey of Literature Combustion Data

The main purposes of the literature survey are (a) to examine the consistency of the literature data and (b) to compile reliable data for model verification. Review of literature data has been carried out for the shock tube ignition and the detailed structures for burner-stabilized premixed flames of ethylene and acetylene. In the following, we shall present the results of literature survey and data comparison.

2.1. Shock-Tube Ignition

Experimental data for ethylene ignition in shock tubes are limited to the studies by Homer and Kistiakowsky (1967), Baker and Skinner (1972), and Jachimowski (1977). The experimental conditions and methods employed in these studies are summarized in Table 1. These experiments are designated as shock mixtures 1-14.

Data comparison is complicated by the differences in the ignition detection method and definition, and the type of shock waves employed in these studies, as indicated in Table 1. A summary of the data is shown in Figure 1, where the ignition delay times are plotted in the form of $\tau(\mu s) / \left\{[C_2H_4]_\circ^\alpha [O_2]_\circ^\beta [Ar]_\circ^\gamma\right\}$, where $[]_o$ denotes the initial reactant concentration (mol/cm^3), and α, β, and γ empirical parameters to be discussed later. Baker and Skinner (1972) reported only τ-versus-T_5 correlations for individual mixtures. The data shown in Figure 1 were generated from their correlations at an approximate temperature interval of 50 K. The experiments of Jachimowski were conducted in incident shock waves. The time elapse between the passage of the shock and the instant of maximum IR emission was scaled from the laboratory times to gas times (Gardiner *et al.*, 1981), and the resulting gas times are plotted in the figure.

Baker and Skinner (1972) presented the correlation equation,

$$\tau(\mu s) = 10^{-5.9} e^{17200/T} [C_2H_4]_\circ^{0.3} [O_2]_\circ^{-1.1} [Ar]_\circ^{0.4} \quad ,$$

on the basis of a least-square fit of their own data. We have derived a more comprehensive correlation equation

$$\tau(\mu s) = 10^{-57.97} T^{14.854} e^{35900/T} [C_2H_4]_\circ^{0.230} [O_2]_\circ^{-0.839} [Ar]_\circ^{0.247}$$

which combines the data of Baker and Skinner (1972) and those of the two other studies. A comparison of the data and the correlation equation is presented in Figure 1. The uncertainty factor of the experimental data shown in Figure 1 is estimated to be 2, as judged by the scatter around the line given by the correlation equation.

The level-off of the correlation-equation curve at temperatures higher than 2000 K may be artificial because it is strongly influenced by the data of Jachimowski (1977), who determined the ignition delay as the time elapse between the shock passage and the post-ignition instant of maximum IR emission.

Our correlation equation is qualitatively the same as that of Baker and Skinner (1972). Specifically, an increase in the initial fuel concentration retards ignition, while a similar increase in oxygen concentration strongly promotes ignition. An increase in pressure tends to slow down the ignition process, as indicated by the positive exponent of the diluent argon concentration.

A similar data analysis was carried out for acetylene ignition in shock tubes. The experimental data are summarized in Table 2. These experiments are designated as shock mixtures 15-33. The data can be plotted in a fashion similar to the ethylene plot, as shown in Figure 2. A correlation equation was obtained as

$$\tau(\mu s) = 10^{-7.035} e^{9770/T} [C_2H_2]_\circ^{-0.236} [O_2]_\circ^{-0.701} [Ar]_\circ^{0.015} \quad ,$$

by fitting the data of shock mixtures 16 through 33, but excluding mixtures 17, 22, 23, and 24. It is seen that most of the data fall within a factor of 2 from the fitted line, with the exception of mixture 17 (Bradley and Kistiakowsky, 1961) and mixture 23 (Jachimowski, 1977). In particular, the data of mixture 17 lie significantly lower than the fit, suggesting that

impurity may be responsible for the small ignition delay times observed in the experiments. The data of mixture 23 lie above the fit, which can be well explained by the fact that the induction times were determined as the post-ignition instant of maximum IR emission. The uncertainty factor in the data is estimated to be 2, as judged by the scatter around the fit.

Unlike the ignition of ethylene, increases in the concentrations of acetylene and oxygen generally facilitate the ignition of the mixture. On the other hand, an increase in the total pressure has a very small effect on the ignition delay times.

2.2. Laminar Burning Velocity

There have been several experimental studies reported for the measurement of the laminar burning velocity of ethylene and acetylene in air at the atmospheric pressure. A review of the literature data is given by Egolfopoulos *et al.* (1990a). In the present study, we adopted the burning velocity data collected in the Princeton counterflow flames (Egolfopoulos *et al.*, 1990b). These data were obtained with a linear extrapolation technique (Wu and Law, 1984), and were re-analyzed using a nonlinear extrapolation technique (Tien and Matalon, 1991) in the work of Sun *et al.* (1997). Both linearly and nonlinearly extrapolated data will be used for comparison with model calculations.

There are only limit amount of burning velocity data of ethylene and acetylene at variable pressures. Egolfopoulos *et al.* (1990) reported the burning velocity data of ethylene in nitrogen diluted air (18% O_2/82% N_2) as a function of the equivalence ratio and at the pressures of 0.5, 1, and 2 atm. In addition, the burning velocities were also determined for a stoichiometric mixture at the additional pressures of 0.25 and 3 atm. Similar data were reported for acetylene burning in a nitrogen diluted air (13%O_2/87%N_2) at the pressures of 0.5 and 1 atm with varying equivalence ratios, along with a single point measurement for a stoichiometric mixture at 0.25 atm. These pressure-dependence data have also been included for the purpose of model verification.

2.3. Burner-Stabilized Flames

The major and minor species profiles determined in burner-stabilized premixed flames offer the possibility of model verification on a level more detailed than that based on the global combustion behavior. However, the species profiles are often collected with the intrusive molecular beam mass spectrometric technique, and are expected to be less certain than the burning velocity and ignition delay. Nonetheless, we have included four burner-stabilized flames for the purpose of model verification. The conditions of these flames are summarized in Table 3. For each fuel, we tested our model against the flame structures for a fuel-lean mixture and a fuel rich mixture. There are additional reliable data on sooting acetylene and ethylene flames. Because the current model includes only species with size up to C_4H_4, these data are not included in the model verification in the current phase of study.

3. Quantum Mechanical and RRKM calculations

3.1. Computational Methodologies

Quantum mechanical calculations were performed with the Gaussian94 program (Frisch *et al*. 1995). Two different methods were employed in the calculation. In the first method, geometries were optimized with the Density Functional Theory (Hohenberg and Kohn, 1964; Kohn and Sham, 1965) with the B3LYP functional (Becke, 1993; Lee *et al.*, 1988) and the 6-31G(d) basis set. For energy calculations, we employed the G2 procedure (Curtiss *et al.*, 1991) at the B3LYP/6-31G(d) geometry. This computational procedure is referred to as the G2(B3LYP) method. In the second method, geometry optimization was carried out using the Complete Active Space Multireference Configuration Interaction (CASSCF) method (Eade and Robb, 1981) with the same basis set. The CASSCF energy was corrected by an MP2-level electron correlation.

Thermal rate coefficients were calculated from the microcanonical rate constants obtained from the RRKM theory (Holbrook *et al.*, 1996; Gilbert and Smith, 1990)

$$k(E) = l_a \frac{Q_r^{\ddagger} W(E^{\ddagger})}{Q_r h \rho(E)} \ ,$$

where l_a is the reaction path degeneracy; $Q_r^{\ddagger}$ and Q_r are respectively the partition functions for inactive rotational degrees of freedom of the transition state and the reactant molecule; $W(E^{\ddagger})$ is the sum of rovibrational energy states of the transition state at energy level $E^{\ddagger}$, $\rho(E)$ is the density of states of the stable species at energy level $E = E^{\ddagger} + E_o$; E_o is the energy barrier; and h is the Planck constant. The direct-count algorithm of Beyer and Swinehart (1973) was used to calculate the sums of energy states, while the densities of states were calculated using the Whitten–Rabinovitch approximation (Whitten and Rabinovitch, 1963; 1964). Active rotations were accommodated using the method of Astholz *et al.* (1979). The thermal rate coefficients were obtained by assuming a steady state for each of the energized species and by implementing weak collision stabilization.

3.2. C_2H_2 + O_2 Reactions

For acetylene oxidation behind shock waves, the radical-chain process was originally thought to be initiated via two possible steps: (a) the C-H bond fission in acetylene and/or (b) the molecular reaction of acetylene with O_2, with the following reaction pathways being previously considered (Gardiner and Walker, 1968; Jachimowski, 1977; Miller et al, 1982),

$$C_2H_2 + O_2 \rightarrow 2CO + 2H \qquad \Delta H = -3.1 \text{ kcal/mol} \qquad (176a)$$

$$C_2H_2 + O_2 \rightarrow CHO + CHO \qquad \Delta H = -34.5 \text{ kcal/mol} \qquad (176b)$$

$$C_2H_2 + O_2 \rightarrow CHCO + OH \qquad \Delta H = -2.7 \text{ kcal/mol} \qquad (176c)$$

$$C_2H_2 + O_2 \rightarrow CH_2CO + O \qquad \Delta H = -6.3 \text{ kcal/mol} \qquad (176d)$$

Recent theoretical (Bauschlicher and Langhoff, 1991) and experimental (Ervin *et al.*, 1990) results placed the C-H bond energy (BDE) of acetylene in the 133 - 134 kcal/mol range. Such a BDE value essentially rules out the C-H bond fission as the most efficient initiation step. Hidaka *et al.* (1996) recently showed in their shock tube study at temperatures between 1050 and 1600 K that acetylene ignition cannot be adequately predicted without the molecular

reaction 176. Such a conclusion was also reached in an early work of Miller *et al.* (1982) It was shown that the ignition delay times can be predicted if channel 176a was included in the kinetic scheme with a rate expression of $k_{176a} = 1\times10^{12}$ exp[–28(kcal/mol)/RT] ($cm^3mol^{-1}s^{-1}$) (Hidaka *et al.*, 1996). We note that this rate expression remains to be a fit to the experimental data. The small activation energy associated with such a molecular reaction is yet to be understood from fundamental consideration of potential energy surfaces. In addition, it was concluded from previous studies (Miller *et al.*, 1982; Hidaka *et al.* 1996) that specific reaction channel(s) for the molecular reaction cannot be distinguished by kinetic modeling, in that any channel (176a-d) with an appropriately chosen rate coefficient can reproduce the experimental ignition delay data. This situation further demonstrates the need to examine the relevant reaction pathway on the basis of fundamental consideration of reaction energetics.

We considered two possible pathways for the reaction of acetylene with molecular oxygen. The first pathway is the direct attack of O_2 on the triple C≡C bond, forming a hot adduct, which may isomerize to a number of isomers, as depicted in Figure 3. The dissociation of the hot isomers leads to the products consistent with reactions 176b-c. The energy barrier of O_2 attachment to the π bond in acetylene, leading to the $H\dot{C}=CH–O–\dot{O}$ biradical, was examined at the G2(B3LYP) and CASSCF levels of theory. Both methods yielded 55 kcal/mol for the energy barrier. We note that Sheng and Bozzelli (1998) reported the results of *ab initio* calculations for the same reaction. At the B3LYP/6-31G(d) and BHANDH/6-31G(d) levels of theory without considering the configuration interaction and basis set extension for energy calculations, the C_2H_2-to-O_2 addition energy barrier was found to be 30-35 kcal/mol. Despite of the lower energy barrier for the entrance channel reported by Sheng and Bozzelli (1998), the maximal energy barriers along their proposed pathways, leading to the final dissociated products, were still between 51 and 66 kcal/mol. Thus, it is reasonable to conclude on the basis of the two studies that the energy barrier along the first pathway is close to or greater than 55 kcal/mol.

Recognizing that the energy barrier reported in the literature (Kiefer and Von Drasek, 1990; Smith *et al.* 1992) for the isomerization of acetylene to vinylidene is 41-45 kcal/mol, and the resulting singlet vinylidene could react with O_2 without an appreciable energy barrier, we examine this second possibility. Figure 4 presents the energy diagram, computed at the G2(B3LYP) level of theory. It is seen that the mechanism depicted in the figure can be viewed as an analog of acetylene dimerization via vinylidene formation and its further reaction but the overall reaction of C_2H_2 with O_2 leading to dissociated products is significantly more exothermic. The addition of H_2CC to O_2 leads to the formation of the biradical adduct with an exothermicity of 63 kcal/mol. The biradical may isomerize to a number of isomers or it may dissociate to $CH_2 + CO_2$ and $CH_2CO + O$. The isomers may also dissociate to HCO + HCO, $CH_2O + CO$, HCO + H + CO. All of the dissociative reactions are chemically activated and highly exothermic, as such the reaction of acetylene and molecule oxygen should lead to

$$\begin{aligned} C_2H_2+O_2 \rightarrow \quad H_2CC + O_2 &\rightarrow CH_2O + CO \\ &\rightarrow HCO + H + CO \\ &\rightarrow HCO + HCO \\ &\rightarrow CH_2 + CO_2 \\ &\rightarrow CH_2CO + O \end{aligned}$$

The first four product channels can be inferred (Baulch *et al.* 1992) from the experimental measurements for the reaction

$$CH_2CO + O \rightarrow \text{products}$$

where CH_2O, CO, CO_2, OH, and H were measured as the products. Based on the analysis described above, the vinylidene pathway should have an overall energy barrier equal to that of the C_2H_2-to-H_2CC**:** isomerization, which is considerably lower than that of the oxygen attachment to acetylene previously discussed. It follows that the preferred initiation reactions in acetylene oxidation is

$$C_2H_2 + M \rightarrow H_2CC + M \qquad (175)$$

$$H_2CC + O_2 \rightarrow \text{products} \qquad (176e)$$

Because reaction 175 is always in close equilibrium, an overall rate coefficient can be written as

$$C_2H_2 + O_2 \rightarrow \text{products} \qquad (176)$$

with its rate coefficient given by

$$k = K_{175} \times k_{176e} = 4.6\times10^{15}T^{-0.54} \exp[-45\ (\text{kcal/mol})/RT]\ \ \text{cm}^3\text{mol}^{-1}\text{s}^{-1}$$

where K_{175} is the equilibrium constant of reaction 175, and $k_{176e} = 1\times10^{13}$ $\text{cm}^3\text{mol}^{-1}\text{s}^{-1,}$ based on the analogous reaction of singlet methylene with molecular oxygen. The branching ratio to various products cannot be accurately determined from the present study, but this is not critical for the problem of acetylene ignition because any radical produced from reaction 176 (with the exception of CH2O + CO) will quickly induce the growth of a radical pool by their subsequent chain-branching reactions. In this present study, we used the $CH_2 + CO_2$ channel as the product channel.

3.3. CH_3CO System

The reactions considered involves the bimolecular combination and the chemically activated reactions of $CH_2CO + H$ and $CH_3 + CO$, i.e.,

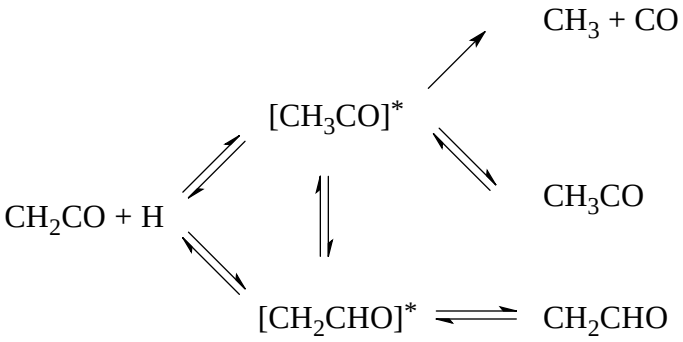

The vinoxy (CH_2CHO) radical is one of the major intermediate during ethylene and acetylene oxidation. Specifically, vinoxy is produced from the reaction between vinyl (C_2H_3) and molecular oxygen,

$$C_2H_3 + O_2 \rightarrow CH_2CHO + H\ , \qquad (192)$$

and decomposes quickly to $CH_3 + CO$ and $CH_2CO + H$,

$$CH_2CHO\ (+M) \rightarrow CH_3 + CO\ (+M) \qquad (201)$$

$$CH_2CHO\ (+M) \rightarrow CH_2CO + H\ (+M)\ . \qquad (-178)$$

Because the second decomposition reaction releases the H atom, which is much more reactive than the CH_3 radical, the branching radio may influence the prediction of the global and detailed combustion characteristics for ethylene and acetylene combustion. There have not been any experimental measurements for this branching ratio, other than some evidence that the first reaction is significantly faster than the second. Tsang (1986) evaluated the rate coefficients of CH_3 + CO recombination, but two new measurements (Baldwin *et al.*, 1987; Bencsura *et al.*, 1992) have emerged since then. The European kinetic data compilation (Baulch *et al.*, 1994) did include the two new studies in their kinetic data evaluation, but the recommendation for the limiting-pressure rate coefficients and the fall-off broadening factor are valid only up to 500 K. In the present study, we extrapolated the low temperature data to high temperatures with RRKM calculations.

Figure 5 presents the potential energy diagram of the reaction. The initial energies are computed at the G2(B3LYP) level of theory. The values are shown in the parentheses in Figure 5. The computed energies were then compared to the enthalpies of formation found in the compilation of Burcat (1996). Minor corrections were made to the stable geometries. The transition-state energies were also slightly adjusted to fit the RRKM rate coefficients to the experimental data. Using the RRKM parameters shown in Table 4 and the potential energies shown in Figure 5, we computed the second-order rate coefficient of CH_3 + CO combination, and compare the theoretical results with selected experimental data of Bencsura *et al.* (1992) and Baldwin *et al.* (1987), as shown in Figure 6. A $\langle \Delta E \rangle_{down}$ value of 260 cm^{-1} was used for helium to fit the data of Bencsura *et al.* (1992), and the data of Baldwin *et al.* (1987) were fitted with $\langle \Delta E \rangle_{down}$ = 100 cm^{-1} for argon. The pressure dependent rate coefficients were fitted in Troe's formula (Gilbert *et al.* 1982) and shown in Appendix A.

The rate coefficient was also computed for the chemically activated reaction

$$CH_2CO + H \rightarrow CH_3 + CO\ . \qquad (180)$$

Comparison with the experimental data is shown in Figure 7. RRKM calculations reveal that the pressure has little influence on the rate coefficient of this reaction. Unlike the recommendation of Baulch *et al.* (1992), which is based on an extrapolation of the low-temperature data, out RRKM results show a significant upward curvature on an Arrhenius plot at high temperatures, and support the high-temperature data of Frank *et al.* (1986). The RRKM results can be represented by a modified Arrhenius equation as

$$k = 1.5\times10^{9}\ T^{1.43}\ \exp(-1350/T)\ \mathrm{cm^3mol^{-1}s^{-1}}$$ over range 200 - 2500 K

3.4. C_3H_4 and C_3H_5 Systems

The reactions of propyne and allene mutual isomerization and of propyne + H, allene + H, and $CH_3 + C_2H_2$ were studied with quantum mechanical and RRKM calculations. The quantum mechanical calculations were performed at the G2(B3LYP) level of theory. The results have been reported in a journal article (Davis *et al.* 1999), which is attached as Appendix B.

4. Detailed Kinetic Model

The detailed kinetic model compiled in the present study consists of 52 species and 367 elementary reactions. This model was compiled for ethylene and acetylene combustion and is based on a series of works reported in the past (Sun *et al.* 1996, Wang *et al.*, 1996, Davis *et al.* 1998b, Wang and Frenklach, 1997). The small-species chemistry is largely based on the GRI-Mech (Frenklach *et al.* 1995). Whenever possible, we used Troe's fall-off formalism (Gilbert *et al.*, 1983) to describe the pressure dependence of the rate coefficients for unimolecular dissociation and bimolecular combination reactions. The kinetic model retains a reasonable number of C_3 and C_4 species to ensure proper simulation under the fuel-rich conditions and to make it possible for expansion of the kinetic model to include large hydrocarbon chemistry.

4.1. H_2/O_2 Chemistry

The H/O chemistry was taken from the GRIMech (Frenklach *et al.* 1995), with the exception of the reactions

$$HO_2 + H \rightarrow OH + OH$$

$$HO_2 + H \rightarrow H_2 + O_2 ,$$

whose rate coefficients were taken from the recent work of Mueller *et al.* (1998).

4.2. C_1 Chemistry

The C_1 chemistry is largely based on the GRIMech. The reaction of triplet methylene with molecular oxygen was found to exert a large influence on the ignition characteristics of acetylene. Two product channels were considered, including

$$CH_2 + O_2 \rightarrow HCO + OH \quad (55)$$

$$CH_2 + O_2 \rightarrow CO_2 + H + H \quad (56)$$

We adopted the total rate coefficient from the GRIMech compilation (Frenklach *et al.* 1995), and assigned the branching ratio $k_{55}/(k_{55}+k_{56}) = 0.8$, based on the CO-to-$CO_2$ ratio detected in the work of Bley *et al.* (1992) and Dombrowsky and Wagner (1992).

The bimolecular combination and chemically activated reactions of CH_3 and HCO were included in the kinetic model, with their rate coefficients derived from an RRKM analysis. These reactions are

$$CH_3 + HCO\ (+M) \rightarrow CH_3CHO\ (+M) \quad (99)$$

$$CH_3CO + H\ (+M) \rightarrow CH_3CHO\ (+M) \quad (211)$$

$$CH_2CHO + H\ (+M) \rightarrow CH_3CHO\ (+M) \quad (202)$$

$$CH_3CO + H \rightarrow CH_3 + HCO \quad (212)$$

$$CH_2CHO + H \rightarrow CH_3 + HCO \quad (204)$$

$$CH_2CHO + H \rightarrow CH_3CO + H \quad (203)$$

The motivation for this RRKM analysis is again the need to consider the destruction reactions of vinoxy (CH_2CHO), a product of vinyl oxidation by molecular oxygen.

4.3. C_2 Chemistry

Among reactions pertinent to ethylene and acetylene oxidation, the sum of the rate coefficients of the reaction

$$C_2H_2 + O \rightarrow HCCO + H \quad (155)$$

$$C_2H_2 + O \rightarrow CH_2 + CO \quad (156)$$

was taken from the GRIMech compilation, but the branching ratio was assigned to be $k_{155}/(k_{155}+k_{156}) = 0.8$, based on the work of Michael and Wagner (1990). The reaction of vinyl + O was split into two channels,

$$C_2H_3 + O \rightarrow CH_2CO + H \quad (188)$$

$$C_2H_3 + O \rightarrow CH_3 + CO\ , \quad (189)$$

based on Donaldson *et al.* (1995). The total rate coefficient of 9.6×10^{13} $cm^3mol^{-1}s^{-1}$ was adopted from the compilation of Tsang and Hampson (1996).

The reaction between vinyl and molecular oxygen influences very significantly the combustion characteristics of ethylene. Slagle *et al.* (1984) determined the mechanism of the reaction to be

$$C_2H_3 + O_2 \rightarrow HCO + CH_2O\ . \quad (193)$$

at 298 and 600 K. Westmoreland (1996) and Bozzelli and Dear (1993) employed the QRRK technique to calculated the branching ratios of the reaction and reported that vinoxy + H may be a significant product channel. Since these two studies, a new mechanism has been proposed by Carpenter (1993, 1995). This mechanism involves the cyclization of the $C_2H_3O_2$ adduct radical to a three-member-ring dioxiranyl radical. Recently, Mebel *et al.* (1996) performed *ab initio* and RRKM calculations for the multichannel rate coefficients of the $C_2H_3 + O_2$ reactions, and concluded that the $HCO + CH_2O$ channel has the highest rate constant, and at $T > 900$ K, the $CH_2CHO + O$ are the major products. At very high temperatures, the channel producing $C_2H_2 + HO_2$ becomes competitive. Based on this latter study, we specified the following reactions for the reaction of vinyl + O_2,

$$C_2H_3 + O_2 \rightarrow C_2H_2 + HO_2 \quad (191)$$

$$C_2H_3 + O_2 \rightarrow CH_2CHO + O \quad (192)$$

$$C_2H_3 + O_2 \rightarrow HCO + CH_2O\ , \quad (193)$$

and adopted the RRKM rate parameters of Mebel *et al.* (1996).

The kinetics of CH_3CO and CH_3CHO was included in the kinetic model. The rate parameters were taken mainly from Tsang and Hampson (1986) for CH_3CO and from Baulch *et al.* (1994) for CH_3CHO.

The rate parameters of the H-abstraction of ethylene by the H atom

$$C_2H_4 + H \rightarrow C_2H_3 + H_2 \quad (226)$$

were updated, based on the recent work of Knyazev *et al.* (1996), who experimentally determined k_{226} in the temperature range 499-947 K and performed *ab initio* studies and transition state calculations. Their rate expression yields a rate constant at 1200 K which is about a factor of 2 lower than the compilation of the GRI-Mech.

4.4. C_3 and C_4 Chemistry

The C_3 and C_4 chemistry becomes relevant for fuel rich combustion. In the present model, we included the chemistry of propyne, allene and propene, and incorporated the results of Davis *et al.* (1998a, 1998b), who studied the pyrolysis and oxidation kinetics of propyne and propene in laminar flames and in a flow reactor. The chemistry of C_4H_2 and C_4H_4 is also included in the kinetic model. The rate parameters for the relevant reactions were taken from Wang and Frenklach (1997). The inclusion of the C_3 and C_4 chemistry not only ensures the fuel-rich chemistry is adequately accounted for by the present model, it also provides an easy extension of the kinetic model to include the chemistry of higher hydrocarbons.

5. Simulation of Shock-Tube Experiments

5.1. Ethylene Oxidation in Shock Tubes

The shock tube simulation was performed using the Sandia Chemkin-II codes (Kee *et al.*, 1989) with a constant-density model for experiments conducted behind reflected shock waves and with the Sandia Shock code (Mitchell and Kee, 1982) for incident shock waves. When possible, the computational ignition was defined in the same fashion as the experiment.

Figures 8-11 presents the experimental data and computational results for ethylene oxidation in shock tubes. A total 13 mixtures were used for data comparison, covering a wide range of equivalence ratio, pressure, and temperature. The ignition delay data shown in Figure 11 are derived from the correlation equations reported by Baker and Skinner (1972), and are not the actually data points. In addition, the experimental ignition delay data with values greater than 2000 μs are not shown in the figure. Excessively long induction-time data are expected to be inaccurate because of the growth of non-ideality and the decay of shock wave at long reaction time after shock passage.

In general, the shock-tube ignition delay times were reasonably well predicted, keeping in mind that the uncertainty factor in the experimental data is a factor of 2. The experimental data of Jachimowski (1977) were collected in incident shock waves under the condition of extremely short induction times, ~10 μs. Although measurements with such short induction times are extremely difficult, the agreement is surprisingly good between experiment and simulation (see Figure 9).

Jachimowski (1977) also reported the maximum of concentration product, [CO][O], based on the ultraviolet emission intensity at 0.37 μm due to $CO + O \rightarrow CO_2 + h\nu$. These data provide a more unambiguous and stringent test for the kinetic model. Figure 10 presents the comparison of the experimental and computed maximum [CO][O]. It is seen that the experimental data are nicely predicted by the current model.

The current kinetic model does not predict well the ignition delay times of shock mixtures 6 and 7 reported by Baker and Skinner (1972). Both mixtures are fuel-rich with the

equivalence ratio equal to 2. It is conceivable that the kinetic model is inadequate in predicting the ignition of fuel-rich ethylene mixtures. At the same time, one should recognize that experimental ignition point may be difficult to define, as it is based on the maximum intensity of light emission after shock passage. The detailed temporal profiles computed for these two mixtures reveal that the oxidation appears to be a slow process, and thus it is difficult to pinpoint the ignition point experimentally.

Because the experimental data for ethylene ignition are rather old and scarce, the current modeling effort suggests the need for additional data especially in the middle temperature range of 1200 - 1800 K, where only one series of study was reported.

5.2. Acetylene Oxidation in Shock Tubes

Figures 12-20 presents comparisons of experimental data and computational results for acetylene oxidation in shock tubes. Some 17 mixtures were included for the purpose of model verification. Again, the predictions for ignition delay times are generally very good, both qualitatively and quantitatively. In almost all cases, the prediction is well within the uncertainty of the data reported for these mixtures.

In addition to the ignition delay, more stringent tests for the model were carried by comparing the experimental data with the numerical predictions for species concentrations during the oxidation of acetylene. Figure 15 shows the experimental and computed maximum [O][CO] for two mixtures reported by Jachimowski (1977). It is seen that the experimental data are well predicted by the current model. On the other hand, the prediction is not satisfactory for the temporary CO_2 concentration profiles reported by Hidaka *et al.* (1996), as seen in Figure 20.

We also compared the model predictions for the laser Schlieren profiles measured prior to the ignition of acetylene, as seen in Figure 18. These profiles characterize the induction-zone exothermicity during acetylene oxidation in shock tubes.

5.3. Mechanisms of Acetylene and Ethylene Oxidation in Shock Tubes

The mechanistic feature of the oxidation of hydrocarbons in shock tube is that upon shock heating of the fuel-oxygen-diluent mixture, the initiation reactions generate an initial radical pool. Over a finite period of reaction, the radical pool, albeit small, grows exponentially in size via a chain reaction mechanism, although at this stage the consumption of the fuel is insignificant. The chain mechanism eventually causes the mixture to ignite, during and after which the fuel is quickly consumed, products are formed, and heat is released over a reaction time considerably shorter than the time to ignition.

The radical-chain initiation reaction is an essential part in our understanding of the mechanism of spontaneous ignition of fuel-oxygen mixtures. Two types of initiation reactions have been previously considered, namely, the H-abstraction of fuel by molecular oxygen and the unimolecular dissociation of the fuel. Here, we uncover a third possible initiation reaction mechanism. This mechanism is dominated by the production of vinylidene, followed by the oxidation of vinylidene by molecular oxygen. The theoretical justification for the mechanism of the initial radical production in acetylene oxidation has been discussed in section 3.2. The agreement between experimental data and theoretical prediction seen in Figures 12-20 further confirms that the reaction sequence given by (175) and (176) is responsible for the production of the initial radical pool. Thus, like the dimerization mechanism of acetylene pyrolysis below 1800 K (Kiefer and Von Drasek, 1990) acetylene oxidation in shock tubes is initiated by the isomerization of acetylene to vinylidene. The initial radical pool is then established via the reaction of vinylidene and molecular oxygen.

For ethylene oxidation in shock tubes, we identified the following reaction sequence, again involving vinylidene formation via 1,1-elimination in ethylene, followed by the reaction of vinylidene with molecular oxygen, as the process which leads to the production of initial free radicals,

$$C_2H_4 (+M) \rightarrow H_2CC + H_2 \qquad ()$$

$$H_2CC + O_2 \rightarrow \text{radical products} \qquad ()$$

An additional issue relevant to acetylene ignition concerns the reaction between methylene and molecular oxygen. Hidaka *et al.* (1996) concluded that in order to predict the early production of CO_2 in their experiments, the products must be assigned as CO_2 + 2H• for the reaction of the triplet methylene with O_2. This conclusion is in an apparent disagreement with the LS experiments of Hwang *et al.* (1987), who concluded on the basis of computer modeling of LS profiles that CO_2 could not be the major product of the **:**CH_2 + O_2 reaction. This conclusion was supported later by the direct experimental investigations (Dombrowsky and Wagner, 1992; Bley et al, 1992) of the same reaction. Our computer simulation results indicate that Hidaka *et al.*'s data can be well predicted with •CHO + •OH as the only channel of the **:**CH_2 + O_2 reaction, without having to consider CO_2 + 2H• as the products.

6. Simulation of Laminar Burning Velocity

Figure 21 presents the comparison between experimental and computed laminar burning velocity of ethylene and acetylene in air at atmospheric pressure. The current model predicts the ethylene data much better than our previous version (Sun *et al.*, 1996). The model still predicts lower burning velocities than the experimental data for moderately fuel-rich acetylene-air mixtures, although the data on the fuel-lean side of stoichiometry are well accounted for by the kinetic model.

Burning velocities at reduced and elevated pressures were also included for model comparison. Figure 22 shows the variation of burning velocity as a function of pressure and equivalence ratio for mixtures of ethylene in a N_2 diluted air (O_2/N_2 = 18/82). It is seen that agreement between experiment and model is quite good. Figure 23 presents the variation of the experimental and computational burning velocity as a function of pressure for a stoichiometric mixture of ethylene in the N_2 diluted air. It is seen that the pressure dependence is well captured by simulation, although the predicted burning velocities are higher than the experimental data by ~2-3 cm/s for pressure greater or equal than 0.5 atm.

Figures 24 and 25 present the similar plots for the pressure dependence of the burning velocity of acetylene in an N_2 diluted mixture (O_2/N_2 = 13/87). For stoichiometric and fuel-rich mixtures, the model predictions are larger than the experimental data, which is opposite to the trend observed for the acetylene-air mixtures shown in Figure 21, where the predictions are seen to be smaller than the experimental data for the fuel-rich conditions. A first order sensitivity analysis does not show that for burning velocity predictions the influential reactions are different between the acetylene-air and acetylene-N_2-diluted air mixtures. It is likely that a further improvement of the kinetic mechanism cannot be achieved before the acetylene data are re-examined.

7. Simulation of Burner-Stabilized Flames

For the simulation of Flames 1 and 2, we followed the suggestion of Bhargava and Westmoreland (1998a, b) and lowered the measured flame temperature by 100 K to account for the probe effect. In addition, the temperature profile was shifted downstream by 0.05 cm to account for perturbation caused by the thermocouple, and the species profiles were moved 0.09 cm toward the burner surface to account for the quartz probe effect.

Figure 26 presents the mole fraction profiles of the major species in Flame 1, a fuel-rich ethylene flame reported by Bhargava and Westmoreland (1998a). It is seen that the kinetic model predicts the species profiles very well. Figure 27 shows the experimental and computed mole fraction profiles of H and OH. The agreement is better than 40%. Figures 28 and 29 present the comparison of model and experiment for 16 minor species. It is seen that peak concentrations of most species are predicted to within a factor of 2. The width and the shapes of the mole fraction profiles are also reasonably well predicted.

Figure 30 presents the mole fraction profiles of major species in Flame 2 (Bhargava and Westmoreland, 1998b). It is seen that the agreement between model and experiment worsen for this fuel-lean ethylene flame. In particular, the model underpredicts quite significantly CO_2 concentrations in the post flame zone. It is likely that this difference is caused by the

discrepancy between model and experiment for the concentrations of the major radical species, as shown in Figure 31. The present model predicts the peak mole fractions of O and H to be 2 times higher than the experimental counterparts. In addition, the peak OH concentration was also over-predicted by about 50%. First order sensitivity tests show that the differences between model and experiment cannot be easily accounted for by adjusting the rate parameters in the kinetic model within the uncertainty of these parameters. Figures 32 and 33 show the comparison for 12 minor species measured in Flame 2.

For the two acetylene flames (Flames 3 and 4), the agreement between model and experiment is generally good, as seen in Figures 34 through 37. For Flame 3, most of the minor species concentrations were predicted to within the experimental uncertainties. Overpredictions for C_3H_3 and C_4H_2 are likely to be caused by the lack of molecular mass growth processes in the present kinetic model. The discrepancy between model and experiment for CH_4 at distances close to the burner is likely to be caused by the recombination of methyl and the H atom on the burner surface. Such an effect is not account for by the numerical simulation.

8. Summary

In this work, we proposed a comprehensive kinetic model for acetylene and ethylene combustion. The kinetic model has been compiled on basis of both critical review of the recent literature kinetic data and theoretical calculations using modern quantum mechanical tools and the RRKM method. The kinetic parameters were taken from experimental/theoretical sources without invoking ad hoc adjustments. The comprehensiveness of the model is demonstrated by extensive verification tests against a variety of combustion data, including ignition behaviors, laminar flame propagation, and detailed structure of burner stabilized flames. It is shown that most of the reliable combustion data are well predicted by the kinetic model.

Through this study, we have concluded that the source of the initial radical pool in ethylene and acetylene oxidation in shock tubes originate from reaction pathways of vinylidene.

In the case of acetylene oxidation, the initiation reactions involves the isomerization of acetylene to vinylidene, followed by the reaction of vinylidene and molecular oxygen to produce the initial radical pool. For ethylene oxidation, the initiation steps are vinylidene formation via 1,1-elimination of H_2 in ethylene, followed again by the reaction between vinylidene and molecular oxygen. This is a significant finding as we have expanded the two previously understood initiation mechanisms of radical chain reactions, namely, unimolecular dissociation of the parent fuel and the H-abstraction of the fuel by molecular oxygen, to three possible mechanisms. Based on preliminary analysis of reaction energetics, it is likely that the new mechanism involving vinylidene and other carbene species dominates the initiation reactions for a large body of alkene compounds.

9. References

Astholz, D. C., Troe, J. and Wieters, W. J. (1979) *J. Chem. Phys*. **70**, 5107.

Baker, J. A. and Skinner, G. B. (1972) *Combust. Flame* **19**, 347.

Baldwin, P., Canosa-Mas, C. E., Frey, H. M. and Walsh, R. (1987) *Int. J. Chem. Kinet.* **19**, 997.

Baulch, D. L., Cobos, C. J., Cox, R. A., Frank, P., Hayman, G., Just, Th., Kerr, J. A., Murrells, T., Pilling, M. J., Troe, J., Walker, R. W. and Warnatz, J. (1992) *J. Phys. Chem. Ref. Data* **21**, 411.

Baulch, D. L., Cobos, C. J., Cox, R. A., Frank, P., Hayman, G., Just, Th., Kerr, J. A., Murrells, T., Pilling, M. J., Troe, J., Walker, R. W. and Warnatz, J. (1994) *J. Phys. Chem. Ref. Data* 23: 847.

Bauschlicher, C. W., Jr. and Langhoff, S. R., (1991) *Chem. Phys. Lett.* **177**, 133.

Becke, A. D. (1993) *J. Chem. Phys.* **98**, 5648.

Bencsura, A., Kuyazev, V. D., Slagle, I. R., Gutman, D. and Tsang, W. (1992) *Ber. Bunsenges. Phys. Chem.* **96**, 1338.

Beyer, T. and Swinehart, D. F. (1973) *Comm. Assoc. Comput. Machines* **16**, 379.

Bhargava, A. and Westmoreland, P. R. (1998a) *Combust. Flame* **113**, 333.

Bhargava, A. and Westmoreland, P. R. (1998b) *Combust. Flame* **115**, 456.

Bley, U., Temps, F., Wagner, H. Gg. and Wolf, M., (1992) *Ber. Bunsenges. Phys. Chem.* **96**, 1043.

Bozzelli, J. W. and Dean, A. M. (1993) *J. Phys. Chem.* **97**, 4427.

Bradley, J. N. and Kistiakowsky, G. B. (1961) *J. Chem. Phys.* **35**, 264.

Burcat, A. and McBride, B. (1997) *1997 Ideal Gas Thermodynamic Data for Combustion and Air-Pollution Use*, Technion Aerospace Engineering (TAE) Report # 804, Israel.

Carpenter, B. K. (1993) *J. Am. Chem. Soc.* **115**, 9806.

Carpenter, B. K. (1995) *J. Phys. Chem.* **99**, 9801.

Carr, R. W., Gay, I. D., Glass, G. P. and Niki, H. (1968) *J. Chem. Phys.* **49**, 846.

Curtiss, L. A., Raghavachari, K., Trucks, G. W. and Pople, J. A. (1991) *J. Chem Phys.* **24** 7221.

Dagaut, P., Boettner, J.-C. and Cathonnet, M. (1990) *Int. J. Chem. Kinet.* **22**, 641.

Davis, S. G., Law, C. K. and Wang, H. (1998a) "Propyne Pyrolysis in a Flow Reactor: An Experimental, RRKM, and Detailed Kinetic Modeling Study," *J. Phys. Chem.*, submitted.

Davis, S. G., Law, C. K. and Wang, H. (1998b) "Propene Pyrolysis and Oxidation Kinetics in Flow Reactors and in Laminar Flames," *Combust. Flame*, submitted.

Dombrowsky, C. H. and Wagner, H. Gg. (1992) *Ber. Bunsenges. Phys. Chem.* **96**, 1048.

Donaldson, D. J., Okuda, I. V. and Sloan, J. J. (1995) *Chem. Phys.* **193**, 37.

Eade, R. H. E. and Robb, M. A. (1981) *Chem. Phys. Lett.* **148**, 183.

Eberius, K. H., Hoyermann, K. and Wagner, H. Gg. (1973) *Fourteenth Symposium (International) on Combustion*, The Combustion Institute, Pittsburgh, p. 147.

Egolfopoulos, F. N., Zhu, D. L. and Law, C. K. (1990a) "Laminar Flame Speeds of Mixtures of C_2-Hydrocarbons with Oxygen and Nitrogen," MAE Report # 1891, Princeton University.

Egolfopoulos, F. N., Zhu, D. L. and Law, C. K. (1990b) *Twenty-Third Symposium (International) on Combustion*, The Combustion Institute, Pittsburgh, p. 471.

Ervin, K. M., Gronert, S., Barlow, S. E., Gilles, M. K., Harrison, A. G., Bierbaum, V. M., DePuy, C. H., Lineberger, W. C. and Ellison, G. B. (1990) *J. Am. Chem. Soc.* **112**, 5750.

Frank, P., Bhaskaran, K. A. and Just, Th. (1986) *J. Phys. Chem.* **90**, 2226.

Frenklach, M., Wang, H., Goldenberg, M., Smith, G. P., Golden, D. M., Bowman, C. T., Hanson, R. K., Gardiner, W. C. and Lissianski, V. (1995) *GRI-Mech–An Optimized Detailed Chemical Reaction Mechanism for Methane Combustion*, GRI Technical Report No. GRI-95/0058.

Gardiner, W. C., Jr. (1961) *J. Chem. Phys.* **35**, 2252.

Gardiner, W. C., Jr. and Walker, B. F. (1968) *J. Chem. Phys.* **48** 5279.

Gardiner, W. C., Jr., Walker, B. F., and Wakefield, C. B. (1981) *Shock Waves in Chemistry*, A. Lifshitz Ed., Marcel Dekker, New York, p.319.

Gilbert, R. G. and Smith, S. C. (1990) *Theory of Unimolecular and Recombination Reactions*; Blackwell Scientific: Oxford.

Gilbert, R. G., Luther, K. and Troe, J. (1983) *Ber. Bunsenges. Phys. Chem*. **87**, 169.

Hidaka, Y., Eubank, C. S., Gardiner, W. C. Jr. and Hwang, S. M. (1984) *J. Phys. Chem.* **88**, 1006.

Hidaka, Y., Hattori, K., Okuno, T., Inami, K., Abe, T. and Koike, T. (1996) *Combust. Flame* **107**, 401.

Hidaka, Y., Tanaka, Y., Kawano, H. and Suga, M. (1981) *Mass. Spectros.* **29**, 191.

Hohenberg, P. and Kohn, W. (1964) *Phys. Rev. B* **136**, 864.

Holbrook, K. A., Pilling, M. J. and Robertson, S. H. (1996) *Unimolecular Reactions*, 2nd ed., Wiley, Chichester.

Homer, J. B. and Kistiakowsky, G. B. (1967) *J. Chem. Phys.* **47**, 5290.

Hwang, S. M., Gardiner, W. C., Jr., Frenklach, M. and Hidaka, Y. (1987) *Combust. Flame* **67**, 65.

Jachimowski, C. J. (1977) *Combust. Flame* **29**, 55.

Kee, R. J., Dixon-Lewis, G., Warnatz, J., Coltrin, M. E. and Miller, J. A., (1986) *A Fortran Computer Code Package for the Evaluation of Gas-Phase Multicomponent Transport Properties*, Sandia Report SAND86-8246.UC-32, Sandia, Albuquerque, New Mexico.

Kee, R. J., Grcar, J. F., Smooke, M. D. and. Miller, J. A. (1987) *A Fortran Program for Modeling Steady Laminar One-Dimensional Flames*, Sandia Report SAND85-8240.UC-4, Sandia, Albuquerque, New Mexico.

Kee, R.J., Rupley, F.M. and Miller, J.A. (1989) *Chemkin II: A Fortran Chemical Kinetics Package for the Analysis of Gas-Phase Chemical Kinetics*, Sandia Report SAND 89-8009B, Sandia, Albuquerque, New Mexico.

Kiefer, J. H. and Von Drasek, W. A., (1990) *Int. J. Chem. Kinet.* **22** 747.

Kistiakowsky, G. B. and Richards, L. W. (1962) *J. Chem. Phys.* **36**, 1707.

Knyazev V. D. and Slagle I. R. (1996) *J. Phys. Chem.* **100**, 16899.

Kohn, W. and Sham, L. J. (1965) *Phys. Rev. A* **140**, 1133.

Lee, C., Yang, W. and Parr, R. G. (1988) *Phys. Rev. B* **37** 785.

M. J. Frisch, G. W. Trucks, H. B. Schlegel, P. M. W. Gill, B. G. Johnson, M. A. Robb, J. R. Cheeseman, T. Keith, G. A. Petersson, J. A. Montgomery, K. Raghavachari, M. A. Al-Laham, V. G. Zakrzewski, J. V. Ortiz, J. B. Foresman, J. Cioslowski, B. B. Stefanov, A. Nanayakkara, M. Challacombe, C. Y. Peng, P. Y. Ayala, W. Chen, M. W. Wong, J. L. Andres, E. S. Replogle, R. Gomperts, R. L. Martin, D. J. Fox, J. S. Binkley, D. J. Defrees, J. Baker, J. P. Stewart, M. Head-Gordon, C. Gonzalez and J. A. Pople (1995) Gaussian 94, Revision D.4, Gaussian, Inc., Pittsburgh.

Michael, J. V. and Wagner, A. F. (1990) *J. Phys. Chem.* **94**, 2453.

Michael, J. V., Nava, D. F., Payne, W. A. and Stief, L. J. (1979) *J. Chem. Phys.* **70**, 5222.

Miller, J. A., Mitchell, R. E., Smooke, M. D. and Kee, R. J. (1982) *Nineteenth Symposium (International) on Combustion*, The Combustion Institute, Pittsburgh, p. 181.

Mitchell, R. E. and Kee, R. J. (1982) *A General Purpose Computer Code for Predicting Chemical Kinetic Behavior behind Incident and Reflected shocks*, Sandia Report SAND82-8205, Sandia, Albuquerque, New Mexico.

Mueller, M. A., Kim, T. J., Yetter, R. A. and Dryer, F. L. (1998) "Flow reactor studies and kinetic modeling of the H_2/O_2 reactions." *Int. J. Chem. Kinet.* submitted.

Sheng, C. and Bozzelli, J. W. (1998) Twenty-Seventh International Symposium on Combustion, work-in-progress poster W4B27, Boulder, Colorado.

Slagle, I. R., Park, J.-Y., Heaven, M. C., and Gutman, D. (1984) *J. Am. Chem. Soc.* **106**, 4356.

Slemr, F. and Warnek, P. (1975) *Ber. Bunsenges. Phys. Chem.* **79**, 152.

Smith, B. J., Smernik, R. and Radom, L., (1992) *Chem. Phys. Lett.* **188**, 589, and refs 1-6 cited therein.

Stubbeman, R. F. and Gardiner, W. C., Jr. (1961) *J. Phys. Chem.* **68**, 3169.

Sun, C. J., Sung, C. J., Wang, H. and Law, C. K. (1996) *Combust. Flame* **107**, 321.

Tien, J. H. and Matalon, M. (1991) *Combust Flame* **84**, 238.

Tsang, W. and Hampson, R. F. (1986) *J. Phys. Chem. Ref. Data* **15**, 1087.

Umemoto, H., Tsunashima, S., Sato, S., Washida, N. and Hatakeyama, S. (1984) *Bull. Chem. Soc. Japan* **57**, 2578.

Wang, H. and Frenklach, M. (1997) *Combust. Flame*, **110**, 173.

Wang, H., Hahn, T. O., Sung, C. J., and Law, C. K. (1996) *Combust. Flame* **105**, 291.

Warnatz, J. (1981) *Eighteenth Symposium (International) on Combustion*, The Combustion Institute, Pittsburgh, p. 369.

Westbrook, C. K. and Dryer, F. L. (1984) *Prog. Energy Combust. Sci.* **10**, 1.

Westmoreland, P. R. (1992) *Combust. Sci. Technol.* **82**, 151.

Westmoreland, P. R., Howard, J. B. and Longwell, J. P. (1986) *Twenty-First Symposium (International) on Combustion*, The Combustion Institute, Pittsburgh, p. 773.

Whitten, G. Z. and Rabinovitch, B. S. (1963) *J. Chem. Phys*. **38**, 2466.

Whitten, G. Z. and Rabinovitch, B. S. (1964) *J. Chem. Phys*. **41**, 1883.

Wu, C. K. and Law, C. K. (1984) *Twentieth Symposium (International) on Combustion*, The Combustion Institute, Pittsburgh, p. 1941.

Table 1. Shock-Tube Ignition Delay of Ethylene-Oxygen-Argon Mixtures.

Shock No.	ϕ	Mole Percent C_2H_4	Mole Percent O_2	P_5 or P_2 (atm)	T_5 or T_2 (K)	Method	Reference
1	0.5	0.5	3.0	0.6-0.8	1505-2225	Reflected shock wave IR emission from CO + CO_2 (10% of the final CO + CO_2 conc.)	Homer & Kistiakowsky (1967)
2	1.5	0.5	1.0	0.6-0.7	1540-2325		
3	1.0	1.0	3.0	3	1112-1556	Reflected shock wave Maximum light emission (maximum point close to that of a rapid pressure rise)	Baker & Skinner (1972)
4	0.5	0.5	3.0	3	1118-1430		
5	1.0	0.25	0.75	12	1176-1531		
6	2.0	2.0	3.0	3	1117-1616		
7	2.0	1.0	1.5	3	1155-1747		
8	0.5	1.0	6.0	3	1080-1440		
9	0.13	0.25	6	3	1058-1418		
10	0.5	0.25	1.5	3	1100-1628		
11	2.0	0.5	0.75	3	1166-1876		
12	0.5	1	6	1.2-1.6	1800-2301	Incident shock wave Maximum IR emission due to $CO + O \rightarrow CO_2 + h\nu$	Jachimowski (1977)
13	1.0	2	6	1.2-1.7	1815-2339		
14	1.5	3	6	1.3-1.7	1868-2311		

Table 2. Shock-Tube Ignition Delay of Acetylene-Oxygen-Argon Mixtures.

Shock No.	ϕ	Mole Percent C_2H_2	Mole Percent O_2	P_5 or P_2 (atm)	T_5 or T_2 (K)	Method	Reference
15	0.78	1.0	3.2	0.1-0.2	1370-2455	Incident shock wave UV emission from OH (10% maximum value)	Stubbeman & Gardiner (1961)
16	1.65	1.35	2.04	0.09-0.16	1610-2050	Incident shock wave X-ray densitometry	Gardiner (1961)
17	3.21	10.8	8.4	0.19-0.28	954-1090	Reflected shock wave Onset of CO & H_2O production (TOF mass spec.)	Bradley & Kistiakowsky (1961)
18	0.32	0.57	4.43	0.06-0.12	1293-1994	Reflected shock wave	Kistiakowsky & Richards (1962)
19	3.45	2.9	2.1	0.09-0.13	1694-2049	Onset of vacuum UV	
20	1.67	2.0	3.0	0.07-0.16	1391-2371	radiation	
21	1.56	0.5	0.8	0.6-0.76	1580-2300	Reflected shock wave	Homer & Kistiakowsky (1967)
22[a]	-	0.5	1.0	0.6-0.7	1430-2400	IR emission from CO & CO_2 (10% maximum value)	
23	0.67	1.0	3.75	1.2-1.5	1823-2322	Reflected shock wave	Jachimowski (1977)
24[b]	-	1.0	5.5	1.3-1.6	1907-2302	Maximum IR emission due to $CO + O \rightarrow CO_2 + h\nu$	
25	2.0	2.0	2.5	~0.6	1171-1705	Reflected shock wave	Hidaka *et al.* (1981)
26	0.71	1.0	3.5	~0.6	1169-1710	Onset of O_2 disappearance	
27	1.0	1.0	2.5	~0.6	1197-1859		
28	1.0	0.5	1.25	0.22-0.34	1528-2173	Incident shock wave	Hidaka *et al.* (1984)
29	0.25	0.5	5.0	0.19-0.30	1346-1949	Maximum LS density gradients	
30	0.49	0.5	2.54	1.1-2.0	1092-1565	Reflected shock wave	Hidaka *et al.* (1996)
31	0.5	1.0	5.0	1.1-1.7	1051-1393	Onset of IR emission	
32	1.0	0.5	1.25	1.3-2.1	1206-1627	from CO_2	
33	1.0	1.0	2.5	1.2-1.8	1135-1446		
34	2.0	2.0	2.5	1.3-1.9	1177-1467		

[a] With an additional 0.5% H_2. [b] with an additional 1% C_2H_4.

Table 3. Laminar Premixed Flat Flames for Model Verification

No.	Reactants	ϕ	p (Torr)	v_0 (cm/s)	T_{max} (K)	Reference
1	$0.194C_2H_4$-$0.306O_2$-0.5Ar	1.9	20	62.5	2090	Bhargava and Westmoreland, 1998a
2	$0.086C_2H_4$-$0.345O_2$-0.569Ar	0.75	30	30	1925	Bhargava and Westmoreland, 1998b
3	$0.465C_2H_2$-$0.485O_2$-0.05Ar	2.4	20	50	1900	Westmoreland *et al.*, 1986
4	$0.03C_2H_2$-$0.97O_2$	0.077	76	57	>1300	Eberius *et al.* 1973

Table 4. RRKM Parameters for the Reaction of CH_3CO.

CH_3CO	Freq (cm^{-1})	454.6 839.3 943.7 1038.0 1355.0 1455.2 1458.3 1898.9 2982.9 3070.7 3073.7
	B_0 (cm^{-1})	0.321(1,2) - inactive 6.433(3,1) - active 2.761(1,1) - active
	L-J param.	σ = 3.97 Å, ε/k_B = 436 K
TS1	Freq (cm^{-1})	250.7 399.5 449.9 529.3 690.4 991.8 1137.7 1399.2 2184.3 3144.3 3232.2
	B_0 (cm^{-1})	0.299(1,2) - inactive 2.962(1,1) - active
	Path deg.	1
TS2	Freq (cm^{-1})	219.7 434.7 458.1 766.0 1408.7 1412.8 2066.3 3071.2 3231.6 3240.7
	B_0 (cm^{-1})	0.211(1,2) - inactive 5.780(3,1) - active 1.891(1,1) - active
	Path deg.	1
TS3	Freq (cm^{-1})	421.2 622.6 834.6 1021.8 1114.3 1224.4 1452.9 1805.4 1867.3 3014.3 3189.7
	B_0 (cm^{-1})	0.329(1,2) - inactive 3.328(1,1) - active
	Path deg.	2
CH_2CHO	Freq (cm^{-1})	450.1 494.8 737.4 956.8 965.0 1144.5 1387.4 1465.6 1541.2 2906.1 3110.4 3218.8
	B_0 (cm^{-1})	0.351(1,2) - inactive 2.235(1,1) - active
	Path deg.	2
	L-J param.	σ = 3.97 Å, ε/k_B = 436 K
TS4	Freq (cm^{-1})	321.0 483.5 522.3 575.7 621.5 989.8 1128.1 1405.8 2109.3 3132.8 3243.2
	B_0 (cm^{-1})	0.320(1,2) - inactive 2.887(1,1) - active
	Path deg.	1

Equilibrium constants

$CH_2CO + H = CH_3 + CO$	$K_{eq} = 3.04\times10^{1}\ T^{-0.53} \exp(21400/T)$
$CH_3 + CO = CH_3CO$	$K_{eq} = 1.55\times10^{-5}\ T^{0.97} \exp(5810/T)$

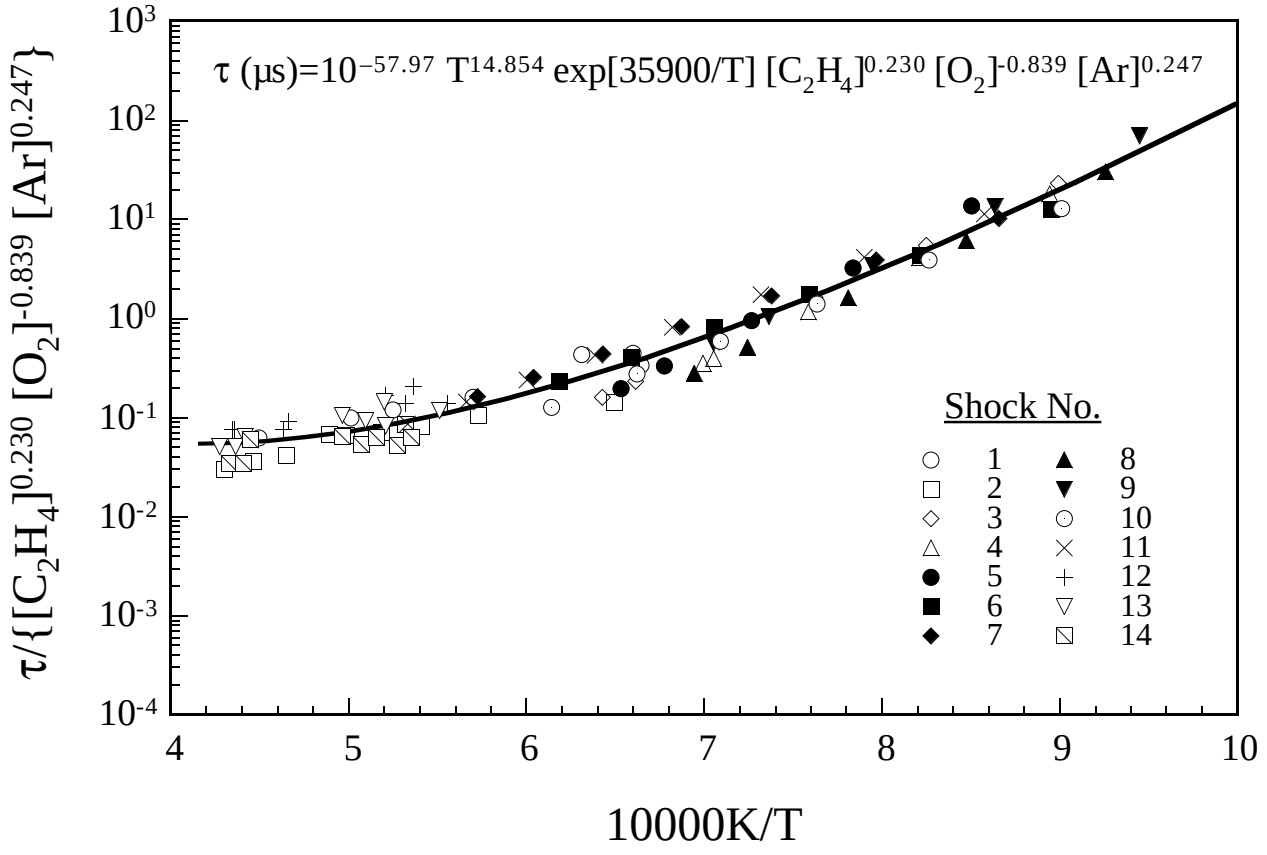

Figure 1. Literature shock-tube ignition data of ethylene-oxygen-argon mixtures. Symbols are experimental data, line is the correlation equation given in the panel. See Table 1 for reference sources and mixture conditions.

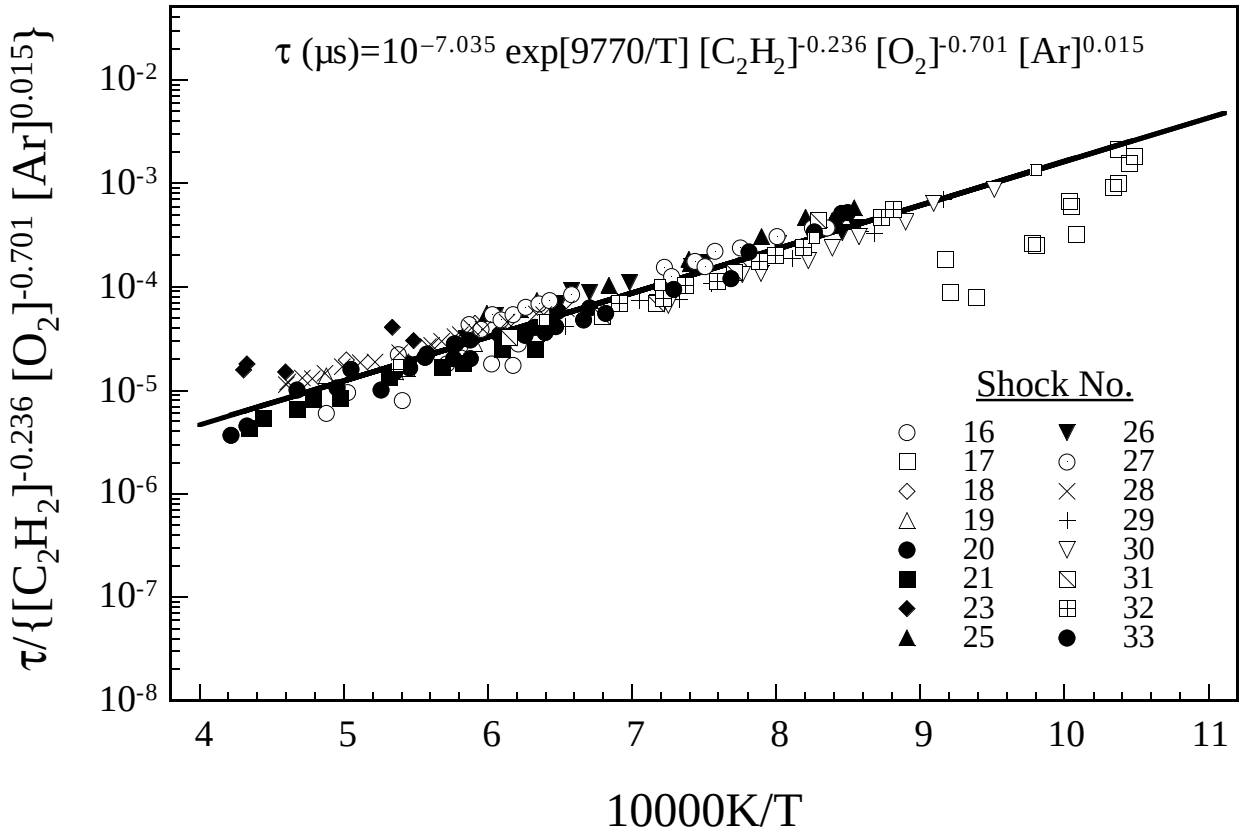

Figure 2. Literature shock-tube ignition data of acetylene-oxygen-argon mixtures. Symbols are experimental data, line is the correlation equation given in the panel.. See Table 2 for reference sources and mixture conditions.

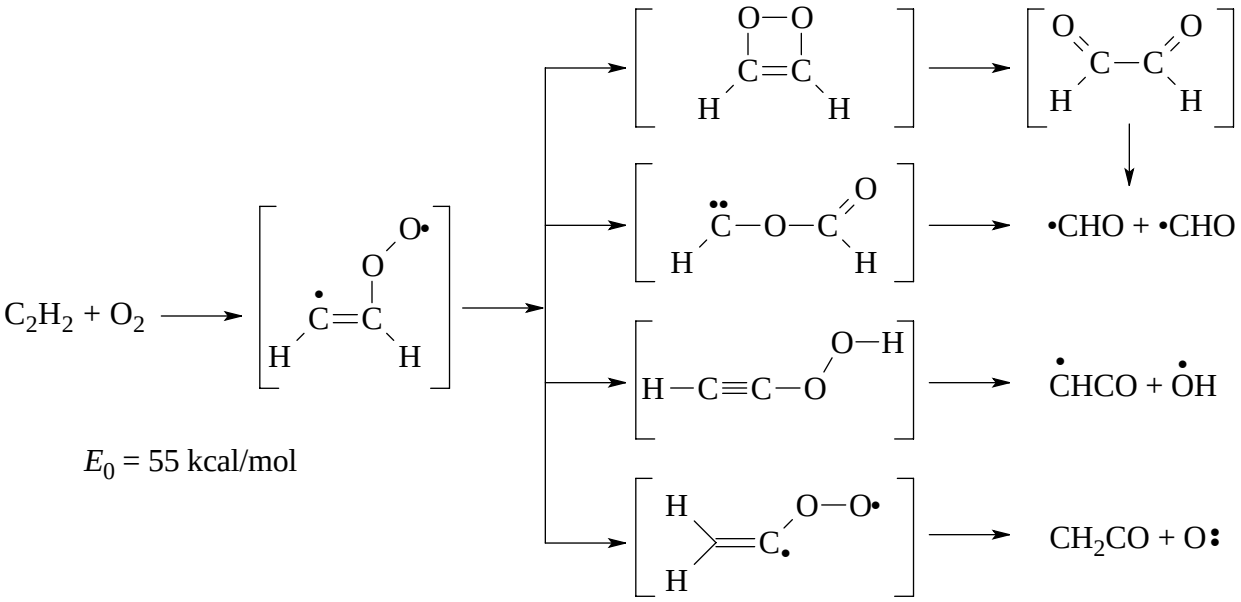

Figure 3. Reaction pathways following molecular oxygen attack on the π bond in acetylene. The bracket denotes that the species is a rovibrationally excited adduct.

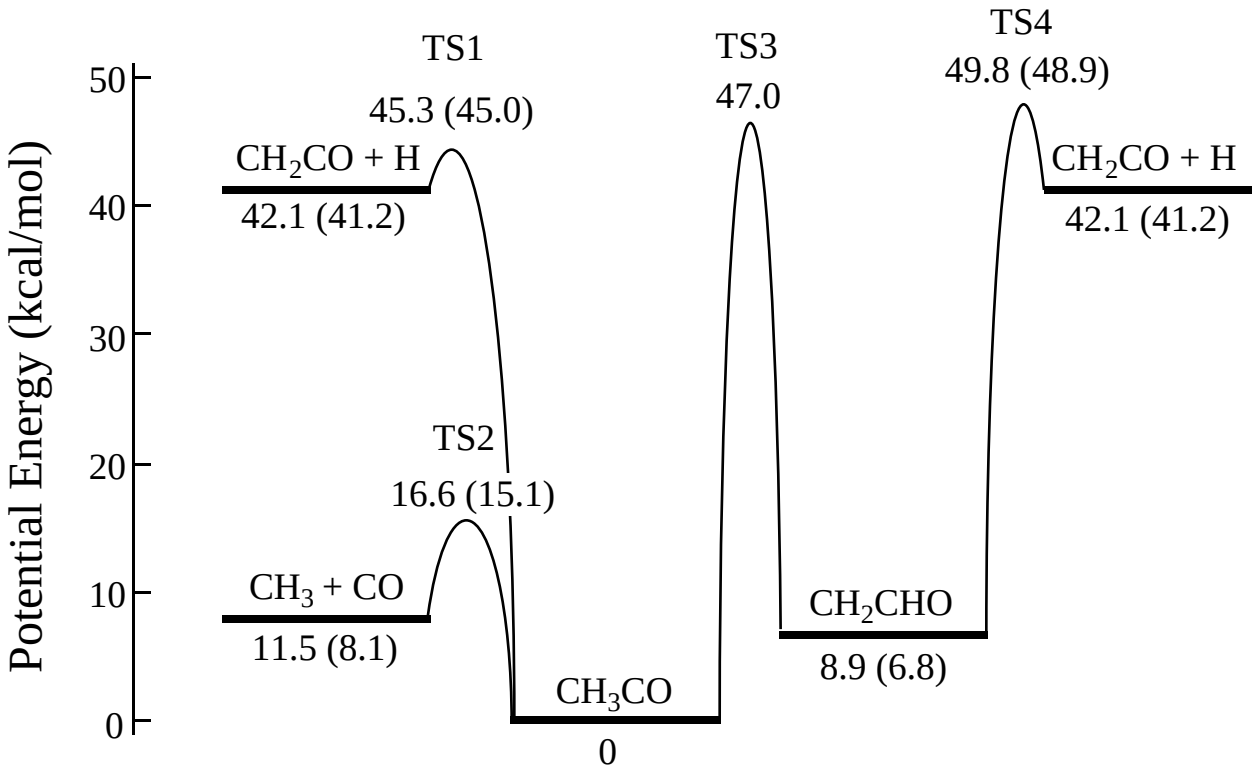

Figure 5. Potential energy diagram of the CH_3CO reactions. The energy values in parentheses are obtained at the G2(B3LYP) level of theory.

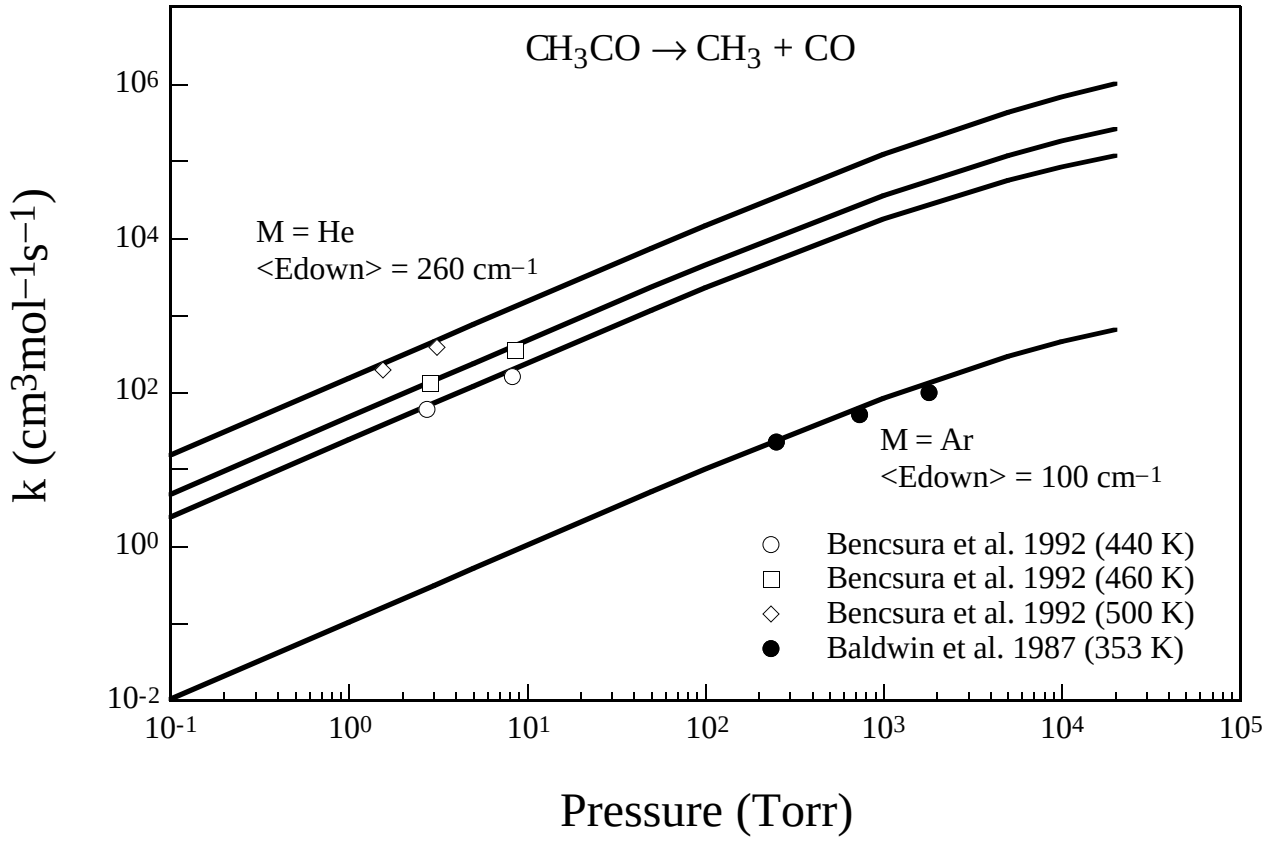

Figure 6. Comparison of theoretical prediction and experimental data for the pressure fall-off of the rate coefficients of $CH_3CO \rightarrow CH_3 + CO$.

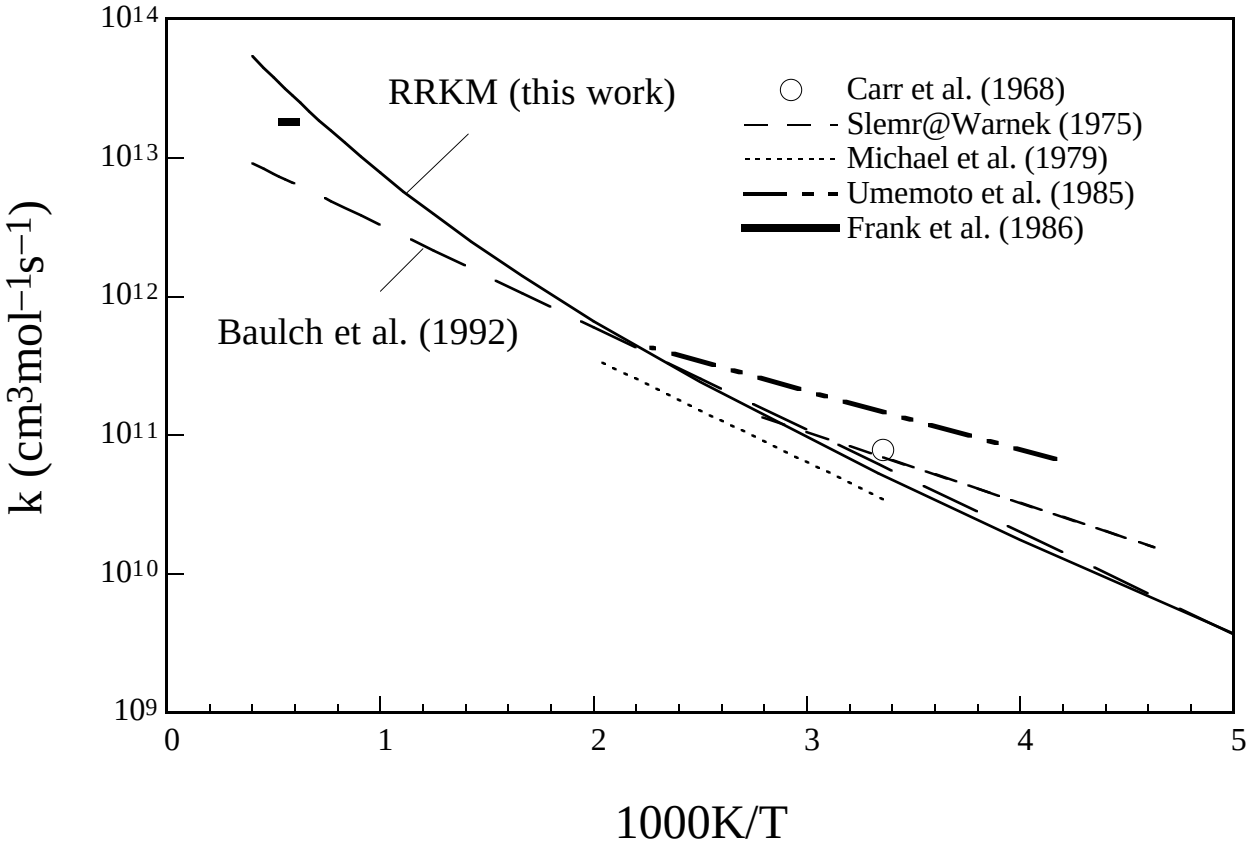

Figure 7. Comparison of theoretical prediction and experimental data for the rate coefficient of $CH_2CO + H \rightarrow CH_3 + CO$.

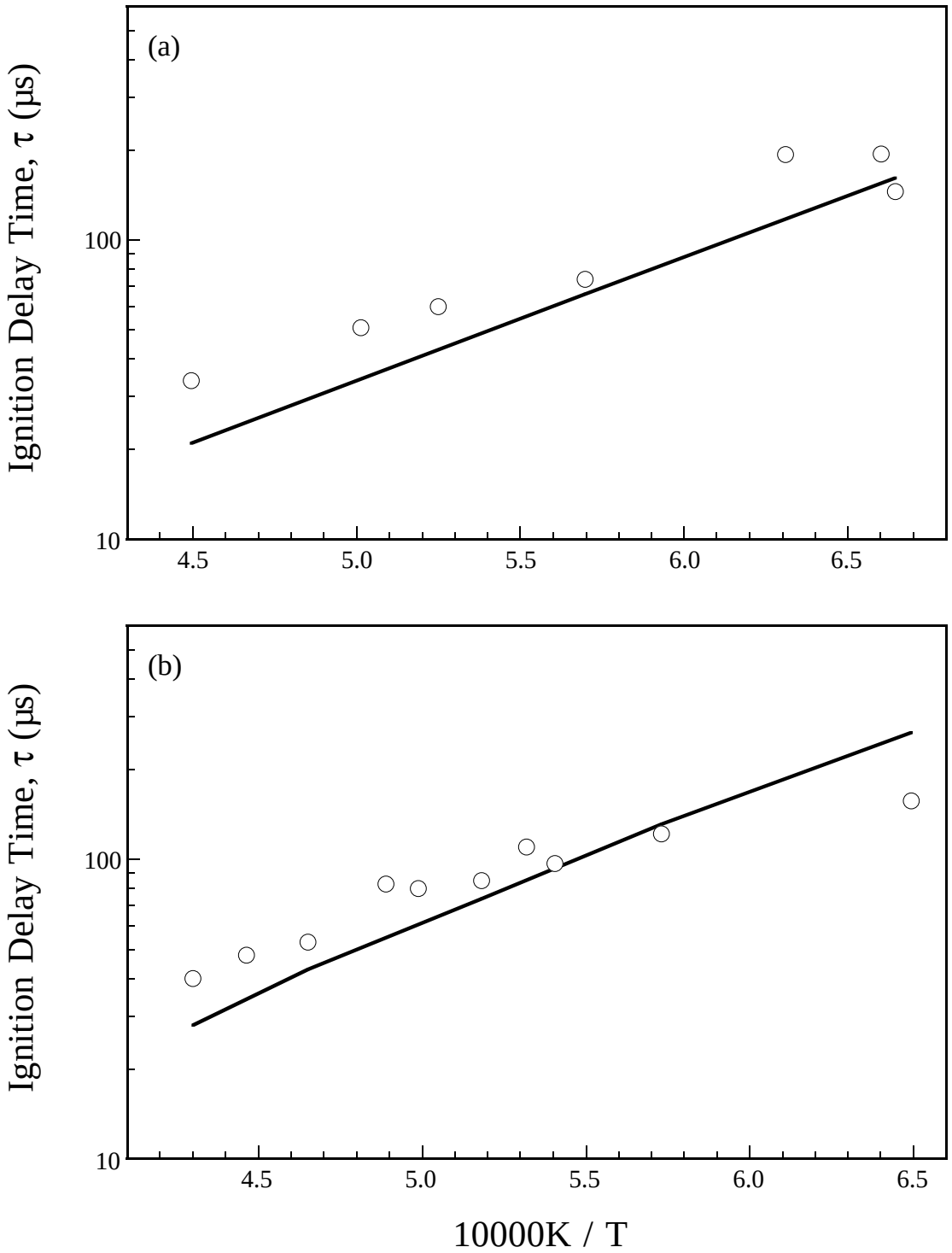

Figure 8. Comparison of experimental (symbols, Homer and Kistiakowsky, 1967) and computed (lines) ignition delay times behind reflected shock waves for the mixtures of (a) $0.5\%C_2H_4$-$3\%O_2$ (shock mixture 1, see Table 1) and (b) $0.5\%C_2H_4$-$1\%O_2$ (shock mixture 2, see Table 1) in argon. The computational ignition delay was determined as the time corresponding to [CO] + [CO_2] equal to 10% of its final value.

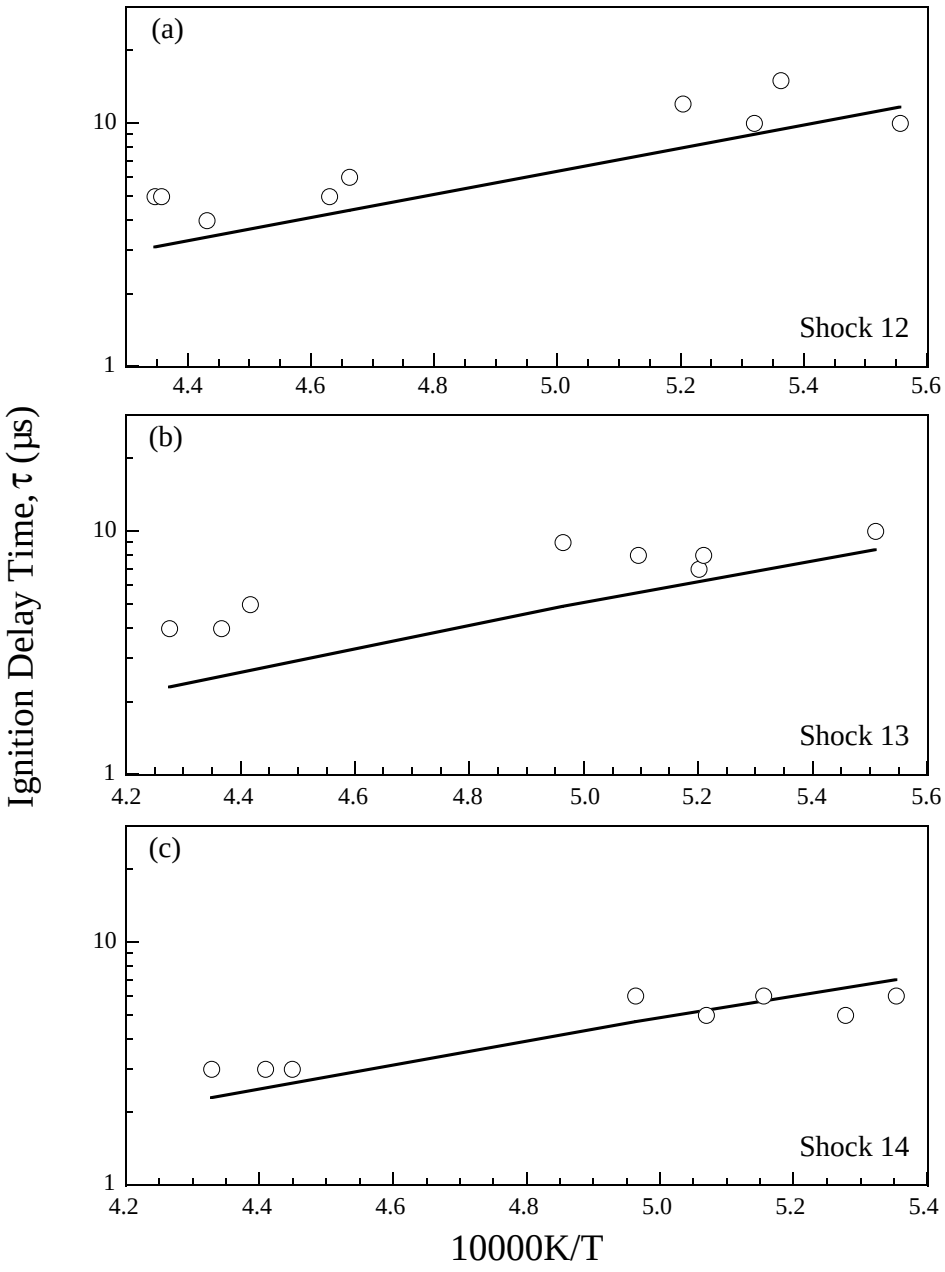

Figure 9. Comparison of experimental (symbols, Jachimowski 1977) and computed (lines) ignition delay times in incident shock waves for the mixtures of (a) 1%C_2H_4-6%O_2, (b) 2%C_2H_4-6%O_2, and (c) 3%C_2H_4-6%O_2 in argon. Other shock conditions can found in Table 1. The computational ignition delay was determined as the laboratory time corresponding to maximum [O][CO].

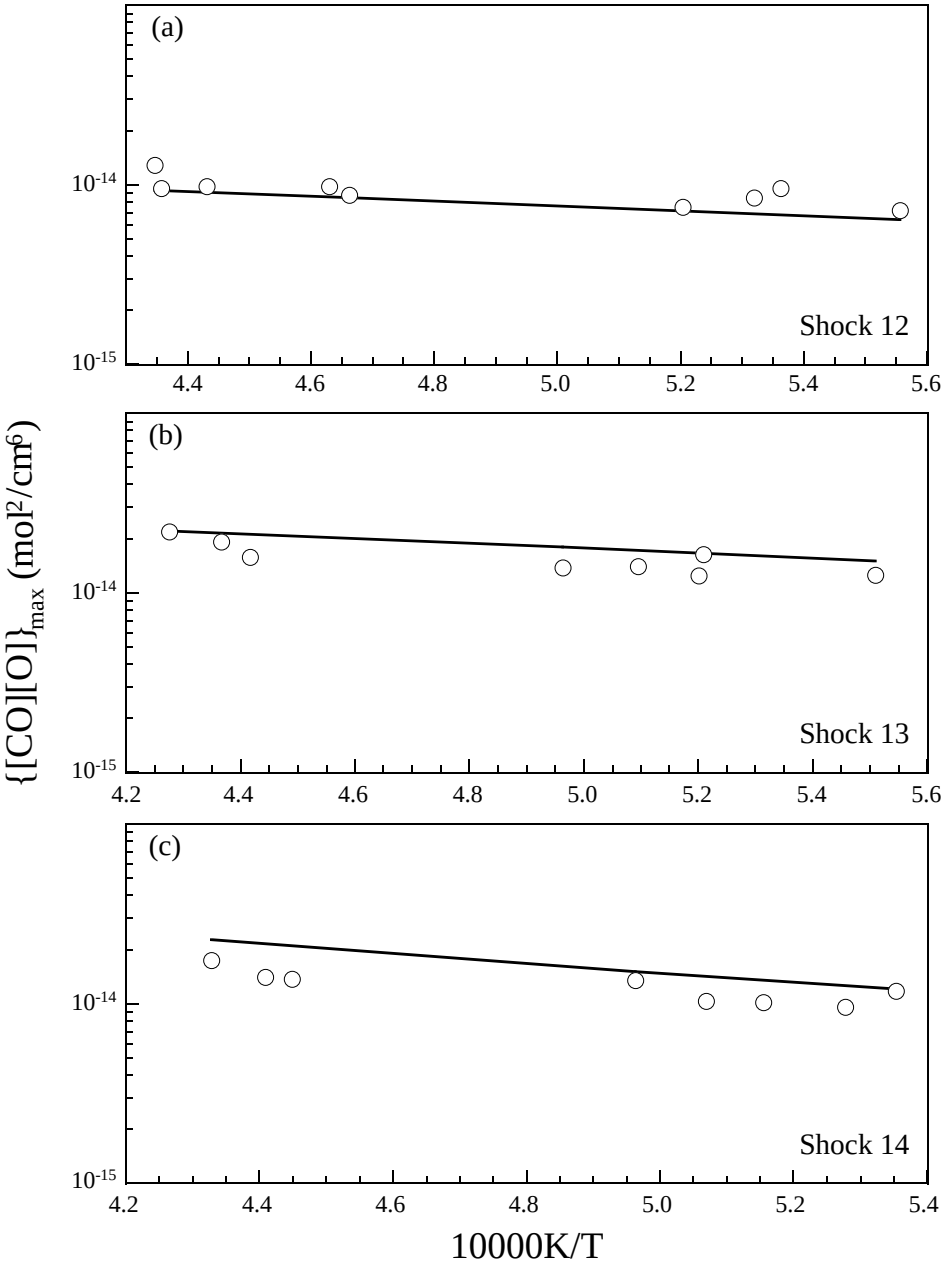

Figure 10. Comparison of experimental (symbols, Jachimowski 1977) and computed (lines) maximum [CO][O] in incident shock waves for the mixtures of (a) 1%C_2H_4-6%O_2, (b) 2%C_2H_4-6%O_2, and (c) 3%C_2H_4-6%O_2 in argon. Other shock conditions can found in Table 1.

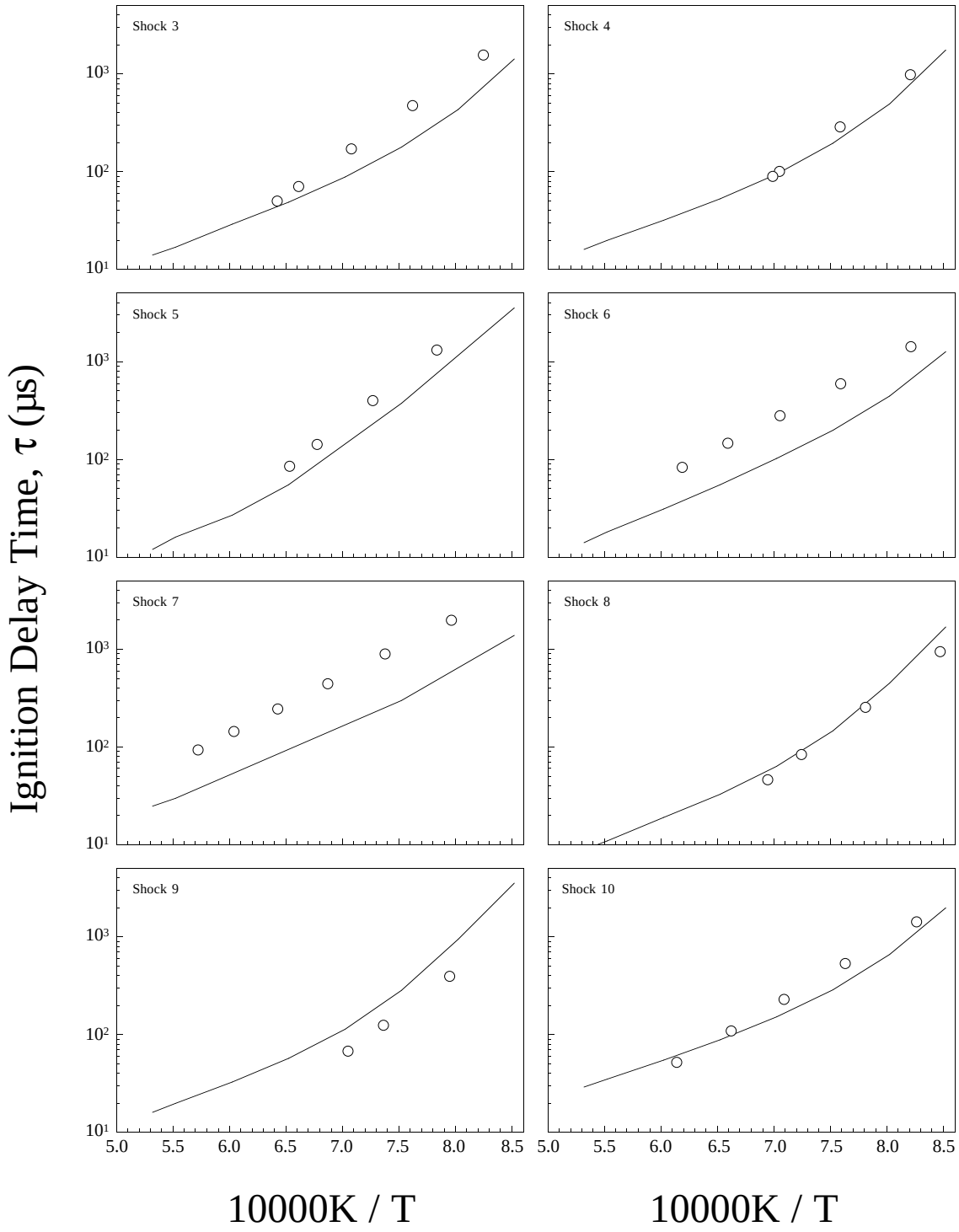

Figure 11. Comparison of experimental (symbols, Baker and Skinner, 1972) and computed (lines) ignition delay times behind reflected shock waves. The computational ignition was determined by the maximum pressure gradient. Shock mixtures (in argon): (3) 1%C_2H_4-3%O_2, (4) 0.5%C_2H_4-3%O_2, (5) 0.25%C_2H_4-0.75%O_2, (6) 2%C_2H_4-3%O_2, (7) 1%C_2H_4-1.5%O_2, (8) 1%C_2H_4-6%O_2, (9) 0.25%C_2H_4-6%O_2, (10) 0.5%C_2H_4-1.5%O_2. The initial pressure for all but one shock mixtures is 3 atm. The pressure of mixture 5 is 12 atm.

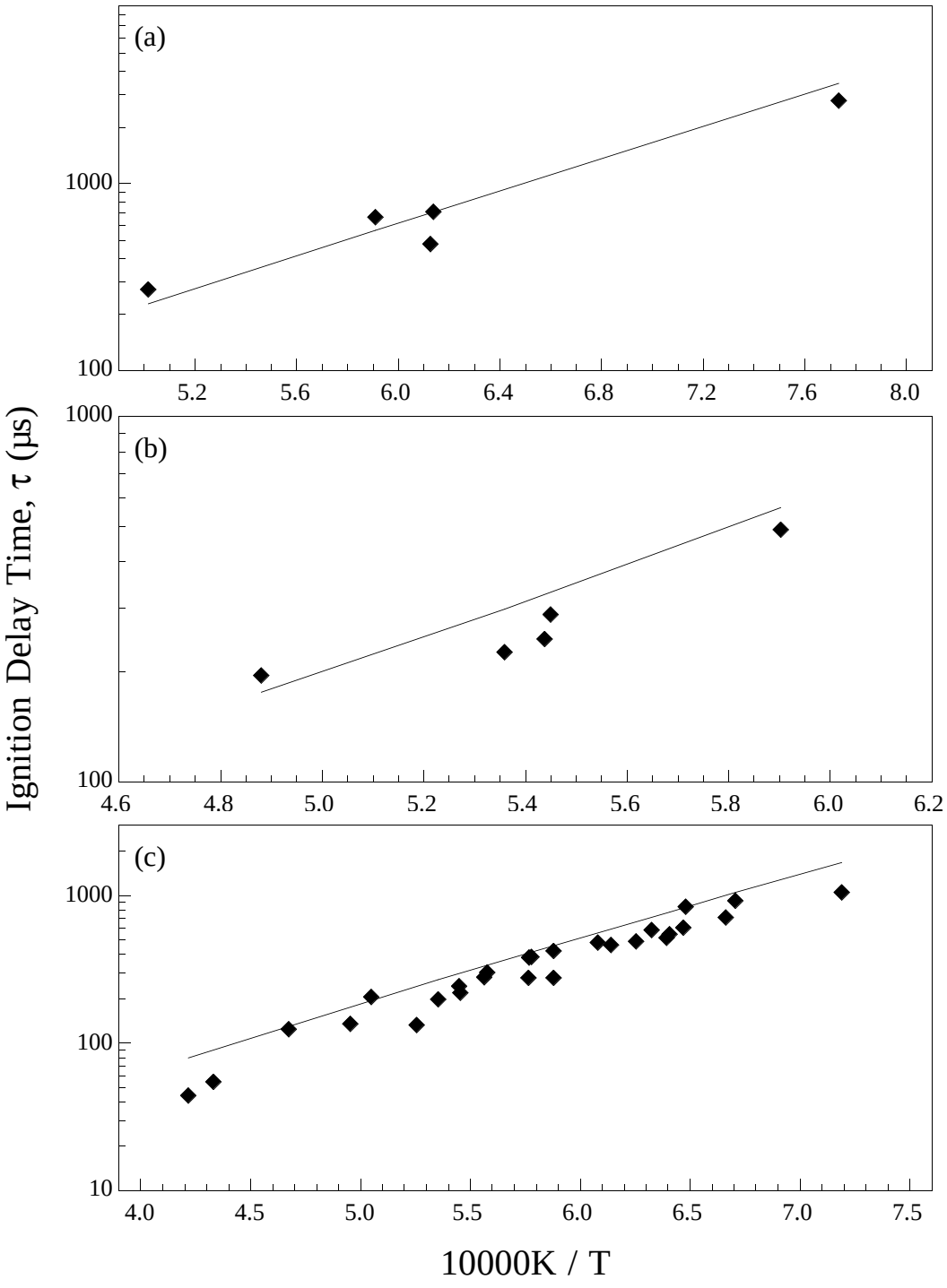

Figure 12. Comparison of experimental (symbols, Kistiakowsky and Richards, 1962) and computed (lines) ignition delay times behind reflected shock waves. The computational ignition was determined by the maximum pressure gradient. Mixture compositions (in argon): (a) 0.57%C_2H_2-4.43%O_2 (shock mixture 18), (b) 2.9%C_2H_2-2.1%O_2 (shock mixture 19), and (c) 2%C_2H_2-3%O_2 (shock mixture 20). See Table 2 for additional experimental conditions.

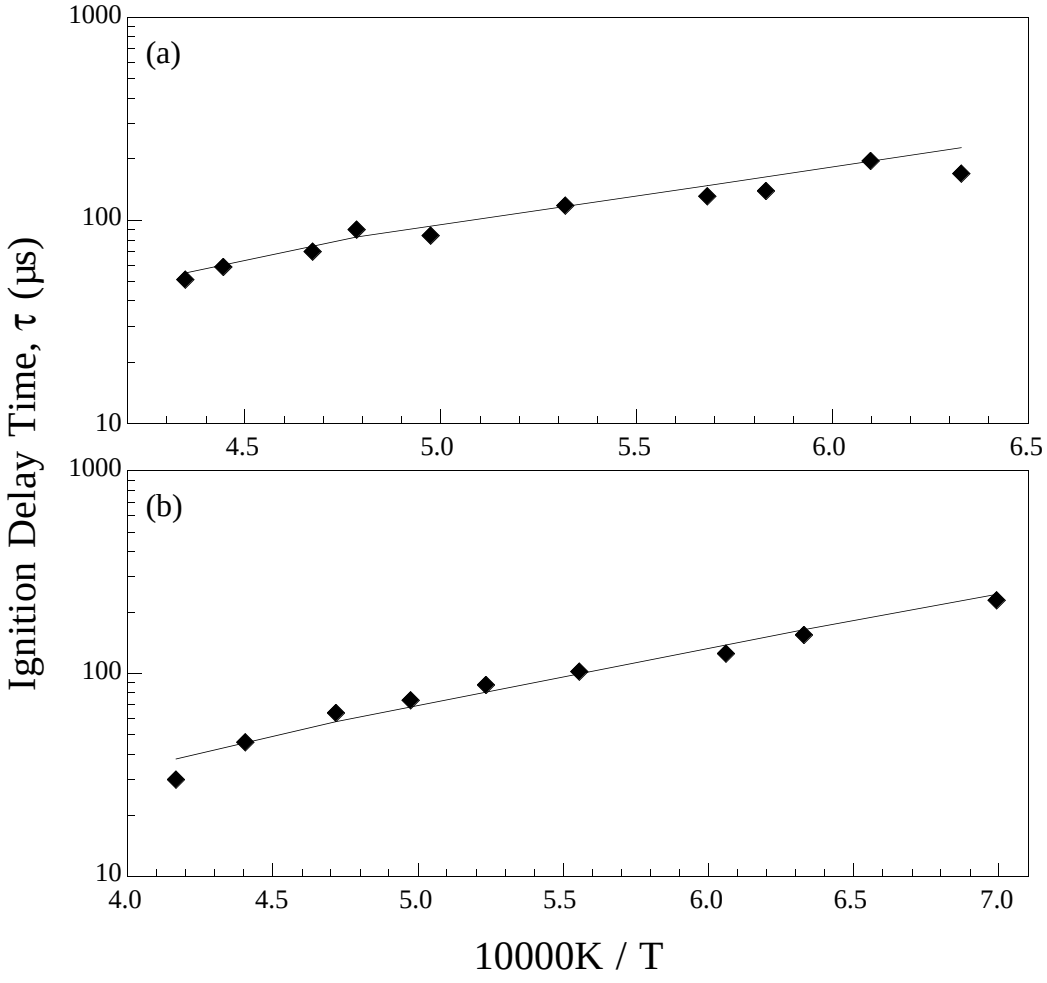

Figure 13. Comparison of experimental (symbols, Homer and Kistiakowsky, 1967) and computed (lines) ignition delay times behind reflected shock waves. The computational ignition delay was determined as the time corresponding to [CO] + [CO_2] equal to 10% of its final value. Mixture compositions (in argon): (a) 0.5%C_2H_2-0.8%O_2 (shock 21), and (b) 0.5%C_2H_2-1.0%O_2-0.5%H_2 (shock 22). See Table 2 for additional experimental conditions.

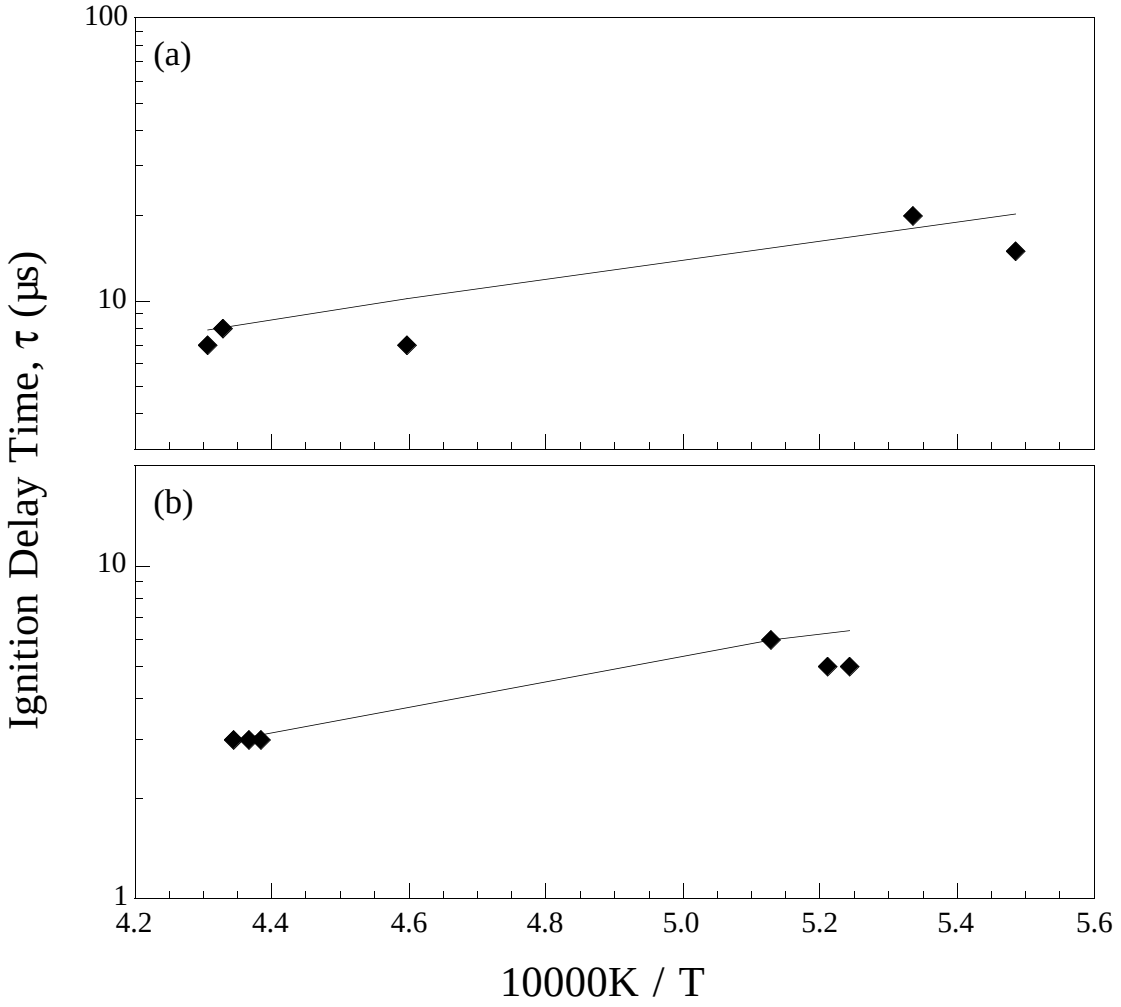

Figure 14. Comparison of experimental (symbols, Jachimowski, 1977) and computed (lines) ignition delay times in incident shock waves. The computational ignition delay was determined as the time corresponding to maximum [O][CO]. Mixture compositions (in argon): (a) 1%C_2H_2-3.75%O_2 (shock mixture 23), and (b) 1%C_2H_2-1%C_2H_4-5.5%O_2 (shock mixture 24). See Table 2 for additional experimental conditions.

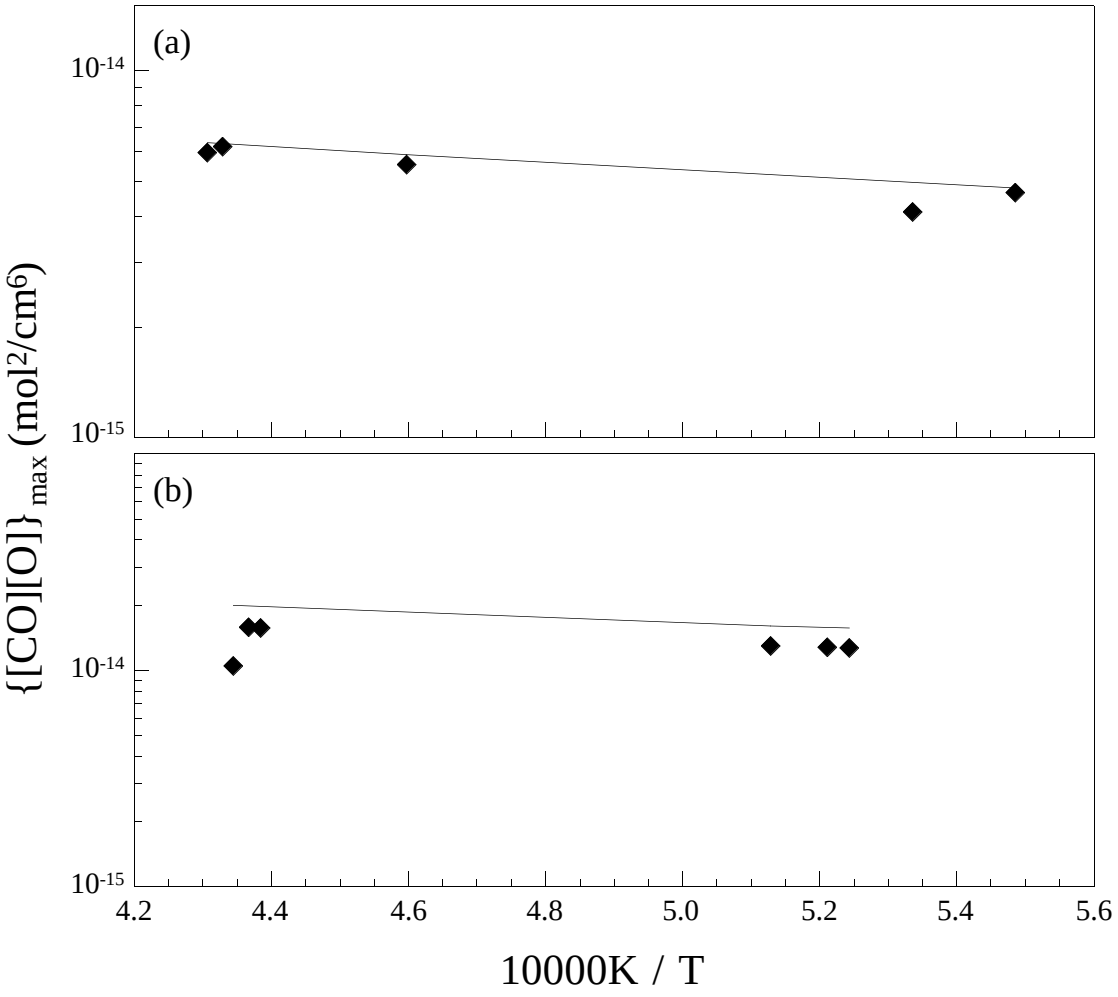

Figure 15. Comparison of experimental (symbols, Jachimowski, 1977) and computed (lines) maximum [O][CO]. Mixture compositions (in argon): (a) 1%C_2H_2-3.75%O_2 (shock mixture 23), and (b) 1%C_2H_2-1%C_2H_4-5.5%O_2 (shock mixture 24). See Table 2 for additional experimental conditions.

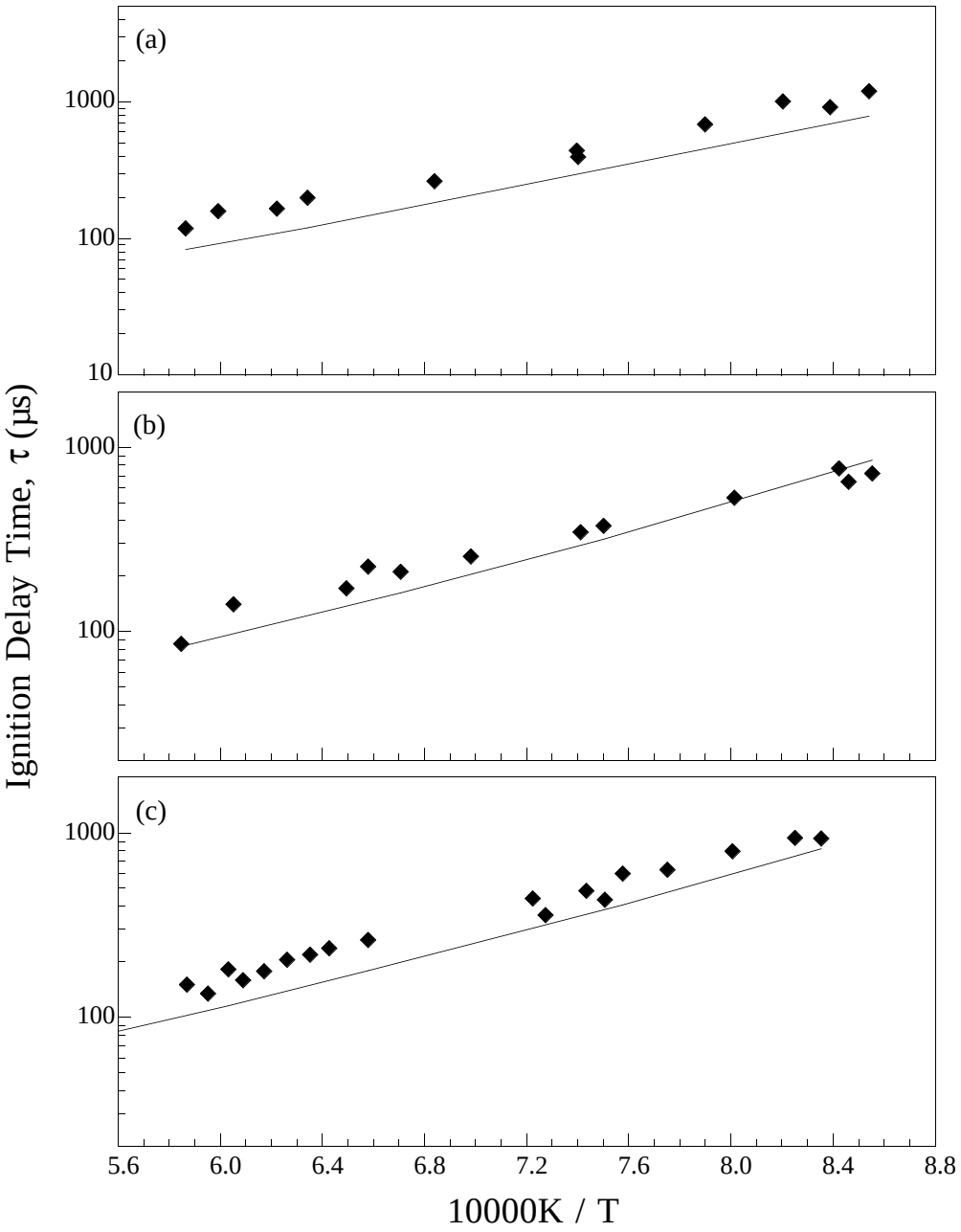

Figure 16. Comparison of experimental (symbols, Hidaka *et al.*, 1981) and computed (lines) ignition delay times behind reflected shock waves. The computational ignition delay was determined by the maximum pressure gradient. Mixture compositions (in argon): (a) 2%C_2H_2-2.5%O_2 (shock mixture 25), (b) 1%C_2H_2-3.5%O_2 (shock 26), and (c) 1%C_2H_2-2.5%O_2 (shock mixture 27). An estimated value of 0.6 atm was used for pressure in the simulation.

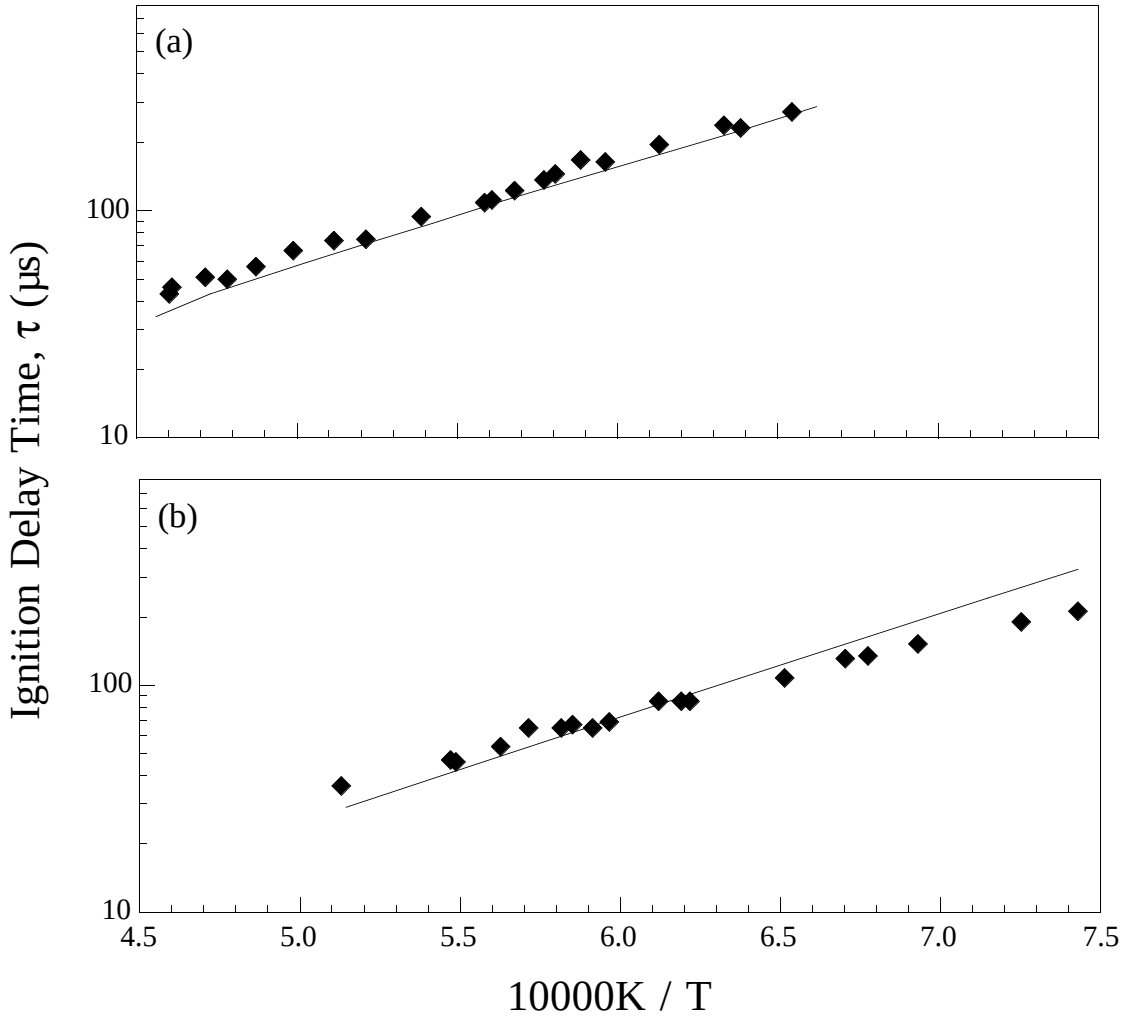

Figure 17. Comparison of experimental (symbols, Hidaka *et al.* 1984) and computed (lines) maximum ignition delay times in incident shock waves. The experimental and computational ignition were determined by the maximum laser-Schlieren density gradient. Shock mixtures (in argon): (28) $0.5\%C_2H_2$-$1.25\%O_2$ and (29) $0.5\%C_2H_2$-$5\%O_2$. See Table 2 for additional experimental conditions.

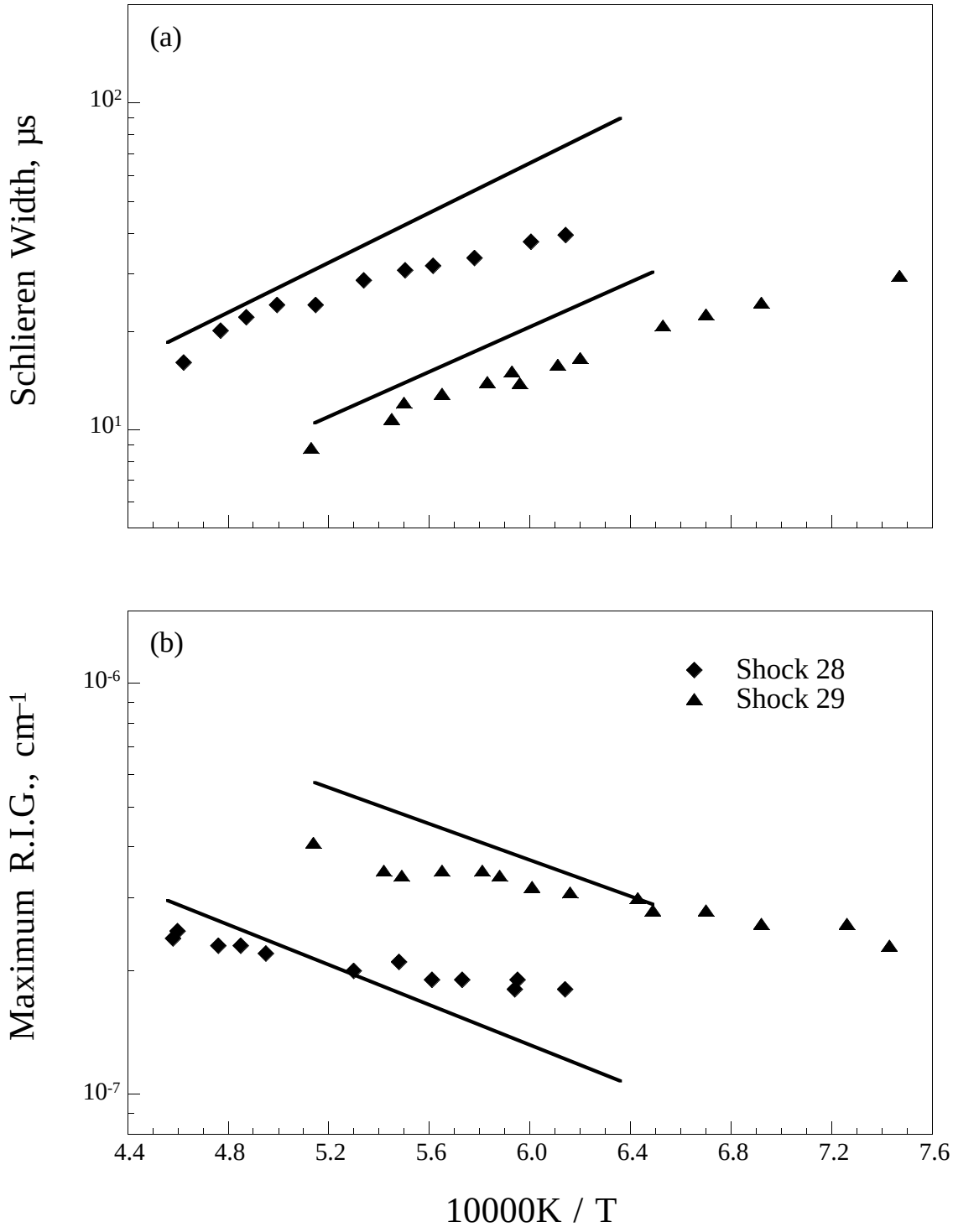

Figure 18. Comparison of experimental (symbols, Hwang *et al.* 1986) and computed (lines) (a) depth of refractive index gradients and (b) full width at half-depth of the refractive index gradient. Shock mixtures (in argon): (28) 0.5%C_2H_2-1.25%O_2 and (29) 0.5%C_2H_2-5%O_2. See Table 2 for additional experimental conditions.

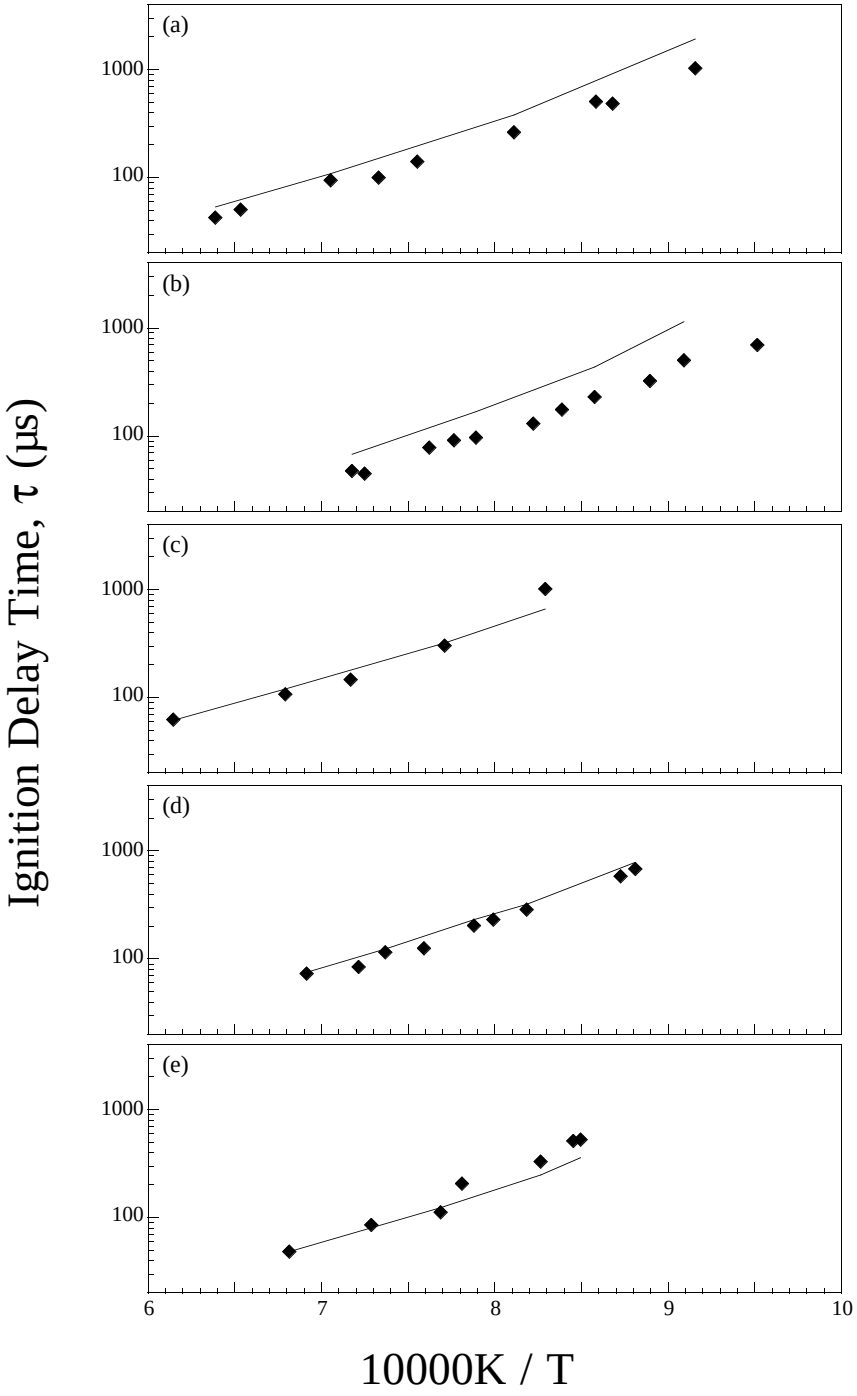

Figure 19. Comparison of experimental (symbols, Hidaka *et al.* 1996) and computed (lines) maximum ignition delay times behind reflected shock waves. The computational ignition was determined by the onset of CO_2 concentration rise. Shock mixtures (in argon): (30) 0.5%C_2H_2-2.54%O_2, (31) 1%C_2H_2-5%O_2, (32) 0.5%C_2H_2-1.25%O_2, (33) 1%C_2H_2-2.5%O_2, and (34) 2%C_2H_2-2.5%O_2. See Table 2 for additional experimental conditions.

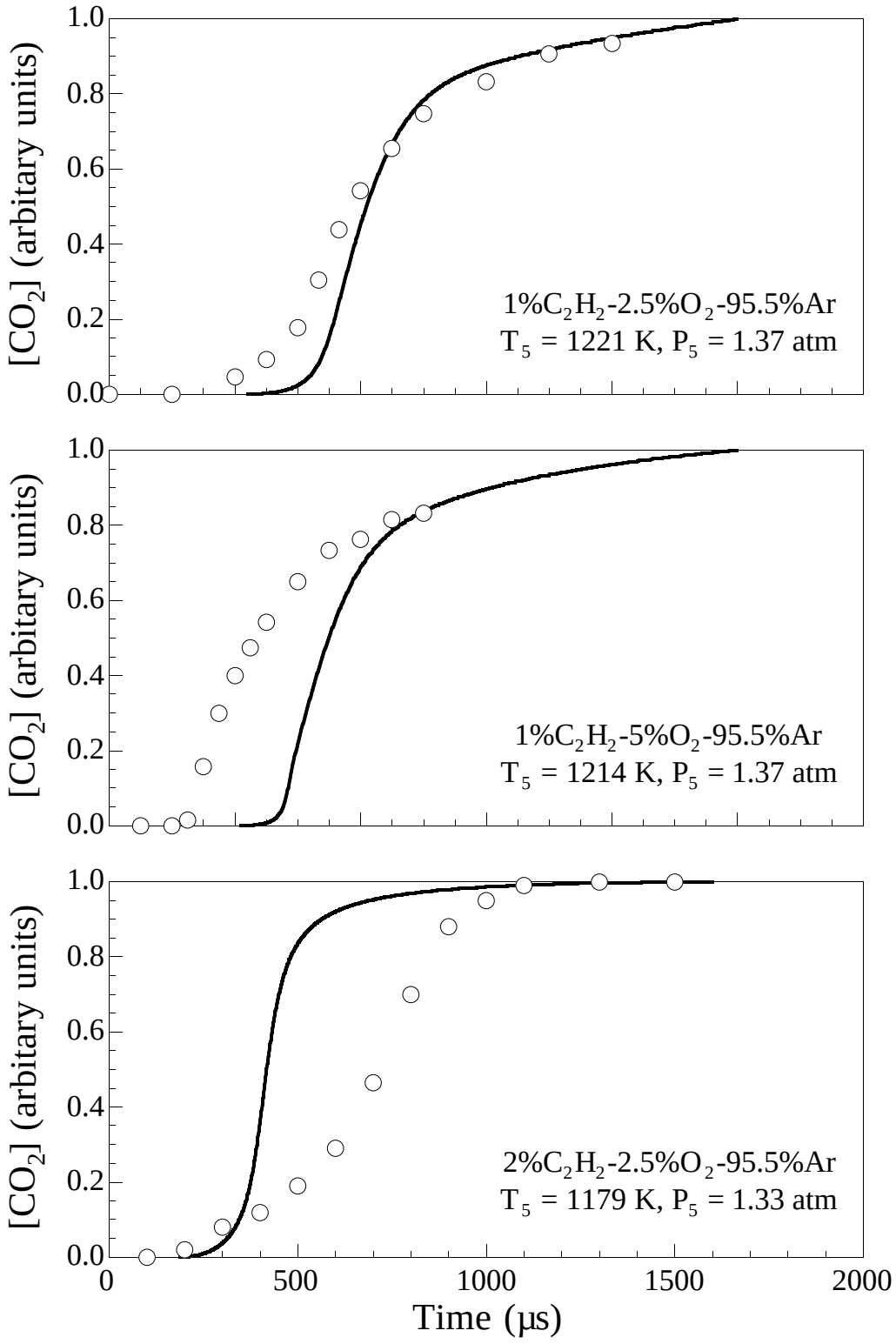

Figure 20. Comparison of experimental (symbols, Hidaka *et al.* 1996) and computed (lines) CO_2 profiles in three shock mixtures.

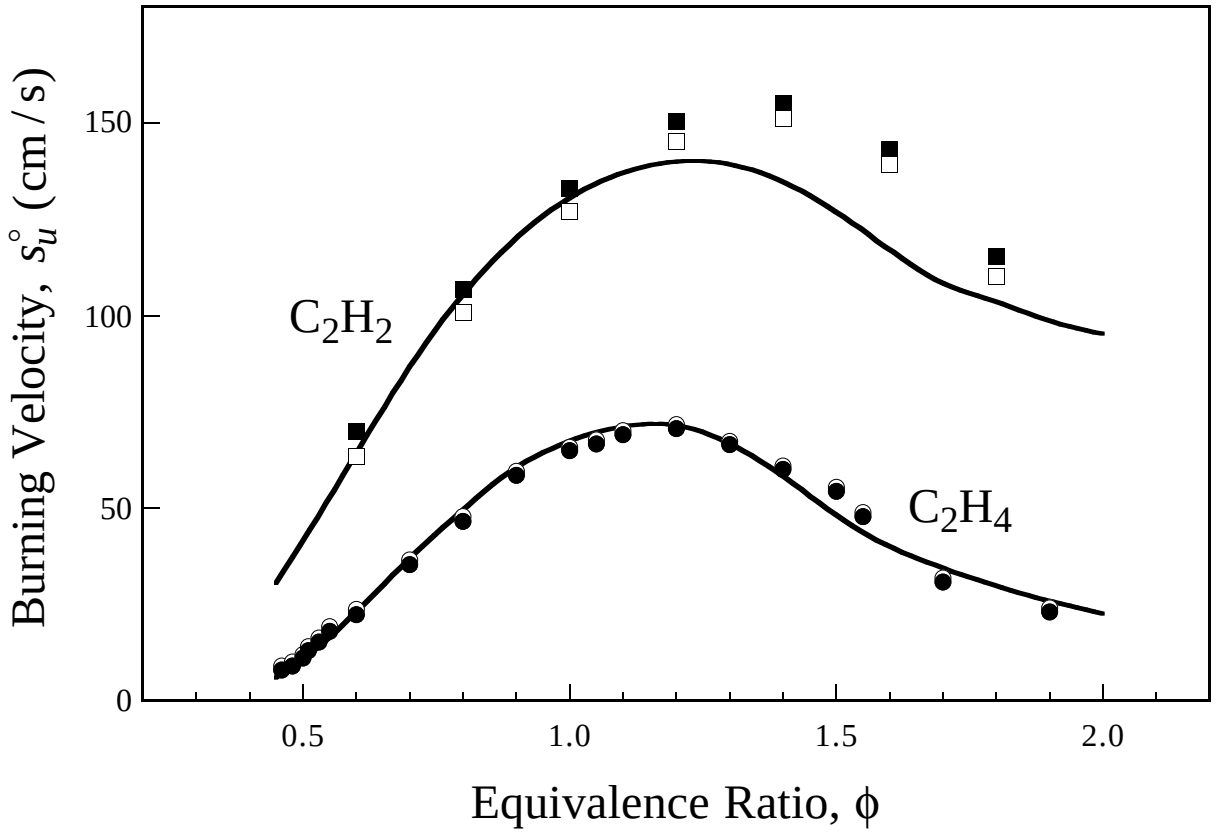

Figure 21. Comparison of measured (symbols, Egolfopoulos *et al.* 1990b) and computed (lines) laminar burning velocity of ethylene and acetylene in air at atmospheric pressure. Filled symbols: linearly extrapolated data, open symbols: nonlinearly extrapolated data.

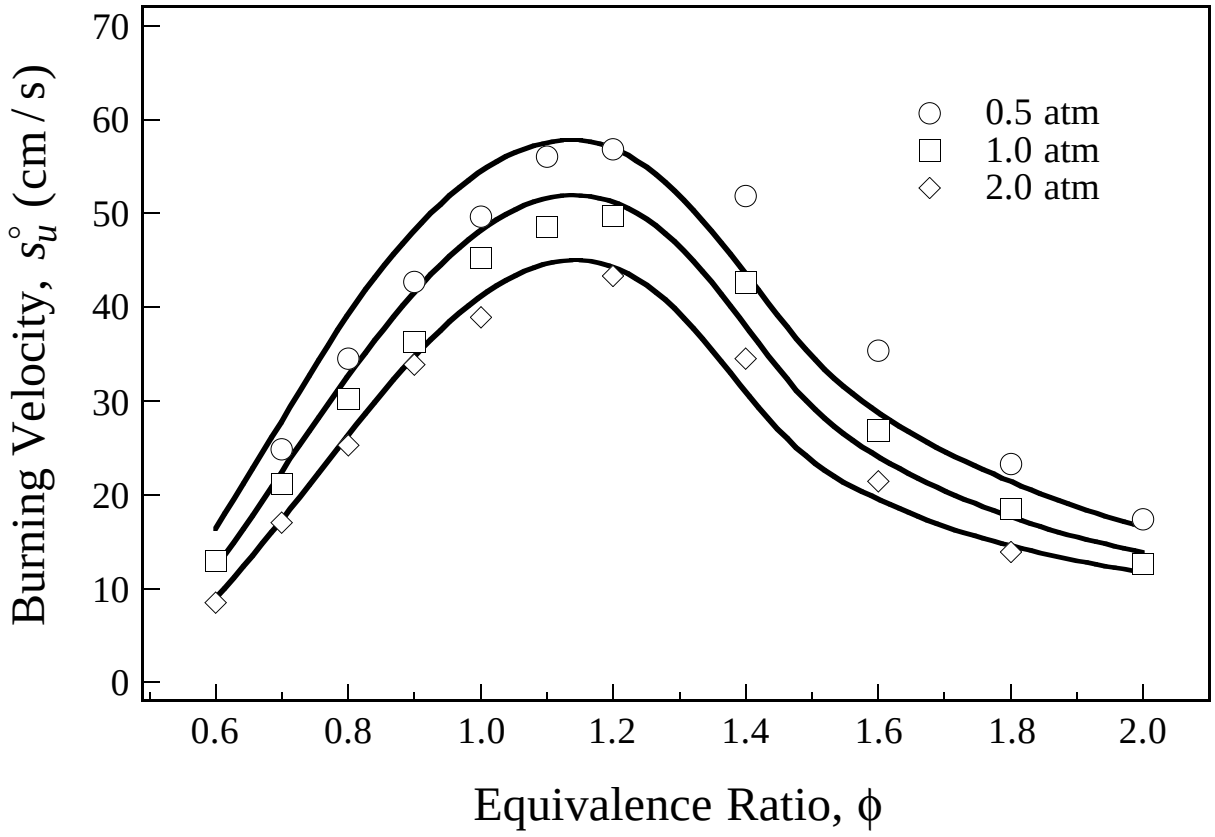

Figure 22. Comparison of measured (symbols, Egolfopoulos *et al.* 1990b) and computed (lines) laminar burning velocity of ethylene in a nitrogen diluted air (O_2/N_2=18/82).

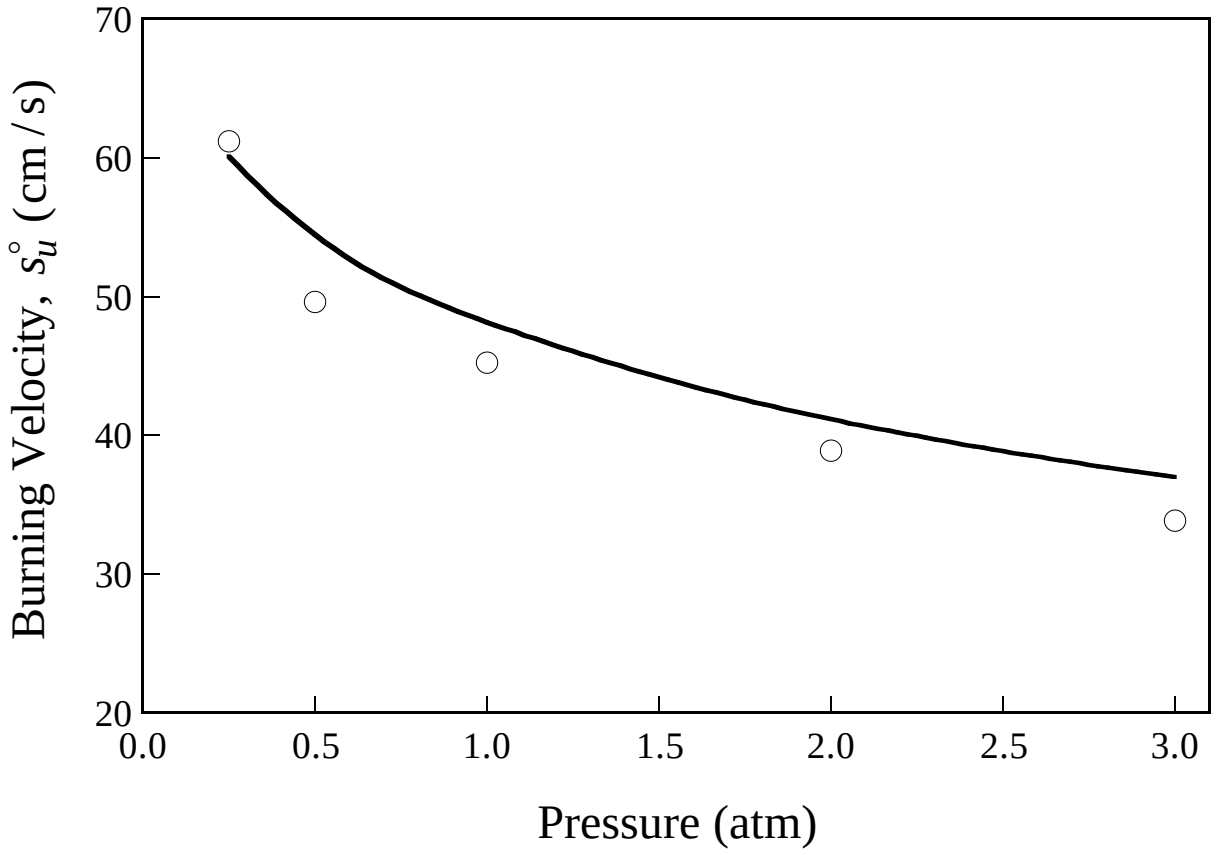

Figure 23. Comparison of measured (symbols, Egolfopoulos *et al.* 1990b) and computed (line) pressure variation of the laminar burning velocity of a stoichiometric mixture of ethylene in a nitrogen diluted air (O_2/N_2=18/82).

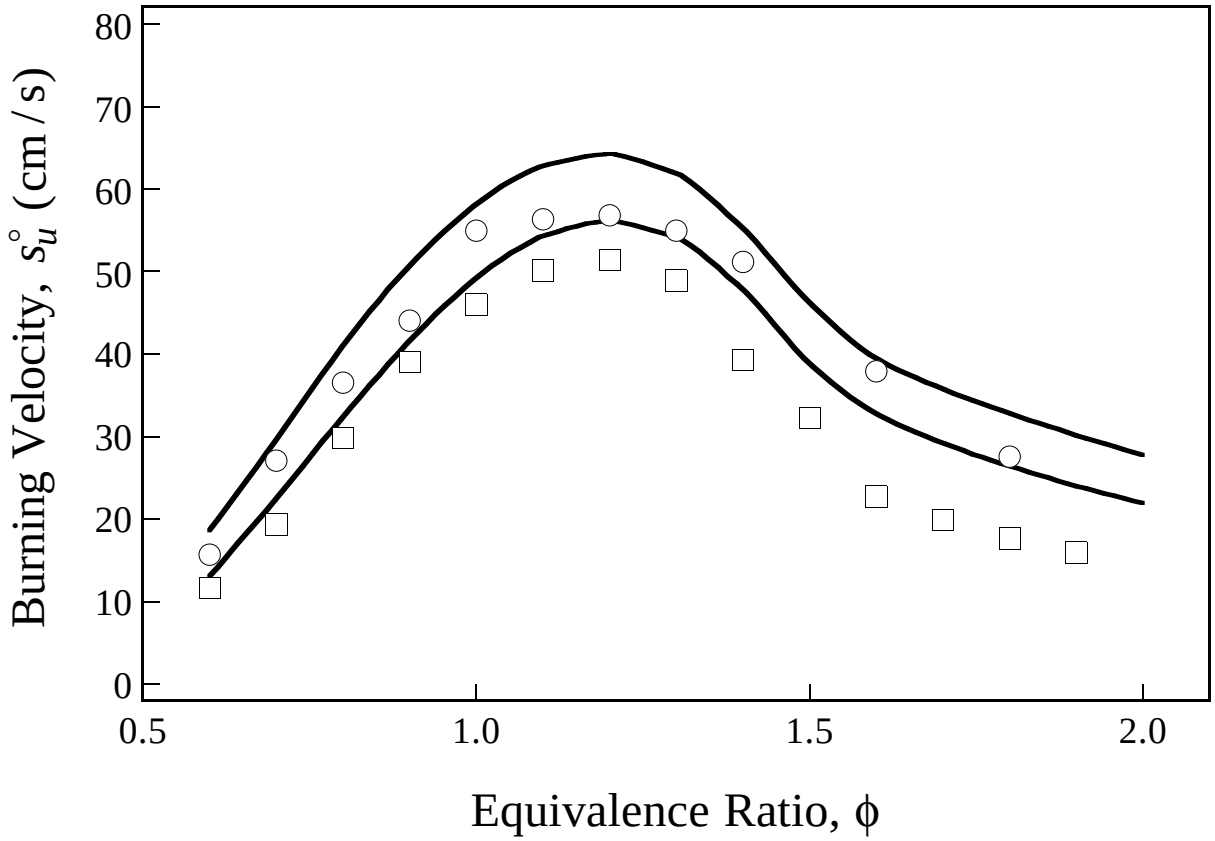

Figure 24. Comparison of measured (symbols, Egolfopoulos *et al.* 1990b) and computed (lines) laminar burning velocity of acetylene in a nitrogen diluted air (O_2/N_2=18/82).

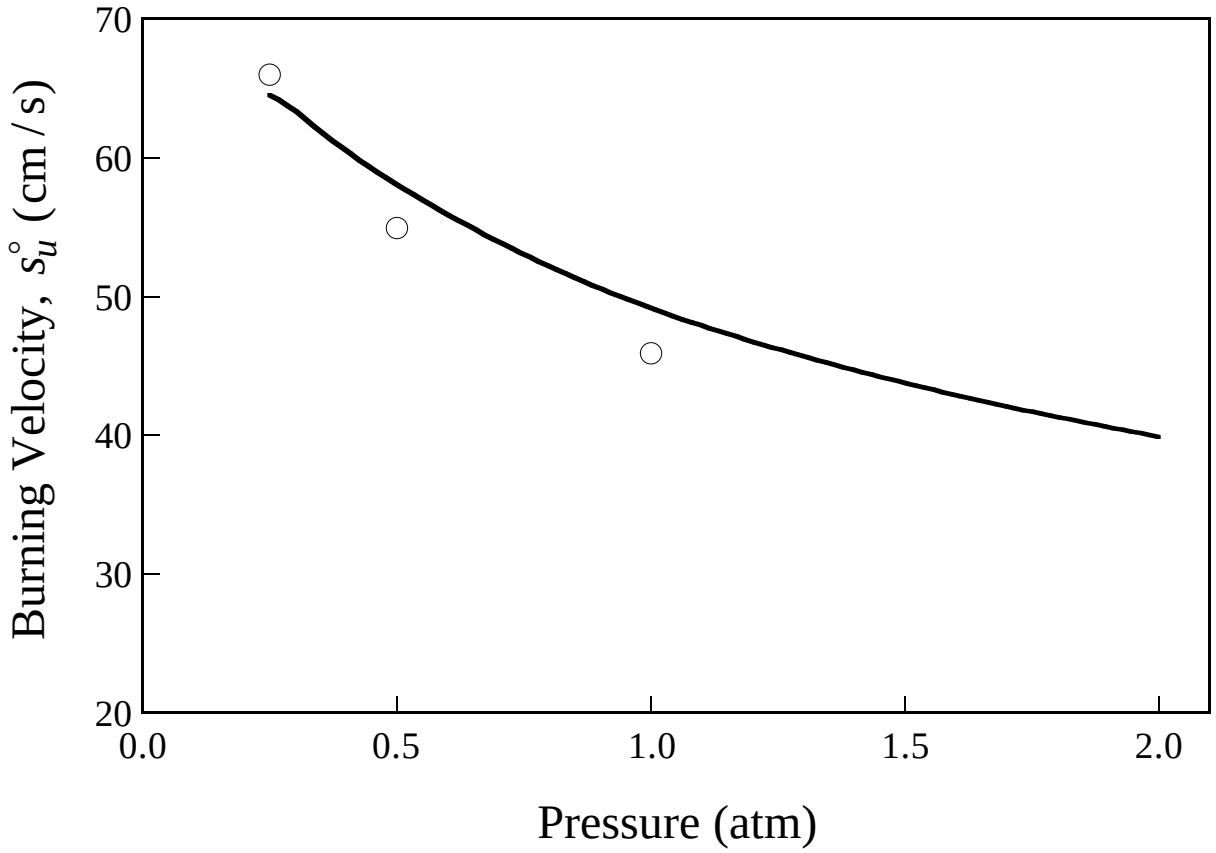

Figure 25. Comparison of measured (symbols, Egolfopoulos *et al.* 1990b) and computed (line) pressure variation of the laminar burning velocity of a stoichiometric mixture of acetylene in a nitrogen diluted air (O_2/N_2=18/82).

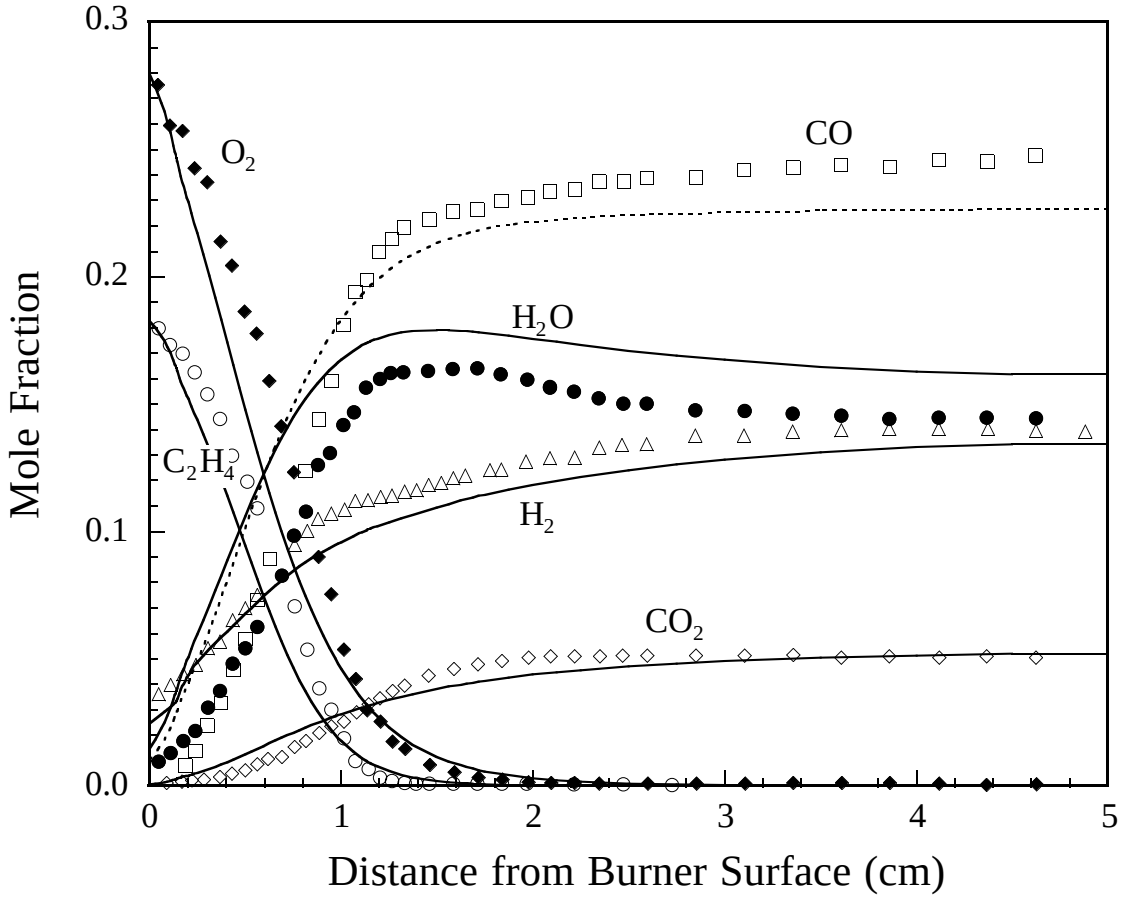

Figure 26. Experimental (Bhargava and Westmoreland, 1998a) and computed major species profiles of Flame 1 (p = 20 Torr, C_2H_4/O_2/50%Ar, ϕ = 1.9).

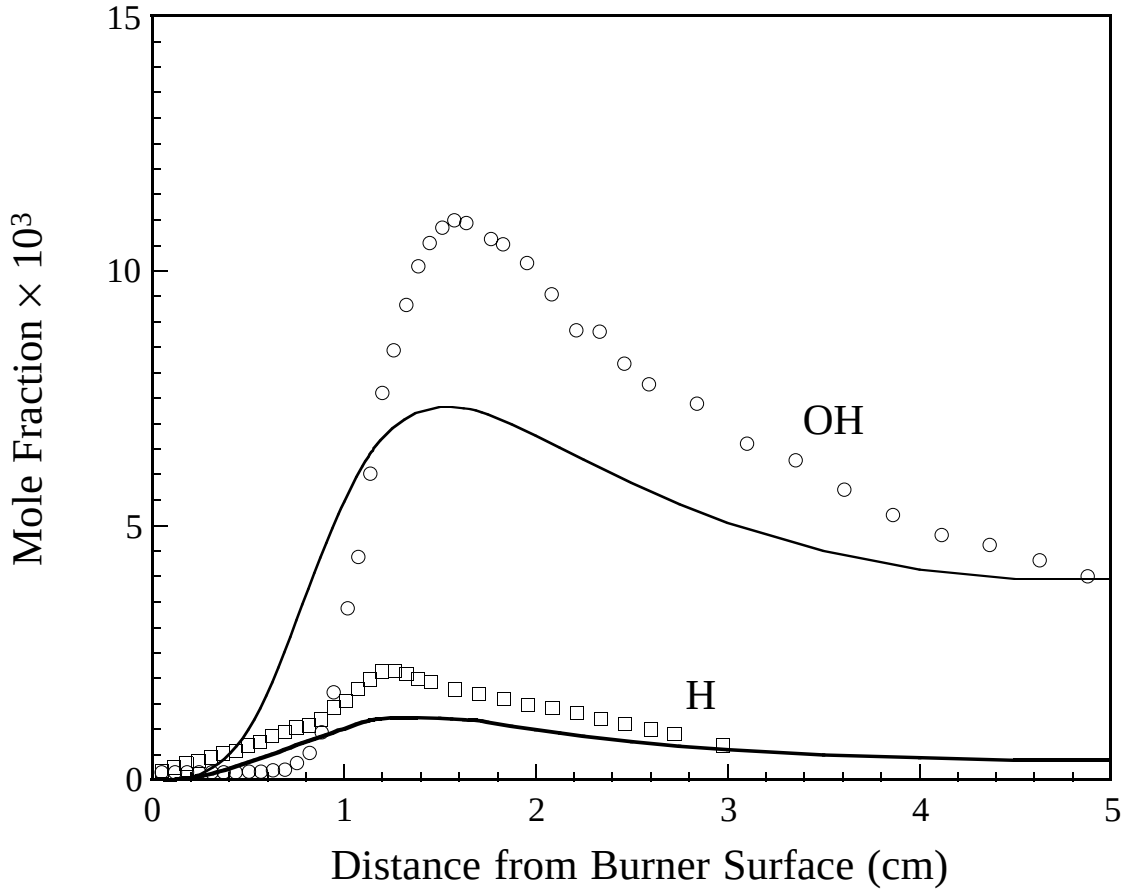

Figure 27. Experimental (Bhargava and Westmoreland, 1998a) and computed H and OH mole fraction profiles of Flame 1 (p = 20 Torr, C_2H_4/O_2/50%Ar, ϕ = 1.9).

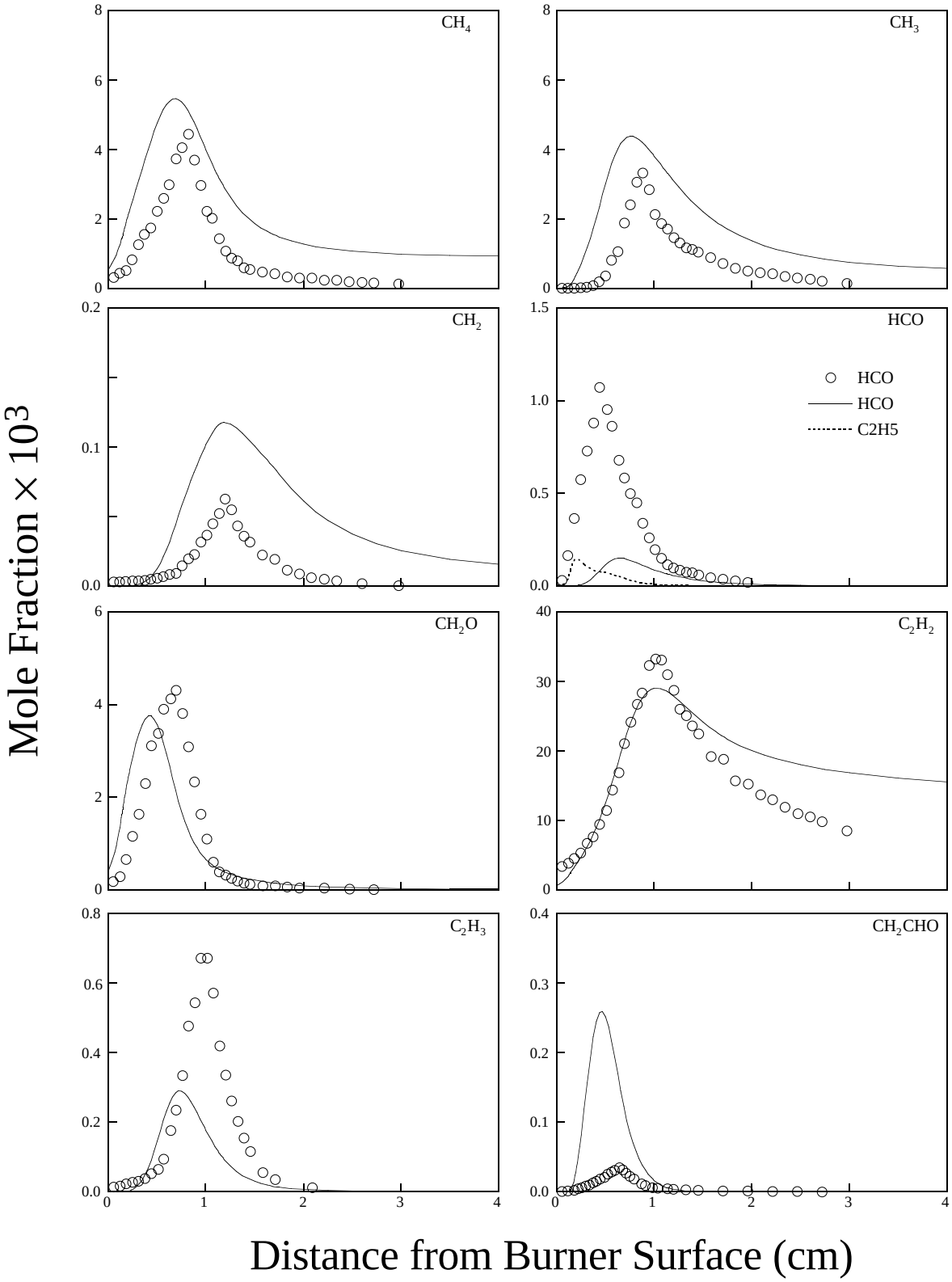

Figure 28. Experimental (Bhargava and Westmoreland, 1998a) and computed minor-species mole fraction profiles of Flame 1 (p = 20 Torr, C_2H_4/O_2/50%Ar, ϕ = 1.9).

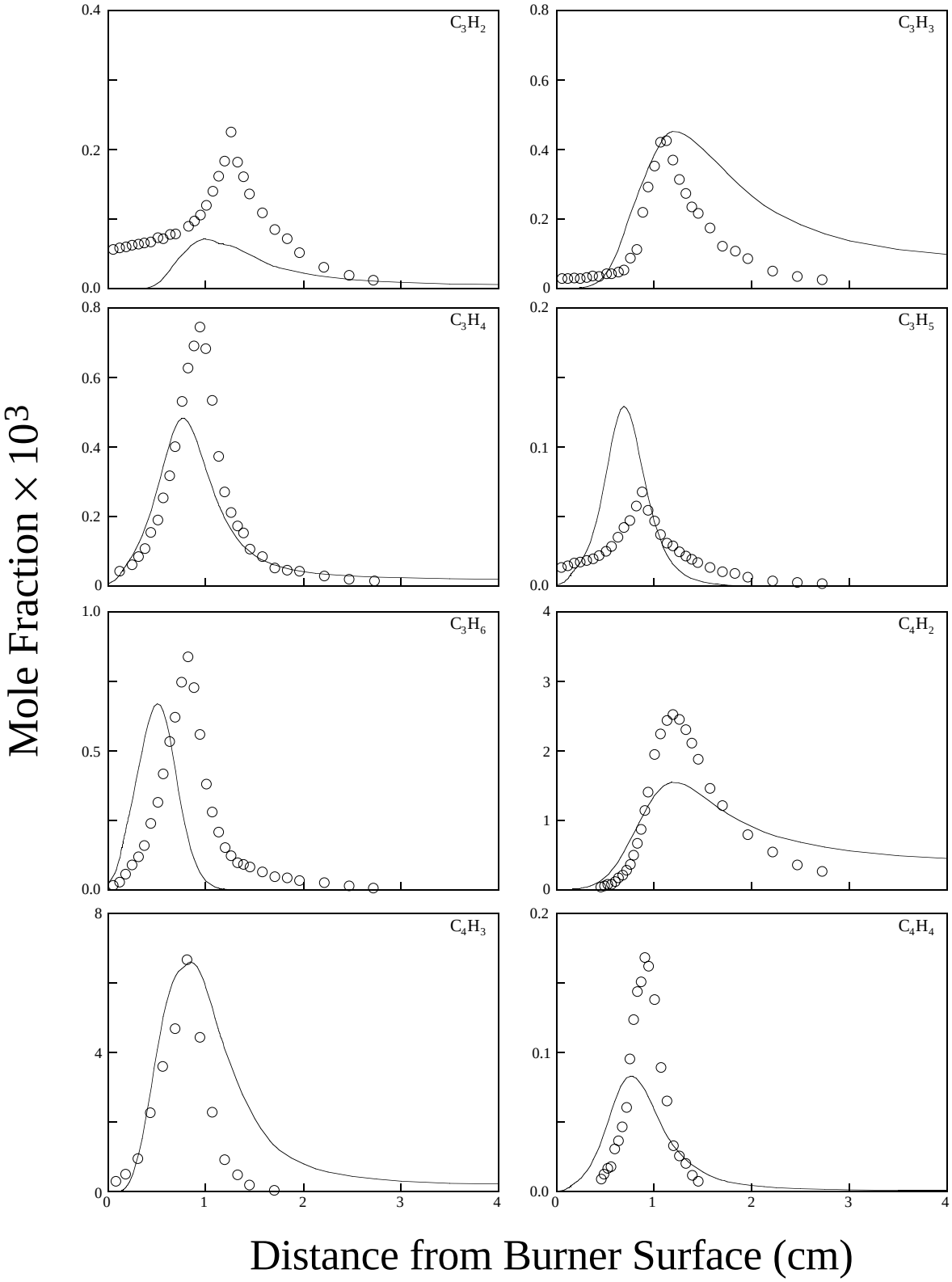

Figure 29. Experimental (Bhargava and Westmoreland, 1998a) and computed minor-species mole fraction profiles of Flame 1 (p = 20 Torr, C_2H_4/O_2/50%Ar, ϕ = 1.9).

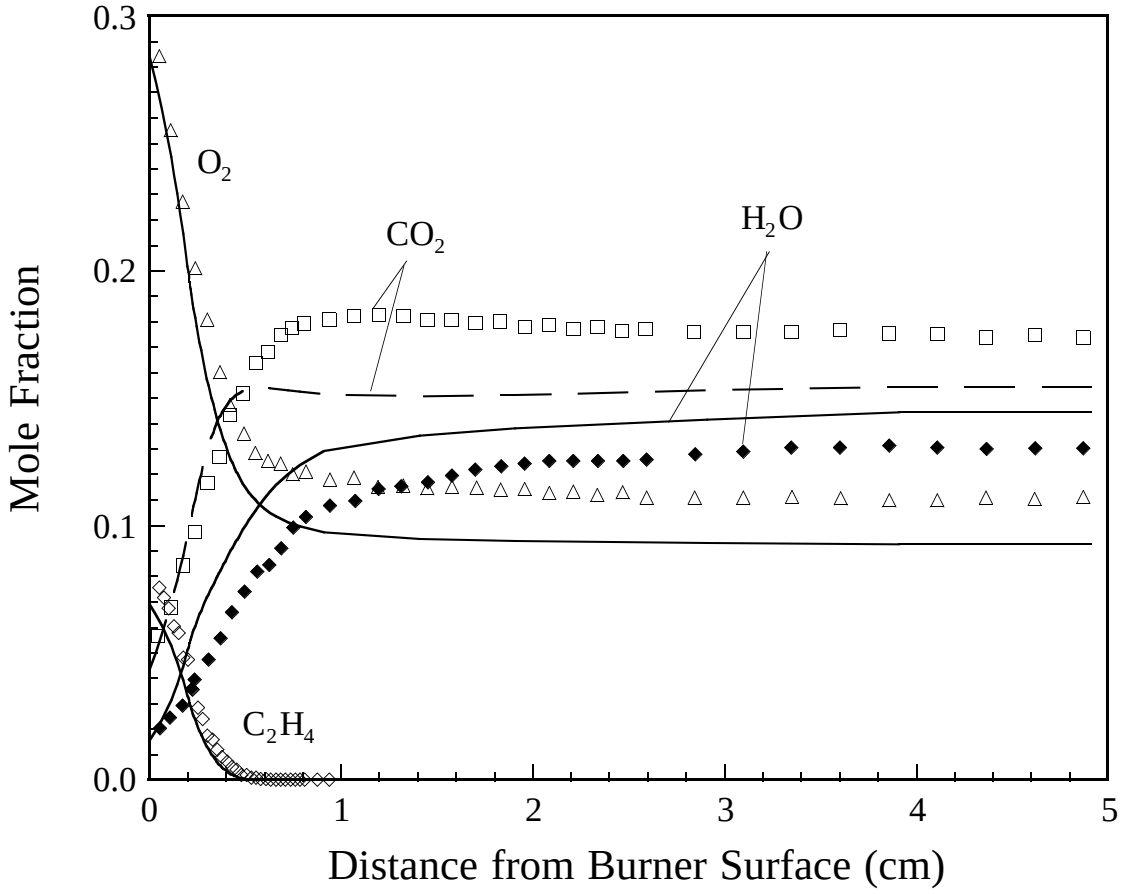

Figure 30. Experimental (Bhargava and Westmoreland, 1998b) and computed major species profiles of Flame 2 (p = 30 Torr, C_2H_4/O_2/56.9%Ar, ϕ = 0.75).

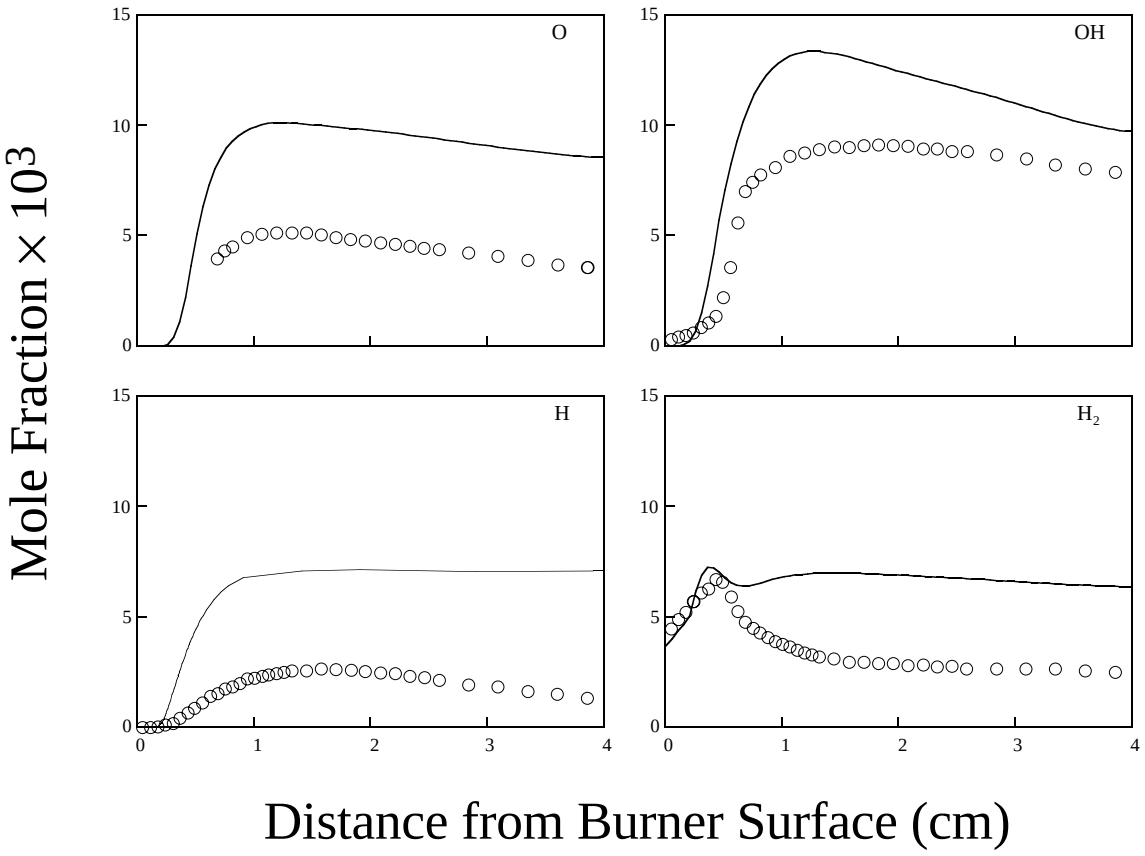

Figure 31. Experimental (Bhargava and Westmoreland, 1998b) and computed minor-species mole fraction profiles of Flame 2 (p = 30 Torr, C_2H_4/O_2/56.9%Ar, ϕ = 0.75).

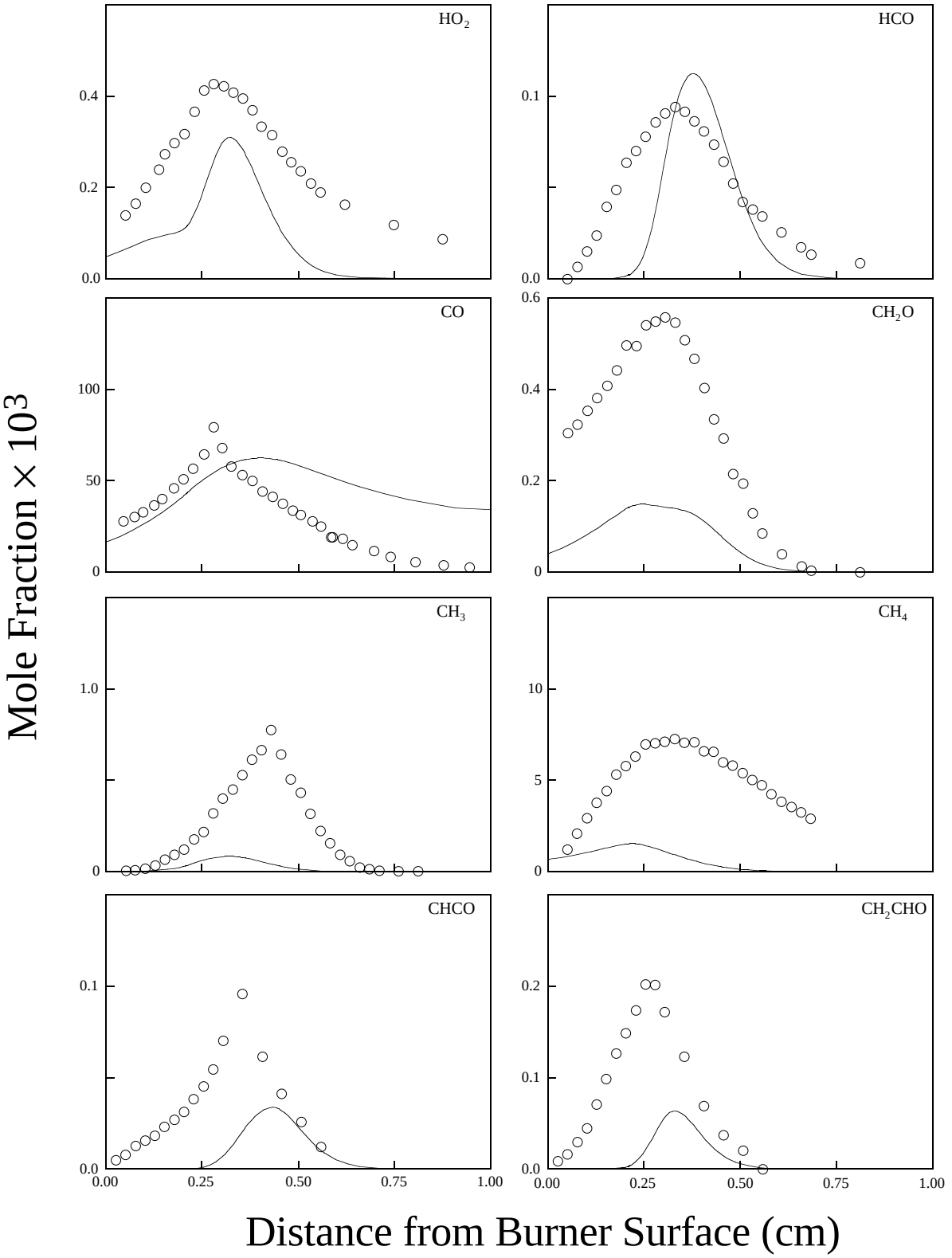

Figure 32. Experimental (Bhargava and Westmoreland, 1998b) and computed minor-species mole fraction profiles of Flame 2 (p = 30 Torr, C_2H_4/O_2/56.9%Ar, ϕ = 0.75).

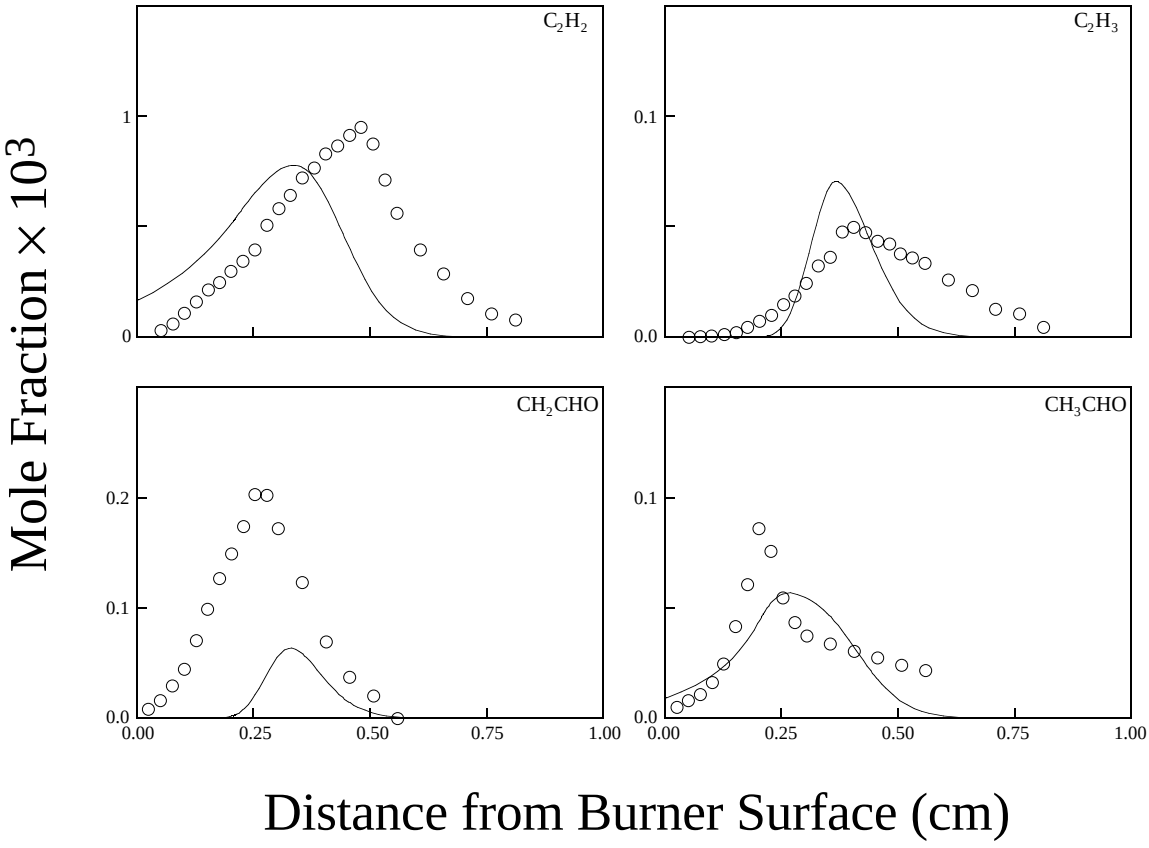

Figure 33. Experimental (Bhargava and Westmoreland, 1998b) and computed minor-species mole fraction profiles of Flame 2 (p = 30 Torr, C_2H_4/O_2/56.9%Ar, ϕ = 0.75).

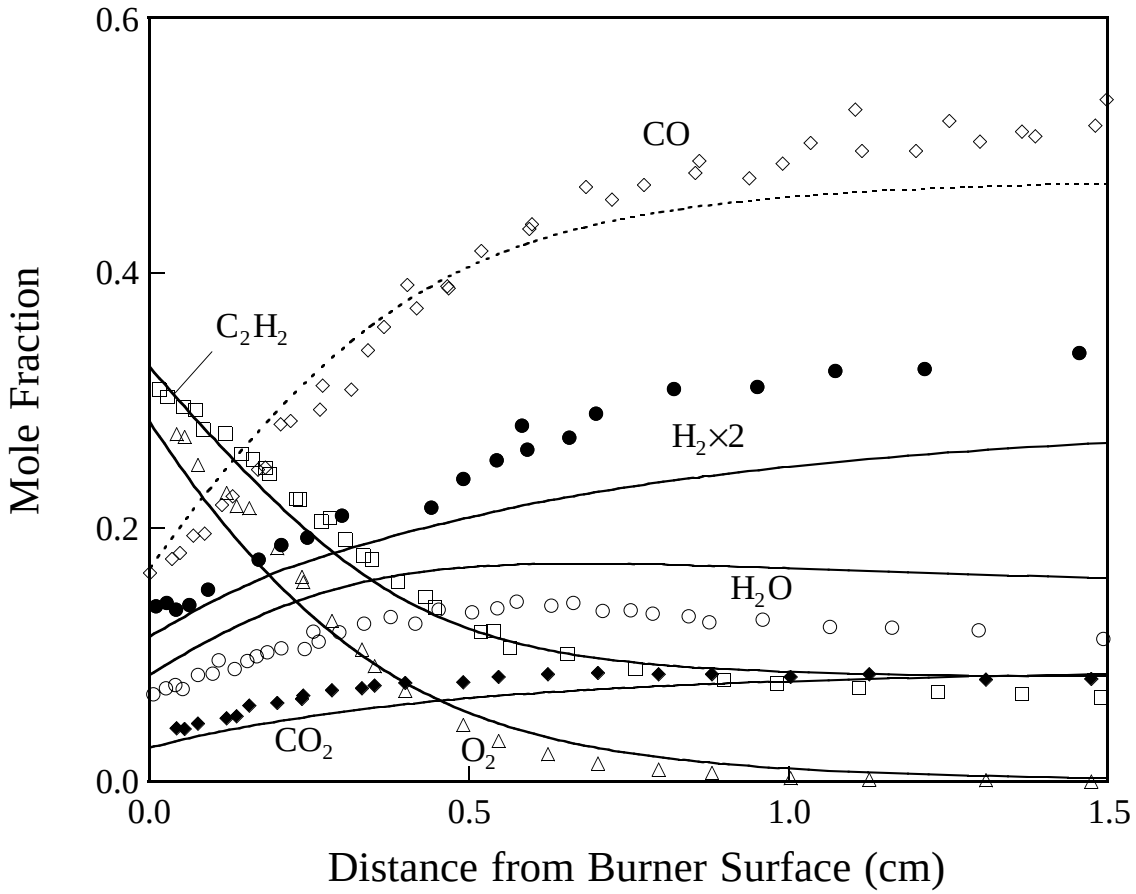

Figure 34. Experimental (Westmoreland *et al.*, 1986) and computed major species profiles of Flame 3 (p = 20 Torr, $C_2H_2/O_2/5\%Ar$, ϕ = 2.4).

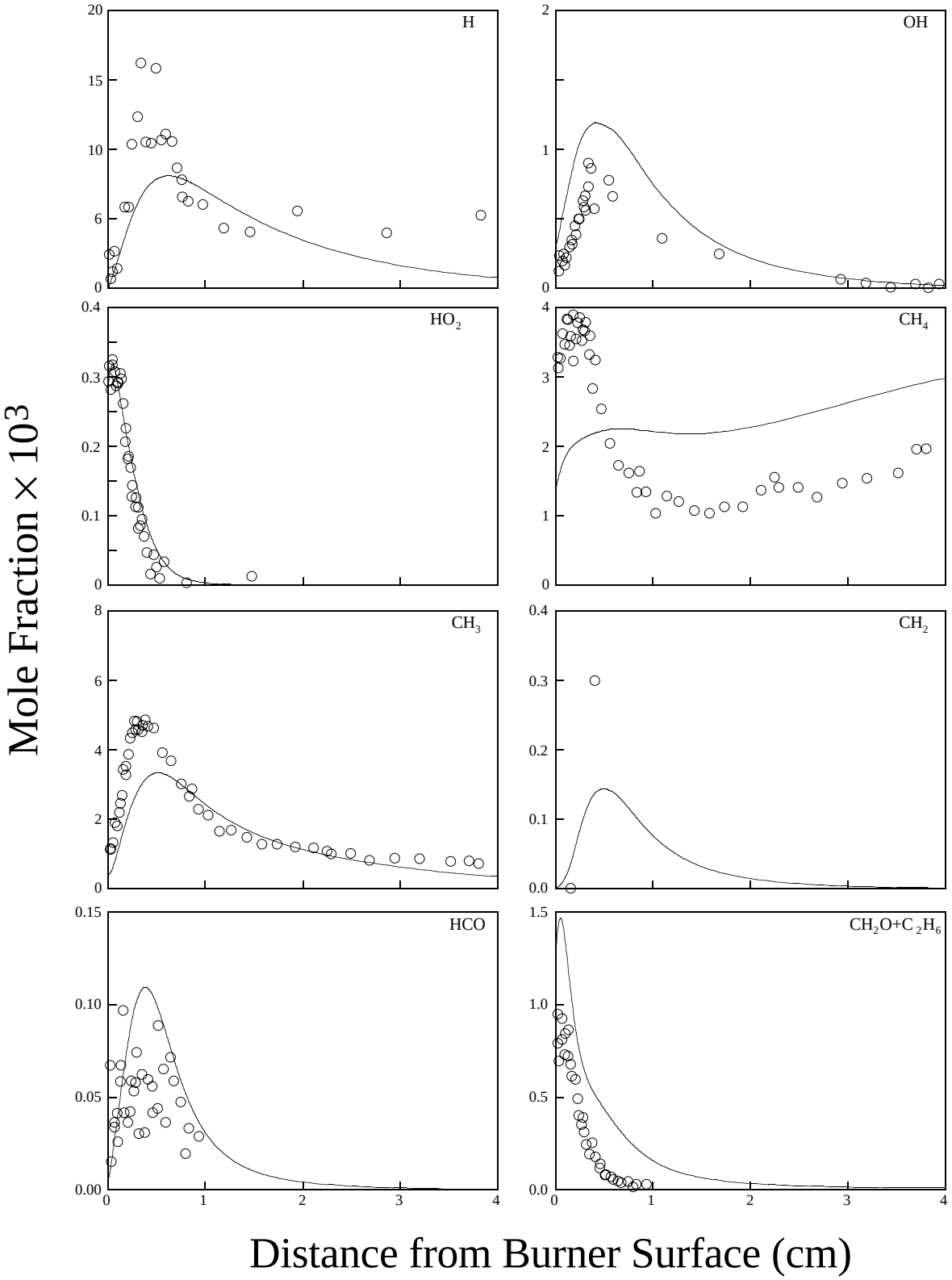

Figure 35. Experimental (Westmoreland *et al.*, 1986) and computed minor-species mole fraction profiles of Flame 3 (p = 20 Torr, $C_2H_2/O_2/5\%Ar$, ϕ = 2.4).

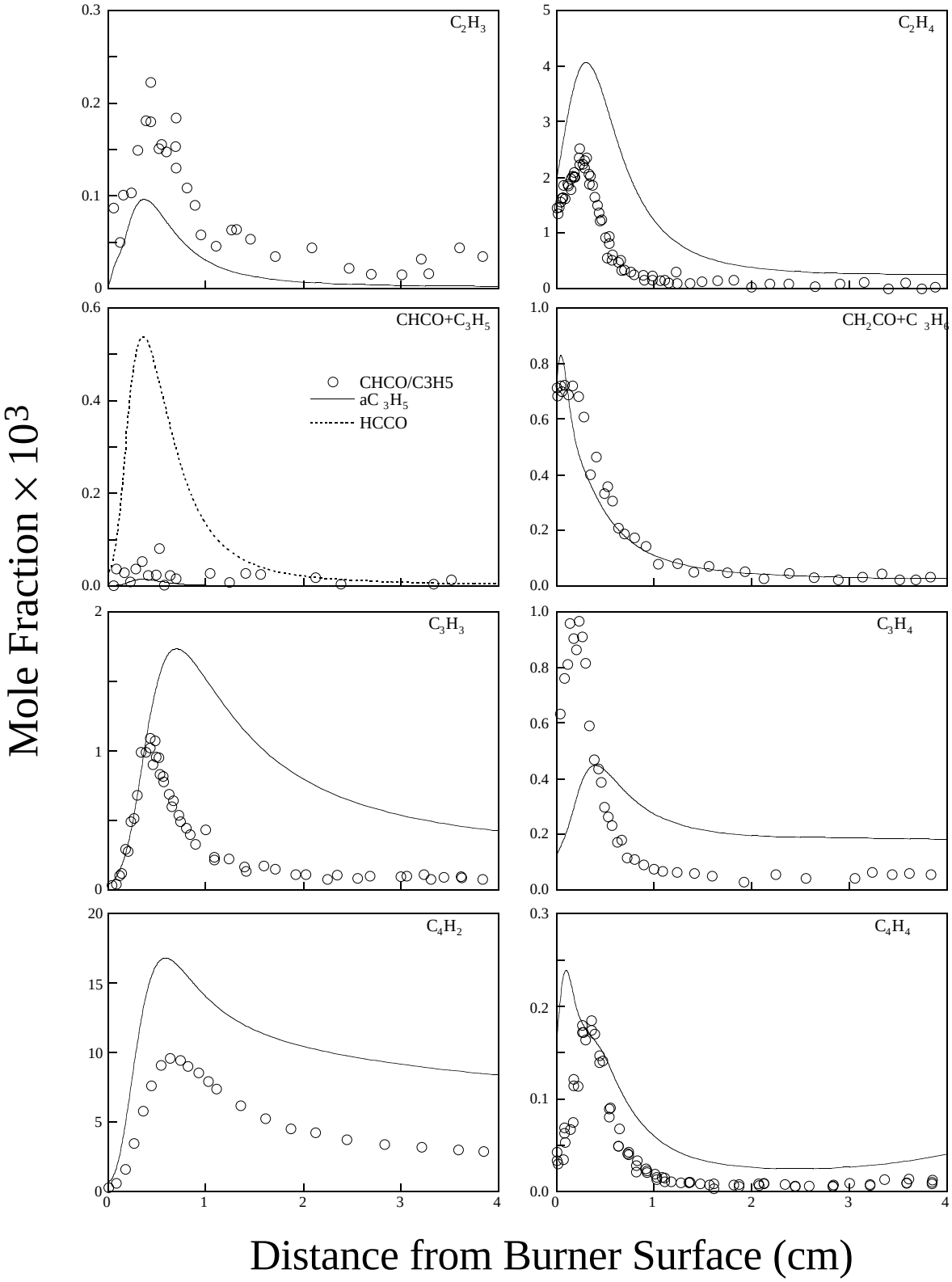

Figure 36. Experimental (Westmoreland *et al.*, 1986) and computed minor-species mole fraction profiles of Flame 3 (p = 20 Torr, $C_2H_2/O_2/5\%Ar$, ϕ = 2.4).

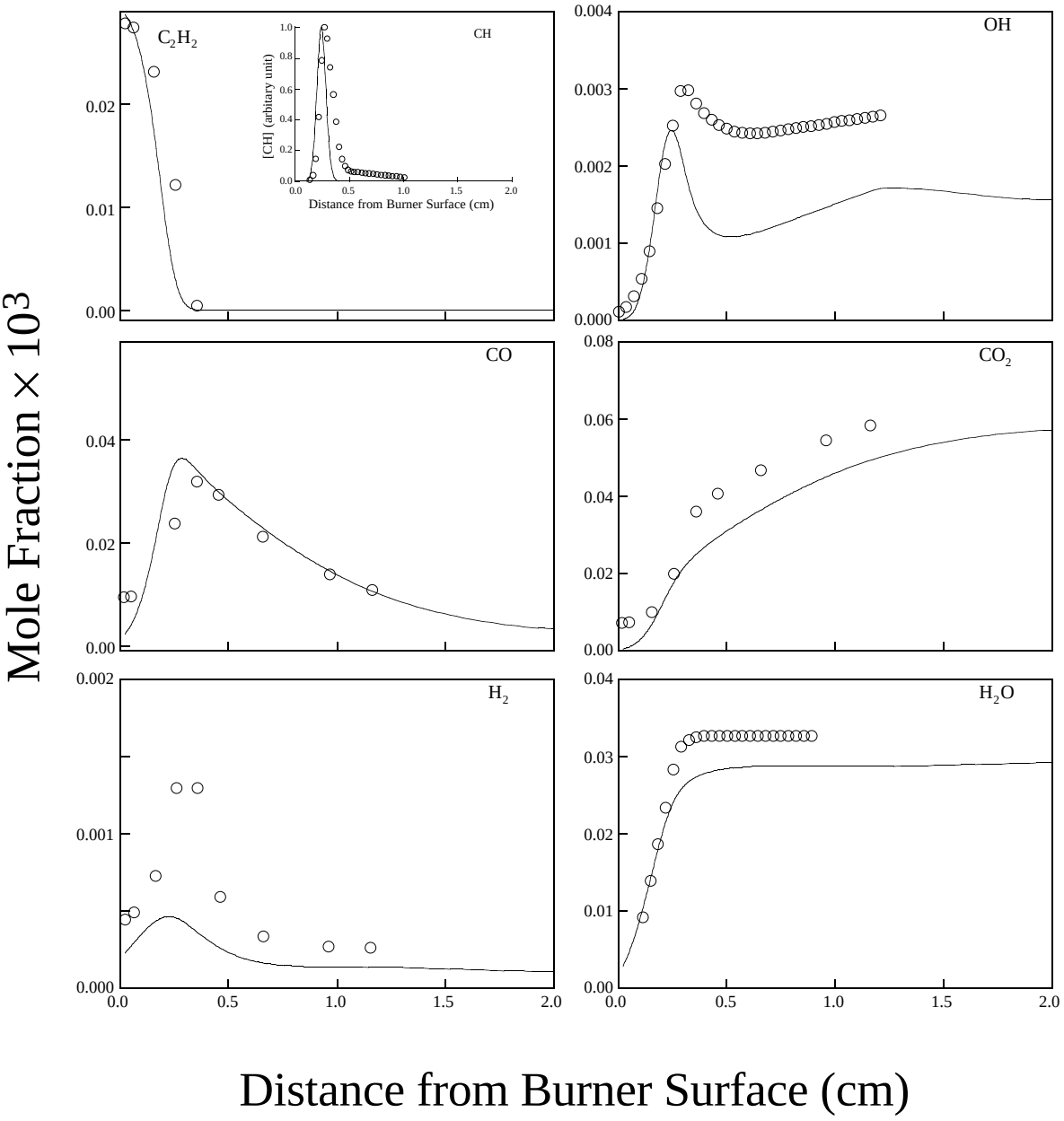

Figure 37. Experimental (Eberius *et al.* 73) and computed species mole fraction profiles of Flame 4 (p = 76 Torr, 3%C_2H_2/97%O_2).

Appendix A. A Comprehensive and Detailed Kinetic Model of Ethylene and Acetylene Oxidation at High Temperatures

SPECIES CONSIDERED

H2	H	O	O2	OH
H2O	HO2	H2O2	C	CH
CH2	CH2*	CH3	CH4	CO
CO2	HCO	CH2O	CH2OH	CH3O
CH3OH	C2H	C2H2	H2CC	C2H3
C2H4	C2H5	C2H6	HCCO	CH2CO
HCCOH	C2O	CH2CHO	CH3CHO	CH3CO
C3H2	C3H3	pC3H4	aC3H4	cC3H4
aC3H5	CH3CCH2	C3H6	C2H3CHO	C4H
C4H2	H2C4O	n-C4H3	i-C4H3	C4H4
AR	N2			

REACTIONS CONSIDERED			(k = A T**b exp(-E/RT)) A	b	E
1. H+O2=O+OH			8.30E+13	0.0	14413.0
2. O+H2=H+OH			5.00E+04	2.7	6290.0
3. OH+H2=H+H2O			2.16E+08	1.5	3430.0
4. OH+OH=O+H2O			3.57E+04	2.4	-2110.0
5. H+H+M=H2+M			1.00E+18	-1.0	0.0
H2	Enhanced by	0.000E+00			
H2O	Enhanced by	0.000E+00			
CH4	Enhanced by	2.000E+00			
CO2	Enhanced by	0.000E+00			
C2H6	Enhanced by	3.000E+00			
AR	Enhanced by	6.300E-01			
C2H2	Enhanced by	3.000E+00			
C2H4	Enhanced by	3.000E+00			
6. H+H+H2=H2+H2			9.00E+16	-0.6	0.0
7. H+H+H2O=H2+H2O			6.00E+19	-1.2	0.0
8. H+H+CO2=H2+CO2			5.50E+20	-2.0	0.0
9. H+OH+M=H2O+M			0.22E+23	-2.0	0.0
H2	Enhanced by	7.300E-01			
H2O	Enhanced by	3.650E+00			
CH4	Enhanced by	2.000E+00			
C2H6	Enhanced by	3.000E+00			
AR	Enhanced by	3.800E-01			
C2H2	Enhanced by	3.000E+00			
C2H4	Enhanced by	3.000E+00			
10. O+H+M=OH+M			5.00E+17	-1.0	0.0
H2	Enhanced by	2.000E+00			
H2O	Enhanced by	6.000E+00			
CH4	Enhanced by	2.000E+00			
CO	Enhanced by	1.500E+00			

Units are in cal, mol, s, and cm.

```
       CO2              Enhanced by    2.000E+00
       C2H6             Enhanced by    3.000E+00
       AR               Enhanced by    7.000E-01
       C2H2             Enhanced by    3.000E+00
       C2H4             Enhanced by    3.000E+00
11. O+O+M=O2+M                                     1.20E+17   -1.0        0.0
       H2               Enhanced by    2.400E+00
       H2O              Enhanced by    1.540E+01
       CH4              Enhanced by    2.000E+00
       CO               Enhanced by    1.750E+00
       CO2              Enhanced by    3.600E+00
       C2H6             Enhanced by    3.000E+00
       AR               Enhanced by    8.300E-01
       C2H2             Enhanced by    3.000E+00
       C2H4             Enhanced by    3.000E+00
12. H+O2+M=HO2+M                                   2.80E+18   -0.9        0.0
       O2               Enhanced by    0.000E+00
       H2O              Enhanced by    0.000E+00
       CO               Enhanced by    7.500E-01
       CO2              Enhanced by    1.500E+00
       C2H6             Enhanced by    1.500E+00
       N2               Enhanced by    0.000E+00
       AR               Enhanced by    0.000E+00
       C2H2             Enhanced by    3.000E+00
       C2H4             Enhanced by    3.000E+00
13. H+O2+O2=HO2+O2                                 3.00E+20   -1.7        0.0
14. H+O2+H2O=HO2+H2O                               1.65E+19   -0.8        0.0
15. H+O2+N2=HO2+N2                                 2.60E+19   -1.2        0.0
16. H+O2+AR=HO2+AR                                 7.00E+17   -0.8        0.0
17. OH+OH(+M)=H2O2(+M)                             7.40E+13   -0.4        0.0
    Low pressure limit:  0.23000E+19 -0.90000E+00 -0.17000E+04
    TROE centering:      0.73460E+00  0.94000E+02  0.17560E+04  0.51820E+04
       H2               Enhanced by    2.000E+00
       H2O              Enhanced by    6.000E+00
       CH4              Enhanced by    2.000E+00
       CO               Enhanced by    1.500E+00
       CO2              Enhanced by    2.000E+00
       C2H6             Enhanced by    3.000E+00
       AR               Enhanced by    7.000E-01
       C2H2             Enhanced by    3.000E+00
       C2H4             Enhanced by    3.000E+00
18. HO2+H=O+H2O                                    3.97E+12    0.0      671.0
19. HO2+H=O2+H2                                    1.66E+13    0.0      820.0
20. HO2+H=OH+OH                                    7.08E+13    0.0      300.0
21. HO2+O=OH+O2                                    2.00E+13    0.0        0.0
22. HO2+OH=O2+H2O                                  4.64E+13    0.0     -500.0
23. HO2+HO2=O2+H2O2                                1.30E+11    0.0    -1630.0
    Declared duplicate reaction...
24. HO2+HO2=O2+H2O2                                4.20E+14    0.0    12000.0
    Declared duplicate reaction...
25. H2O2+H=HO2+H2                                  1.21E+07    2.0     5200.0
26. H2O2+H=OH+H2O                                  1.00E+13    0.0     3600.0
27. H2O2+O=OH+HO2                                  9.63E+06    2.0     4000.0
28. H2O2+OH=HO2+H2O                                1.75E+12    0.0      320.0
    Declared duplicate reaction...
29. H2O2+OH=HO2+H2O                                5.80E+14    0.0     9560.0
    Declared duplicate reaction...
30. CO+O+M=CO2+M                                   6.02E+14    0.0     3000.0
       H2               Enhanced by    2.000E+00
       O2               Enhanced by    6.000E+00
       H2O              Enhanced by    6.000E+00
       CH4              Enhanced by    2.000E+00
       CO               Enhanced by    1.500E+00
       CO2              Enhanced by    3.500E+00
```

```
      C2H6              Enhanced by    3.000E+00
      AR                Enhanced by    5.000E-01
      C2H2              Enhanced by    3.000E+00
      C2H4              Enhanced by    3.000E+00
31. CO+OH=CO2+H                                    4.76E+07    1.2       70.0
32. CO+H2(+M)=CH2O(+M)                             4.30E+07    1.5    79600.0
    Low pressure limit:  0.50700E+28 -0.34200E+01  0.84350E+05
    TROE centering:      0.93200E+00  0.19700E+03  0.15400E+04  0.10300E+05
      H2                Enhanced by    2.000E+00
      H2O               Enhanced by    6.000E+00
      CH4               Enhanced by    2.000E+00
      CO                Enhanced by    1.500E+00
      CO2               Enhanced by    2.000E+00
      C2H6              Enhanced by    3.000E+00
      AR                Enhanced by    7.000E-01
      C2H2              Enhanced by    3.000E+00
      C2H4              Enhanced by    3.000E+00
33. CO+O2=CO2+O                                    2.50E+12    0.0    47800.0
34. CO+HO2=CO2+OH                                  1.50E+14    0.0    23600.0
35. C+OH=CO+H                                      5.00E+13    0.0        0.0
36. C+O2=CO+O                                      5.80E+13    0.0      576.0
37. CH+H=C+H2                                      1.10E+14    0.0        0.0
38. CH+O=CO+H                                      5.70E+13    0.0        0.0
39. CH+OH=HCO+H                                    3.00E+13    0.0        0.0
40. CH+H2=CH2+H                                    1.11E+08    1.8     1670.0
41. CH+H2O=CH2O+H                                  5.71E+12    0.0     -755.0
42. CH+O2=HCO+O                                    3.30E+13    0.0        0.0
43. CH+CO(+M)=HCCO(+M)                             5.00E+13    0.0        0.0
    Low pressure limit:  0.26900E+29 -0.37400E+01  0.19360E+04
    TROE centering:      0.57570E+00  0.23700E+03  0.16520E+04  0.50690E+04
      H2                Enhanced by    2.000E+00
      H2O               Enhanced by    6.000E+00
      CH4               Enhanced by    2.000E+00
      CO                Enhanced by    1.500E+00
      CO2               Enhanced by    2.000E+00
      C2H6              Enhanced by    3.000E+00
      AR                Enhanced by    7.000E-01
      C2H2              Enhanced by    3.000E+00
      C2H4              Enhanced by    3.000E+00
44. CH+CO2=HCO+CO                                  3.40E+12    0.0      690.0
45. HCO+H(+M)=CH2O(+M)                             1.09E+12    0.5     -260.0
    Low pressure limit:  0.13500E+25 -0.25700E+01  0.14250E+04
    TROE centering:      0.78240E+00  0.27100E+03  0.27550E+04  0.65700E+04
      H2                Enhanced by    2.000E+00
      H2O               Enhanced by    6.000E+00
      CH4               Enhanced by    2.000E+00
      CO                Enhanced by    1.500E+00
      CO2               Enhanced by    2.000E+00
      C2H6              Enhanced by    3.000E+00
      AR                Enhanced by    7.000E-01
      C2H2              Enhanced by    3.000E+00
      C2H4              Enhanced by    3.000E+00
46. HCO+H=CO+H2                                    7.34E+13    0.0        0.0
47. HCO+O=CO+OH                                    3.00E+13    0.0        0.0
48. HCO+O=CO2+H                                    3.00E+13    0.0        0.0
49. HCO+OH=CO+H2O                                  5.00E+13    0.0        0.0
50. HCO+M=CO+H+M                                   1.87E+17   -1.0    17000.0
      H2                Enhanced by    2.000E+00
      H2O               Enhanced by    6.000E+00
      CH4               Enhanced by    2.000E+00
      CO                Enhanced by    1.500E+00
      CO2               Enhanced by    2.000E+00
      C2H6              Enhanced by    3.000E+00
      C2H2              Enhanced by    3.000E+00
```

```
      C2H4              Enhanced by    3.000E+00
51. HCO+O2=CO+HO2                                 7.60E+12    0.0      400.0
52. CH2+H(+M)=CH3(+M)                             2.50E+16   -0.8        0.0
    Low pressure limit:  0.32000E+28 -0.31400E+01  0.12300E+04
    TROE centering:      0.68000E+00  0.78000E+02  0.19950E+04  0.55900E+04
      H2                Enhanced by    2.000E+00
      H2O               Enhanced by    6.000E+00
      CH4               Enhanced by    2.000E+00
      CO                Enhanced by    1.500E+00
      CO2               Enhanced by    2.000E+00
      C2H6              Enhanced by    3.000E+00
      AR                Enhanced by    7.000E-01
      C2H2              Enhanced by    3.000E+00
      C2H4              Enhanced by    3.000E+00
53. CH2+H2=H+CH3                                  5.00E+05    2.0     7230.0
54. CH2+O=HCO+H                                   8.00E+13    0.0        0.0
55. CH2+O2=HCO+OH                                 1.06E+13    0.0     1500.0
56. CH2+O2=CO2+H+H                                2.64E+12    0.0     1500.0
57. CH2+OH=CH2O+H                                 2.00E+13    0.0        0.0
58. CH2+OH=CH+H2O                                 1.13E+07    2.0     3000.0
59. CH2+HO2=CH2O+OH                               2.00E+13    0.0        0.0
60. CH2+C=C2H+H                                   5.00E+13    0.0        0.0
61. CH2+CO(+M)=CH2CO(+M)                          8.10E+11    0.5     4510.0
    Low pressure limit:  0.26900E+34 -0.51100E+01  0.70950E+04
    TROE centering:      0.59070E+00  0.27500E+03  0.12260E+04  0.51850E+04
      H2                Enhanced by    2.000E+00
      H2O               Enhanced by    6.000E+00
      CH4               Enhanced by    2.000E+00
      CO                Enhanced by    1.500E+00
      CO2               Enhanced by    2.000E+00
      C2H6              Enhanced by    3.000E+00
      AR                Enhanced by    7.000E-01
      C2H2              Enhanced by    3.000E+00
      C2H4              Enhanced by    3.000E+00
62. CH2+CH=C2H2+H                                 4.00E+13    0.0        0.0
63. CH2+CH2=C2H2+H2                               3.20E+13    0.0        0.0
64. CH2*+N2=CH2+N2                                1.50E+13    0.0      600.0
65. CH2*+AR=CH2+AR                                9.00E+12    0.0      600.0
66. CH2*+H=CH+H2                                  3.00E+13    0.0        0.0
67. CH2*+O=CO+H2                                  1.50E+13    0.0        0.0
68. CH2*+O=HCO+H                                  1.50E+13    0.0        0.0
69. CH2*+OH=CH2O+H                                3.00E+13    0.0        0.0
70. CH2*+H2=CH3+H                                 7.00E+13    0.0        0.0
71. CH2*+O2=H+OH+CO                               2.80E+13    0.0        0.0
72. CH2*+O2=CO+H2O                                1.20E+13    0.0        0.0
73. CH2*+H2O(+M)=CH3OH(+M)                        2.00E+13    0.0        0.0
    Low pressure limit:  0.27000E+39 -0.63000E+01  0.31000E+04
    TROE centering:      0.15070E+00  0.13400E+03  0.23830E+04  0.72650E+04
      H2                Enhanced by    2.000E+00
      H2O               Enhanced by    6.000E+00
      CH4               Enhanced by    2.000E+00
      CO                Enhanced by    1.500E+00
      CO2               Enhanced by    2.000E+00
      C2H6              Enhanced by    3.000E+00
      C2H2              Enhanced by    3.000E+00
      C2H4              Enhanced by    3.000E+00
74. CH2*+H2O=CH2+H2O                              3.00E+13    0.0        0.0
75. CH2*+CO=CH2+CO                                9.00E+12    0.0        0.0
76. CH2*+CO2=CH2+CO2                              7.00E+12    0.0        0.0
77. CH2*+CO2=CH2O+CO                              1.40E+13    0.0        0.0
78. CH2O+H(+M)=CH2OH(+M)                          5.40E+11    0.5     3600.0
    Low pressure limit:  0.12700E+33 -0.48200E+01  0.65300E+04
    TROE centering:      0.71870E+00  0.10300E+03  0.12910E+04  0.41600E+04
      H2                Enhanced by    2.000E+00
```

```
       H2O              Enhanced by    6.000E+00
       CH4              Enhanced by    2.000E+00
       CO               Enhanced by    1.500E+00
       CO2              Enhanced by    2.000E+00
       C2H6             Enhanced by    3.000E+00
       C2H2             Enhanced by    3.000E+00
       C2H4             Enhanced by    3.000E+00
79. CH2O+H(+M)=CH3O(+M)                            5.40E+11    0.5     2600.0
    Low pressure limit:  0.22000E+31 -0.48000E+01  0.55600E+04
    TROE centering:      0.75800E+00  0.94000E+02  0.15550E+04  0.42000E+04
       H2               Enhanced by    2.000E+00
       H2O              Enhanced by    6.000E+00
       CH4              Enhanced by    2.000E+00
       CO               Enhanced by    1.500E+00
       CO2              Enhanced by    2.000E+00
       C2H6             Enhanced by    3.000E+00
       C2H2             Enhanced by    3.000E+00
       C2H4             Enhanced by    3.000E+00
80. CH2O+H=HCO+H2                                  2.30E+10    1.1     3275.0
81. CH2O+O=HCO+OH                                  3.90E+13    0.0     3540.0
82. CH2O+OH=HCO+H2O                                3.43E+09    1.2     -447.0
83. CH2O+O2=HCO+HO2                                1.00E+14    0.0    40000.0
84. CH2O+HO2=HCO+H2O2                              1.00E+12    0.0     8000.0
85. CH2O+CH=CH2CO+H                                9.46E+13    0.0     -515.0
86. CH3+H(+M)=CH4(+M)                              1.27E+16   -0.6      383.0
    Low pressure limit:  0.24770E+34 -0.47600E+01  0.24400E+04
    TROE centering:      0.78300E+00  0.74000E+02  0.29410E+04  0.69640E+04
       H2               Enhanced by    2.000E+00
       H2O              Enhanced by    6.000E+00
       CH4              Enhanced by    2.000E+00
       CO               Enhanced by    1.500E+00
       CO2              Enhanced by    2.000E+00
       C2H6             Enhanced by    3.000E+00
       AR               Enhanced by    7.000E-01
       C2H2             Enhanced by    3.000E+00
       C2H4             Enhanced by    3.000E+00
87. CH3+O=CH2O+H                                   8.43E+13    0.0        0.0
88. CH3+OH(+M)=CH3OH(+M)                           6.30E+13    0.0        0.0
    Low pressure limit:  0.27000E+39 -0.63000E+01  0.31000E+04
    TROE centering:      0.21050E+00  0.83500E+02  0.53980E+04  0.83700E+04
       H2               Enhanced by    2.000E+00
       H2O              Enhanced by    6.000E+00
       CH4              Enhanced by    2.000E+00
       CO               Enhanced by    1.500E+00
       CO2              Enhanced by    2.000E+00
       C2H6             Enhanced by    3.000E+00
       C2H2             Enhanced by    3.000E+00
       C2H4             Enhanced by    3.000E+00
89. CH3+OH=CH2+H2O                                 5.60E+07    1.6     5420.0
90. CH3+OH=CH2*+H2O                                2.50E+13    0.0        0.0
91. CH3+O2=O+CH3O                                  3.08E+13    0.0    28800.0
92. CH3+O2=OH+CH2O                                 3.60E+10    0.0     8940.0
93. CH3+HO2=CH4+O2                                 1.00E+12    0.0        0.0
94. CH3+HO2=CH3O+OH                                1.34E+13    0.0        0.0
95. CH3+H2O2=CH4+HO2                               2.45E+04    2.5     5180.0
96. CH3+C=C2H2+H                                   5.00E+13    0.0        0.0
97. CH3+CH=C2H3+H                                  3.00E+13    0.0        0.0
98. CH3+HCO=CH4+CO                                 8.48E+12    0.0        0.0
99. CH3+HCO(+M)=CH3CHO(+M)                         1.80E+13    0.0        0.0
    Low pressure limit:  0.22000E+49 -0.95880E+01  0.51000E+04
    TROE centering:      0.61730E+00  0.13076E+02  0.20780E+04  0.50930E+04
       H2               Enhanced by    2.000E+00
       H2O              Enhanced by    6.000E+00
       CH4              Enhanced by    2.000E+00
```

```
        CO               Enhanced by    1.500E+00
        CO2              Enhanced by    2.000E+00
        C2H6             Enhanced by    3.000E+00
        C2H2             Enhanced by    3.000E+00
        C2H4             Enhanced by    3.000E+00
100. CH3+CH2O=CH4+HCO                              3.32E+03    2.8     5860.0
101. CH3+CH2=C2H4+H                                4.00E+13    0.0        0.0
102. CH3+CH2*=C2H4+H                               1.20E+13    0.0     -570.0
103. CH3+CH3(+M)=C2H6(+M)                          2.12E+16   -1.0      620.0
     Low pressure limit:  0.17700E+51 -0.96700E+01  0.62200E+04
     TROE centering:      0.53250E+00  0.15100E+03  0.10380E+04  0.49700E+04
        H2               Enhanced by    2.000E+00
        H2O              Enhanced by    6.000E+00
        CH4              Enhanced by    2.000E+00
        CO               Enhanced by    1.500E+00
        CO2              Enhanced by    2.000E+00
        C2H6             Enhanced by    3.000E+00
        AR               Enhanced by    7.000E-01
        C2H2             Enhanced by    3.000E+00
        C2H4             Enhanced by    3.000E+00
104. CH3+CH3=H+C2H5                                4.99E+12    0.1    10600.0
105. CH3+HCCO=C2H4+CO                              5.00E+13    0.0        0.0
106. CH3+C2H=C3H3+H                                2.41E+13    0.0        0.0
107. CH3O+H(+M)=CH3OH(+M)                          5.00E+13    0.0        0.0
     Low pressure limit:  0.86000E+29 -0.40000E+01  0.30250E+04
     TROE centering:      0.89020E+00  0.14400E+03  0.28380E+04  0.45569E+05
        H2               Enhanced by    2.000E+00
        H2O              Enhanced by    6.000E+00
        CH4              Enhanced by    2.000E+00
        CO               Enhanced by    1.500E+00
        CO2              Enhanced by    2.000E+00
        C2H6             Enhanced by    3.000E+00
        C2H2             Enhanced by    3.000E+00
        C2H4             Enhanced by    3.000E+00
108. CH3O+H=CH2OH+H                                3.40E+06    1.6        0.0
109. CH3O+H=CH2O+H2                                2.00E+13    0.0        0.0
110. CH3O+H=CH3+OH                                 3.20E+13    0.0        0.0
111. CH3O+H=CH2*+H2O                               1.60E+13    0.0        0.0
112. CH3O+O=CH2O+OH                                1.00E+13    0.0        0.0
113. CH3O+OH=CH2O+H2O                              5.00E+12    0.0        0.0
114. CH3O+O2=CH2O+HO2                              4.28E-13    7.6    -3530.0
115. CH2OH+H(+M)=CH3OH(+M)                         1.80E+13    0.0        0.0
     Low pressure limit:  0.30000E+32 -0.48000E+01  0.33000E+04
     TROE centering:      0.76790E+00  0.33800E+03  0.18120E+04  0.50810E+04
        H2               Enhanced by    2.000E+00
        H2O              Enhanced by    6.000E+00
        CH4              Enhanced by    2.000E+00
        CO               Enhanced by    1.500E+00
        CO2              Enhanced by    2.000E+00
        C2H6             Enhanced by    3.000E+00
        C2H2             Enhanced by    3.000E+00
        C2H4             Enhanced by    3.000E+00
116. CH2OH+H=CH2O+H2                               2.00E+13    0.0        0.0
117. CH2OH+H=CH3+OH                                1.20E+13    0.0        0.0
118. CH2OH+H=CH2*+H2O                              6.00E+12    0.0        0.0
119. CH2OH+O=CH2O+OH                               1.00E+13    0.0        0.0
120. CH2OH+OH=CH2O+H2O                             5.00E+12    0.0        0.0
121. CH2OH+O2=CH2O+HO2                             1.80E+13    0.0      900.0
122. CH4+H=CH3+H2                                  6.60E+08    1.6    10840.0
123. CH4+O=CH3+OH                                  1.02E+09    1.5     8600.0
124. CH4+OH=CH3+H2O                                1.00E+08    1.6     3120.0
125. CH4+CH=C2H4+H                                 6.00E+13    0.0        0.0
126. CH4+CH2=CH3+CH3                               2.46E+06    2.0     8270.0
127. CH4+CH2*=CH3+CH3                              1.60E+13    0.0     -570.0
```

```
128. CH3OH+H=CH2OH+H2                                 1.70E+07    2.1     4870.0
129. CH3OH+H=CH3O+H2                                  4.20E+06    2.1     4870.0
130. CH3OH+O=CH2OH+OH                                 3.88E+05    2.5     3100.0
131. CH3OH+O=CH3O+OH                                  1.30E+05    2.5     5000.0
132. CH3OH+OH=CH2OH+H2O                               1.44E+06    2.0     -840.0
133. CH3OH+OH=CH3O+H2O                                6.30E+06    2.0     1500.0
134. CH3OH+CH3=CH2OH+CH4                              3.00E+07    1.5     9940.0
135. CH3OH+CH3=CH3O+CH4                               1.00E+07    1.5     9940.0
136. C2H+H(+M)=C2H2(+M)                               1.00E+17   -1.0        0.0
     Low pressure limit:  0.37500E+34 -0.48000E+01  0.19000E+04
     TROE centering:      0.64640E+00  0.13200E+03  0.13150E+04  0.55660E+04
        H2               Enhanced by    2.000E+00
        H2O              Enhanced by    6.000E+00
        CH4              Enhanced by    2.000E+00
        CO               Enhanced by    1.500E+00
        CO2              Enhanced by    2.000E+00
        C2H6             Enhanced by    3.000E+00
        AR               Enhanced by    7.000E-01
        C2H2             Enhanced by    3.000E+00
        C2H4             Enhanced by    3.000E+00
137. C2H+O=CH+CO                                      5.00E+13    0.0        0.0
138. C2H+OH=H+HCCO                                    2.00E+13    0.0        0.0
139. C2H+O2=HCO+CO                                    5.00E+13    0.0     1500.0
140. C2H+H2=H+C2H2                                    4.90E+05    2.5      560.0
141. C2O+H=CH+CO                                      5.00E+13    0.0        0.0
142. C2O+O=CO+CO                                      5.00E+13    0.0        0.0
143. C2O+OH=CO+CO+H                                   2.00E+13    0.0        0.0
144. C2O+O2=CO+CO+O                                   2.00E+13    0.0        0.0
145. HCCO+H=CH2*+CO                                   1.00E+14    0.0        0.0
146. HCCO+O=H+CO+CO                                   1.00E+14    0.0        0.0
147. HCCO+O2=OH+2CO                                   1.60E+12    0.0      854.0
148. HCCO+CH=C2H2+CO                                  5.00E+13    0.0        0.0
149. HCCO+CH2=C2H3+CO                                 3.00E+13    0.0        0.0
150. HCCO+HCCO=C2H2+CO+CO                             1.00E+13    0.0        0.0
151. HCCO+OH=C2O+H2O                                  3.00E+13    0.0        0.0
152. C2H2(+M)=H2CC(+M)                                8.00E+14   -0.5    50750.0
     Low pressure limit:  0.24500E+16 -0.64000E+00  0.49700E+05
        H2               Enhanced by    2.000E+00
        H2O              Enhanced by    6.000E+00
        CH4              Enhanced by    2.000E+00
        CO               Enhanced by    1.500E+00
        CO2              Enhanced by    2.000E+00
        C2H6             Enhanced by    3.000E+00
        C2H2             Enhanced by    2.500E+00
        C2H4             Enhanced by    2.500E+00
153. C2H3(+M)=C2H2+H(+M)                              3.86E+08    1.6    37048.2
     Low pressure limit:  0.25650E+28 -0.34000E+01  0.35799E+05
     TROE centering:      0.19816E+01  0.53837E+04  0.42932E+01 -0.79500E-01
        H2               Enhanced by    2.000E+00
        H2O              Enhanced by    6.000E+00
        CH4              Enhanced by    2.000E+00
        CO               Enhanced by    1.500E+00
        CO2              Enhanced by    2.000E+00
        C2H6             Enhanced by    3.000E+00
        AR               Enhanced by    7.000E-01
        C2H2             Enhanced by    3.000E+00
        C2H4             Enhanced by    3.000E+00
154. C2H2+O=C2H+OH                                    4.60E+19   -1.4    28950.0
155. C2H2+O=HCCO+H                                    1.63E+07    2.0     1900.0
156. C2H2+O=CH2+CO                                    4.08E+06    2.0     1900.0
157. C2H2+OH=CH2CO+H                                  2.18E-04    4.5    -1000.0
158. C2H2+OH=HCCOH+H                                  5.04E+05    2.3    13500.0
159. C2H2+OH=C2H+H2O                                  3.37E+07    2.0    14000.0
160. C2H2+OH=CH3+CO                                   4.83E-04    4.0    -2000.0
```

```
161. C2H2+HCO=C2H3+CO                                 1.00E+07    2.0     6000.0
162. C2H2+CH=C3H2+H                                   3.00E+13    0.0        0.0
163. C2H2+CH2=C3H3+H                                  1.20E+13    0.0     6620.0
164. C2H2+CH2*=C3H3+H                                 2.00E+13    0.0        0.0
165. C2H2+C2H=C4H2+H                                  9.60E+13    0.0        0.0
166. C2H2+C2H(+M)=n-C4H3(+M)                          8.30E+10    0.9     -363.0
     Low pressure limit:  0.12400E+32 -0.47180E+01  0.18710E+04
     TROE centering:      0.10000E+01  0.10000E+03  0.56130E+04  0.13387E+05
        H2               Enhanced by    2.000E+00
        H2O              Enhanced by    6.000E+00
        CH4              Enhanced by    2.000E+00
        CO               Enhanced by    1.500E+00
        CO2              Enhanced by    2.000E+00
        C2H6             Enhanced by    3.000E+00
        C2H2             Enhanced by    2.500E+00
        C2H4             Enhanced by    2.500E+00
167. C2H2+C2H(+M)=i-C4H3(+M)                          8.30E+10    0.9     -363.0
     Low pressure limit:  0.12400E+32 -0.47180E+01  0.18710E+04
     TROE centering:      0.10000E+01  0.10000E+03  0.56130E+04  0.13387E+05
        H2               Enhanced by    2.000E+00
        H2O              Enhanced by    6.000E+00
        CH4              Enhanced by    2.000E+00
        CO               Enhanced by    1.500E+00
        CO2              Enhanced by    2.000E+00
        C2H6             Enhanced by    3.000E+00
        C2H2             Enhanced by    2.500E+00
        C2H4             Enhanced by    2.500E+00
168. C2H2+HCCO=C3H3+CO                                1.00E+11    0.0     3000.0
169. C2H2+CH3=pC3H4+H                                 2.56E+09    1.1    13644.0
170. C2H2+CH3=aC3H4+H                                 5.14E+09    0.9    22153.0
171. C2H2+CH3+M=CH3CCH2+M                             4.00E+24   -3.4    18840.0
172. C2H2+CH3+M=aC3H5+M                               2.20E+55  -11.8    35730.0
173. H2CC+H=C2H2+H                                    1.00E+14    0.0        0.0
174. H2CC+O=CH2+CO                                    1.00E+14    0.0        0.0
175. H2CC+OH=CH2CO+H                                  2.00E+13    0.0        0.0
176. H2CC+O2=CO2+CH2                                  1.00E+13    0.0        0.0
177. H2CC+C2H2(+M)=C4H4(+M)                           3.50E+05    2.1    -2400.0
     Low pressure limit:  0.14000E+61 -0.12599E+02  0.74170E+04
     TROE centering:      0.98000E+00  0.56000E+02  0.58000E+03  0.41640E+04
        H2               Enhanced by    2.000E+00
        H2O              Enhanced by    6.000E+00
        CH4              Enhanced by    2.000E+00
        CO               Enhanced by    1.500E+00
        CO2              Enhanced by    2.000E+00
        C2H6             Enhanced by    3.000E+00
        C2H2             Enhanced by    3.000E+00
        C2H4             Enhanced by    3.000E+00
178. CH2CO+H(+M)=CH2CHO(+M)                           3.30E+14   -0.1     8500.0
     Low pressure limit:  0.38000E+42 -0.76400E+01  0.11900E+05
     TROE centering:      0.33700E+00  0.17070E+04  0.32000E+04  0.41310E+04
        H2               Enhanced by    2.000E+00
        H2O              Enhanced by    6.000E+00
        CH4              Enhanced by    2.000E+00
        CO               Enhanced by    1.500E+00
        CO2              Enhanced by    2.000E+00
        C2H6             Enhanced by    3.000E+00
        AR               Enhanced by    7.000E-01
        C2H2             Enhanced by    3.000E+00
        C2H4             Enhanced by    3.000E+00
179. CH2CO+H=HCCO+H2                                  5.00E+13    0.0     8000.0
180. CH2CO+H=CH3+CO                                   1.50E+09    1.4     2690.0
181. CH2CO+O=HCCO+OH                                  1.00E+13    0.0     8000.0
182. CH2CO+O=CH2+CO2                                  1.75E+12    0.0     1350.0
183. CH2CO+OH=HCCO+H2O                                7.50E+12    0.0     2000.0
```

```
184. HCCOH+H=CH2CO+H                                  1.00E+13    0.0        0.0
185. C2H3+H(+M)=C2H4(+M)                              6.08E+12    0.3      280.0
     Low pressure limit:  0.14000E+31 -0.38600E+01  0.33200E+04
     TROE centering:      0.78200E+00  0.20750E+03  0.26630E+04  0.60950E+04
        H2               Enhanced by    2.000E+00
        H2O              Enhanced by    6.000E+00
        CH4              Enhanced by    2.000E+00
        CO               Enhanced by    1.500E+00
        CO2              Enhanced by    2.000E+00
        C2H6             Enhanced by    3.000E+00
        AR               Enhanced by    7.000E-01
        C2H2             Enhanced by    3.000E+00
        C2H4             Enhanced by    3.000E+00
186. C2H3+H=C2H2+H2                                   3.00E+13    0.0        0.0
187. C2H3+H=H2CC+H2                                   6.00E+13    0.0        0.0
188. C2H3+O=CH2CO+H                                   4.80E+13    0.0        0.0
189. C2H3+O=CH3+CO                                    4.80E+13    0.0        0.0
190. C2H3+OH=C2H2+H2O                                 3.01E+13    0.0        0.0
191. C2H3+O2=C2H2+HO2                                 1.34E+06    1.6     -383.4
192. C2H3+O2=CH2CHO+O                                 3.00E+11    0.3       11.0
193. C2H3+O2=HCO+CH2O                                 4.60E+16   -1.4     1010.0
194. C2H3+HO2=CH2CHO+OH                               1.00E+13    0.0        0.0
195. C2H3+H2O2=C2H4+HO2                               1.21E+10    0.0     -596.0
196. C2H3+HCO=C2H4+CO                                 9.03E+13    0.0        0.0
197. C2H3+CH3=C2H2+CH4                                3.92E+11    0.0        0.0
198. C2H3+CH3(+M)=C3H6(+M)                            2.50E+13    0.0        0.0
     Low pressure limit:  0.42700E+59 -0.11940E+02  0.97698E+04
     TROE centering:      0.17500E+00  0.13406E+04  0.60000E+05  0.10140E+05
        H2               Enhanced by    2.000E+00
        H2O              Enhanced by    6.000E+00
        CH4              Enhanced by    2.000E+00
        CO               Enhanced by    1.500E+00
        CO2              Enhanced by    2.000E+00
        C2H6             Enhanced by    3.000E+00
        AR               Enhanced by    7.000E-01
        C2H2             Enhanced by    3.000E+00
        C2H4             Enhanced by    3.000E+00
199. C2H3+CH3=aC3H5+H                                 1.50E+24   -2.8    18618.0
200. C2H3+C2H2=C4H4+H                                 5.00E+14   -0.7     6700.0
*201. CH2CHO=CH3+CO                                   7.80E+41   -9.1    46900.0
202. CH2CHO+H(+M)=CH3CHO(+M)                          1.00E+14    0.0        0.0
     Low pressure limit:  0.52000E+40 -0.72970E+01  0.47000E+04
     TROE centering:      0.55000E+00  0.89000E+04  0.43500E+04  0.72440E+04
        H2               Enhanced by    2.000E+00
        H2O              Enhanced by    6.000E+00
        CH4              Enhanced by    2.000E+00
        CO               Enhanced by    1.500E+00
        CO2              Enhanced by    2.000E+00
        C2H6             Enhanced by    3.000E+00
        C2H2             Enhanced by    3.000E+00
        C2H4             Enhanced by    3.000E+00
203. CH2CHO+H=CH3CO+H                                 5.00E+12    0.0        0.0
204. CH2CHO+H=CH3+HCO                                 9.00E+13    0.0        0.0
205. CH2CHO+H=CH2CO+H2                                2.00E+13    0.0     4000.0
206. CH2CHO+O=CH2CO+OH                                2.00E+13    0.0     4000.0
207. CH2CHO+OH=CH2CO+H2O                              1.00E+13    0.0     2000.0
208. CH2CHO+O2=CH2CO+HO2                              1.40E+11    0.0        0.0
209. CH2CHO+O2=CH2O+CO+OH                             1.80E+10    0.0        0.0
210. CH3+CO(+M)=CH3CO(+M)                             4.85E+07    1.6     6150.0
     Low pressure limit:  0.78000E+31 -0.53950E+01  0.86000E+04
     TROE centering:      0.25800E+00  0.59800E+03  0.21002E+05  0.17730E+04
        H2               Enhanced by    2.000E+00
```

* Rate parameters are only applicable to a pressure of 1 atm.

```
        H2O               Enhanced by    6.000E+00
        CH4               Enhanced by    2.000E+00
        CO                Enhanced by    1.500E+00
        CO2               Enhanced by    2.000E+00
        C2H6              Enhanced by    3.000E+00
        AR                Enhanced by    7.000E-01
        C2H2              Enhanced by    3.000E+00
        C2H4              Enhanced by    3.000E+00
211. CH3CO+H(+M)=CH3CHO(+M)                          9.60E+13    0.0        0.0
     Low pressure limit:  0.38500E+45 -0.85690E+01  0.55000E+04
     TROE centering:      0.10000E+01  0.29000E+04  0.29000E+04  0.51320E+04
        H2                Enhanced by    2.000E+00
        H2O               Enhanced by    6.000E+00
        CH4               Enhanced by    2.000E+00
        CO                Enhanced by    1.500E+00
        CO2               Enhanced by    2.000E+00
        C2H6              Enhanced by    3.000E+00
        C2H2              Enhanced by    3.000E+00
        C2H4              Enhanced by    3.000E+00
212. CH3CO+H=CH3+HCO                                 8.00E+13    0.0        0.0
213. CH3CO+O=CH2CO+OH                                3.90E+13    0.0        0.0
214. CH3CO+O=CH3+CO2                                 1.50E+14    0.0        0.0
215. CH3CO+OH=CH2CO+H2O                              1.20E+13    0.0        0.0
216. CH3CO+OH=CH3+CO+OH                              3.00E+13    0.0        0.0
217. CH3CO+HO2=CH3+CO2+OH                            3.00E+13    0.0        0.0
218. CH3CO+H2O2=CH3CHO+HO2                           1.80E+11    0.0     8226.0
219. CH3CHO+O2=CH3CO+HO2                             3.00E+13    0.0    39100.0
220. CH3CHO+OH=CH3CO+H2O                             2.35E+10    0.7    -1110.0
221. CH3CHO+H=CH3CO+H2                               4.10E+09    1.2     2400.0
222. CH3CHO+O=CH3CO+OH                               5.80E+12    0.0     1800.0
223. CH3CHO+CH3=CH3CO+CH4                            2.00E-06    5.6     2460.0
224. C2H4(+M)=H2+H2CC(+M)                            8.00E+12    0.4    88770.0
     Low pressure limit:  0.70000E+51 -0.93100E+01  0.99860E+05
     TROE centering:      0.73450E+00  0.18000E+03  0.10350E+04  0.54170E+04
        H2                Enhanced by    2.000E+00
        H2O               Enhanced by    6.000E+00
        CH4               Enhanced by    2.000E+00
        CO                Enhanced by    1.500E+00
        CO2               Enhanced by    2.000E+00
        C2H6              Enhanced by    3.000E+00
        AR                Enhanced by    7.000E-01
        C2H2              Enhanced by    3.000E+00
        C2H4              Enhanced by    3.000E+00
225. C2H4+H(+M)=C2H5(+M)                             1.08E+12    0.5     1820.0
     Low pressure limit:  0.12000E+43 -0.76200E+01  0.69700E+04
     TROE centering:      0.97530E+00  0.21000E+03  0.98400E+03  0.43740E+04
        H2                Enhanced by    2.000E+00
        H2O               Enhanced by    6.000E+00
        CH4               Enhanced by    2.000E+00
        CO                Enhanced by    1.500E+00
        CO2               Enhanced by    2.000E+00
        C2H6              Enhanced by    3.000E+00
        AR                Enhanced by    7.000E-01
        C2H2              Enhanced by    3.000E+00
        C2H4              Enhanced by    3.000E+00
226. C2H4+H=C2H3+H2                                  5.07E+07    1.9    12950.0
227. C2H4+O=OH+C2H3                                  1.51E+07    1.9     3740.0
228. C2H4+O=CH3+HCO                                  1.92E+07    1.8      220.0
229. C2H4+O=CH2+CH2O                                 3.84E+05    1.8      220.0
230. C2H4+OH=C2H3+H2O                                3.60E+06    2.0     2500.0
231. C2H4+O2=C2H3+HO2                                4.22E+13    0.0    60800.0
232. C2H4+HCO=C2H5+CO                                1.00E+07    2.0     8000.0
233. C2H4+CH=aC3H4+H                                 3.00E+13    0.0        0.0
234. C2H4+CH=pC3H4+H                                 3.00E+13    0.0        0.0
```

```
235. C2H4+CH2=aC3H5+H                              2.00E+13    0.0     6000.0
236. C2H4+CH2*=H2CC+CH4                            5.00E+13    0.0        0.0
237. C2H4+CH2*=aC3H5+H                             5.00E+13    0.0        0.0
238. C2H4+CH3=C2H3+CH4                             2.27E+05    2.0     9200.0
239. C2H4+C2H=C4H4+H                               1.20E+13    0.0        0.0
240. C2H5+H(+M)=C2H6(+M)                           5.21E+17   -1.0     1580.0
     Low pressure limit:  0.19900E+42 -0.70800E+01  0.66850E+04
     TROE centering:      0.84220E+00  0.12500E+03  0.22190E+04  0.68820E+04
        H2               Enhanced by    2.000E+00
        H2O              Enhanced by    6.000E+00
        CH4              Enhanced by    2.000E+00
        CO               Enhanced by    1.500E+00
        CO2              Enhanced by    2.000E+00
        C2H6             Enhanced by    3.000E+00
        AR               Enhanced by    7.000E-01
        C2H2             Enhanced by    3.000E+00
        C2H4             Enhanced by    3.000E+00
241. C2H5+H=C2H4+H2                                2.00E+12    0.0        0.0
242. C2H5+O=CH3+CH2O                               1.60E+13    0.0        0.0
243. C2H5+O=CH3CHO+H                               8.02E+13    0.0        0.0
244. C2H5+O2=C2H4+HO2                              2.00E+10    0.0        0.0
245. C2H5+HO2=C2H6+O2                              3.00E+11    0.0        0.0
246. C2H5+HO2=C2H4+H2O2                            3.00E+11    0.0        0.0
247. C2H5+HO2=CH3+CH2O+OH                          2.40E+13    0.0        0.0
248. C2H5+H2O2=C2H6+HO2                            8.70E+09    0.0      974.0
249. C2H5+HCO=C2H6+CO                              1.20E+14    0.0        0.0
250. C2H6+H=C2H5+H2                                1.15E+08    1.9     7530.0
251. C2H6+O=C2H5+OH                                8.98E+07    1.9     5690.0
252. C2H6+OH=C2H5+H2O                              3.54E+06    2.1      870.0
253. C2H6+CH2*=C2H5+CH3                            4.00E+13    0.0     -550.0
254. C2H6+CH3=C2H5+CH4                             6.14E+06    1.7    10450.0
255. C3H2+O=C2H+HCO                                1.00E+13    0.0        0.0
256. C3H2+H=C3H3                                   1.00E+13    0.0        0.0
257. C3H2+OH=HCO+C2H2                              6.80E+13    0.0        0.0
258. C3H2+O2=HCCO+H+CO                             2.00E+12    0.0     1000.0
259. C3H2+CH=C4H2+H                                5.00E+13    0.0        0.0
260. C3H2+CH2=n-C4H3+H                             5.00E+13    0.0        0.0
261. C3H2+CH3=C4H4+H                               5.00E+12    0.0        0.0
262. C3H2+HCCO=n-C4H3+CO                           1.00E+13    0.0        0.0
263. C3H3+H(+M)=aC3H4(+M)                          2.00E+13    0.0        0.0
     Low pressure limit:  0.22900E+57 -0.12554E+02  0.79340E+04
     TROE centering:      0.23400E+00  0.33000E+03  0.48080E+04  0.72620E+04
        H2               Enhanced by    2.000E+00
        H2O              Enhanced by    6.000E+00
        CH4              Enhanced by    2.000E+00
        CO               Enhanced by    1.500E+00
        CO2              Enhanced by    2.000E+00
        C2H6             Enhanced by    3.000E+00
        AR               Enhanced by    7.000E-01
        C2H2             Enhanced by    3.000E+00
        C2H4             Enhanced by    3.000E+00
264. C3H3+H(+M)=pC3H4(+M)                          3.00E+13    0.0        0.0
     Low pressure limit:  0.16000E+58 -0.12590E+02  0.83760E+04
     TROE centering:      0.24500E+00  0.33000E+03  0.37060E+04  0.67770E+04
        H2               Enhanced by    2.000E+00
        H2O              Enhanced by    6.000E+00
        CH4              Enhanced by    2.000E+00
        CO               Enhanced by    1.500E+00
        CO2              Enhanced by    2.000E+00
        C2H6             Enhanced by    3.000E+00
        AR               Enhanced by    7.000E-01
        C2H2             Enhanced by    3.000E+00
        C2H4             Enhanced by    3.000E+00
265. C3H3+H=C3H2+H2                                5.00E+13    0.0     1000.0
```

```
 266. C3H3+O=CH2O+C2H                                2.00E+13    0.0        0.0
 267. C3H3+OH=C3H2+H2O                               2.00E+13    0.0        0.0
 268. C3H3+OH=C2H3+HCO                               4.00E+13    0.0        0.0
 269. C3H3+O2=CH2CO+HCO                              3.00E+10    0.0     2868.0
 270. C3H3+HO2=OH+CO+C2H3                            8.00E+11    0.0        0.0
 271. C3H3+HO2=aC3H4+O2                              1.90E+11    0.0    15000.0
 272. C3H3+HO2=pC3H4+O2                              3.17E+12    0.0    15000.0
 273. C3H3+HCO=aC3H4+CO                              2.50E+13    0.0        0.0
 274. C3H3+HCO=pC3H4+CO                              2.50E+13    0.0        0.0
 275. C3H3+CH=i-C4H3+H                               5.00E+13    0.0        0.0
 276. C3H3+CH2=C4H4+H                                5.00E+13    0.0        0.0
 277. C3H3+CH2*=C4H4+H                               1.00E+14    0.0        0.0
 278. pC3H4(+M)=cC3H4(+M)                            1.80E+12    0.3    60000.0
      Low pressure limit:  0.18900E+46 -0.88710E+01  0.64200E+05
      TROE centering:      0.17400E+00  0.10840E+04  0.20000E+05  0.42670E+04
         H2               Enhanced by    2.000E+00
         H2O              Enhanced by    6.000E+00
         CH4              Enhanced by    2.000E+00
         CO               Enhanced by    1.500E+00
         CO2              Enhanced by    2.000E+00
         C2H6             Enhanced by    3.000E+00
         C2H2             Enhanced by    3.000E+00
         C2H4             Enhanced by    3.000E+00
 279. cC3H4(+M)=aC3H4(+M)                            1.80E+12    0.6    42200.0
      Low pressure limit:  0.40000E+47 -0.91120E+01  0.46900E+05
      TROE centering:      0.00000E+00  0.23600E+03  0.20000E+04  0.15940E+04
         H2               Enhanced by    2.000E+00
         H2O              Enhanced by    6.000E+00
         CH4              Enhanced by    2.000E+00
         CO               Enhanced by    1.500E+00
         CO2              Enhanced by    2.000E+00
         C2H6             Enhanced by    3.000E+00
         C2H2             Enhanced by    3.000E+00
         C2H4             Enhanced by    3.000E+00
*280. pC3H4=aC3H4                                    3.73E+51  -11.4    83917.2
 281. aC3H4+H=C3H3+H2                                1.30E+06    2.0     5500.0
 282. aC3H4+H+M=CH3CCH2+M                            7.76E+44   -8.4    11190.0
         H2               Enhanced by    2.000E+00
         H2O              Enhanced by    6.000E+00
         CH4              Enhanced by    2.000E+00
         CO               Enhanced by    1.500E+00
         CO2              Enhanced by    2.000E+00
         C2H6             Enhanced by    3.000E+00
         C2H2             Enhanced by    3.000E+00
         C2H4             Enhanced by    3.000E+00
 283. aC3H4+H(+M)=aC3H5(+M)                          3.38E+09    1.5     4786.0
      Low pressure limit:  0.75000E+60 -0.12484E+02  0.13678E+05
      TROE centering:      0.00000E+00  0.65000E+03  0.10000E+04  0.34961E+04
         H2               Enhanced by    2.000E+00
         H2O              Enhanced by    6.000E+00
         CH4              Enhanced by    2.000E+00
         CO               Enhanced by    1.500E+00
         CO2              Enhanced by    2.000E+00
         C2H6             Enhanced by    3.000E+00
         C2H2             Enhanced by    3.000E+00
         C2H4             Enhanced by    3.000E+00
 284. aC3H4+O=C2H4+CO                                2.00E+07    1.8     1000.0
 285. aC3H4+OH=C3H3+H2O                              5.30E+06    2.0     2000.0
 286. aC3H4+CH3=C3H3+CH4                             2.00E+12    0.0     7700.0
 287. aC3H4+C2H=C2H2+C3H3                            1.00E+13    0.0        0.0
 288. pC3H4+H=aC3H4+H                                6.27E+17   -0.9    10079.0
 289. pC3H4+H+M=CH3CCH2+M                            1.36E+49   -9.6    13690.0
```

* Rate parameters are only applicable to a pressure of 1 atm.

```
*290. pC3H4+H=aC3H5                                  2.07E+57  -13.4    29212.9
 291. pC3H4+H=C3H3+H2                                1.30E+06    2.0     5500.0
 292. pC3H4+O=HCCO+CH3                               7.30E+12    0.0     2250.0
 293. pC3H4+O=C2H4+CO                                1.00E+13    0.0     2250.0
 294. pC3H4+O=C3H3+OH                                3.45E+04    2.2     4830.0
 295. pC3H4+OH=C3H3+H2O                              1.00E+06    2.0      100.0
 296. pC3H4+CH3=C3H3+CH4                             2.00E+12    0.0     7700.0
 297. pC3H4+C2H=C2H2+C3H3                            1.00E+13    0.0        0.0
 298. aC3H5+H(+M)=C3H6(+M)                           2.00E+14    0.0        0.0
      Low pressure limit:  0.13300E+61 -0.12000E+02  0.59678E+04
      TROE centering:      0.20000E-01  0.10966E+04  0.10966E+04  0.68595E+04
         H2               Enhanced by    2.000E+00
         H2O              Enhanced by    6.000E+00
         CH4              Enhanced by    2.000E+00
         CO               Enhanced by    1.500E+00
         CO2              Enhanced by    2.000E+00
         C2H6             Enhanced by    3.000E+00
         AR               Enhanced by    7.000E-01
         C2H2             Enhanced by    3.000E+00
         C2H4             Enhanced by    3.000E+00
 299. aC3H5+H=aC3H4+H2                               1.80E+13    0.0        0.0
 300. aC3H5+H=H2CC+CH4                               2.00E+13    0.0     2000.0
 301. aC3H5+O=C2H3CHO+H                              6.00E+13    0.0        0.0
 302. aC3H5+OH=C2H3CHO+H+H                           4.20E+32   -5.2    30126.0
 303. aC3H5+OH=aC3H4+H2O                             6.00E+12    0.0        0.0
 304. aC3H5+O2=aC3H4+HO2                             4.99E+15   -1.4    22428.0
 305. aC3H5+O2=CH3CO+CH2O                            1.19E+15   -1.0    20128.0
 306. aC3H5+O2=C2H3CHO+OH                            1.82E+13   -0.4    22859.0
 307. aC3H5+HO2=C3H6+O2                              2.66E+12    0.0        0.0
 308. aC3H5+HO2=OH+C2H3+CH2O                         3.31E+12    0.0        0.0
 309. aC3H5+HCO=C3H6+CO                              6.00E+13    0.0        0.0
 310. aC3H5+CH3=aC3H4+CH4                            3.00E+12   -0.3     -131.0
*311. aC3H5=CH3CCH2                                  9.44E+62  -15.5    79079.6
 312. CH3CCH2+H=pC3H4+H2                             3.34E+12    0.0        0.0
 313. CH3CCH2+H=aC3H5+H                              5.00E+13    0.0        0.0
 314. CH3CCH2+O=CH3+CH2CO                            6.00E+13    0.0        0.0
 315. CH3CCH2+OH=CH3+CH2CO+H                         5.00E+12    0.0        0.0
 316. CH3CCH2+O2=CH3+CO+CH2O                         4.34E+12    0.0        0.0
 317. CH3CCH2+HO2=CH3+CH2CO+OH                       2.00E+13    0.0        0.0
 318. CH3CCH2+HCO=C3H6+CO                            9.00E+13    0.0        0.0
 319. CH3CCH2+CH3=pC3H4+CH4                          1.00E+11    0.0        0.0
 320. C2H3+HCO=C2H3CHO                               1.80E+13    0.0        0.0
 321. C2H3CHO+H=C2H4+HCO                             1.08E+12    0.5     1820.0
 322. C2H3CHO+O=C2H3+OH+CO                           3.00E+13    0.0     3540.0
 323. C2H3CHO+O=CH2O+CH2CO                           1.90E+07    1.8      220.0
 324. C2H3CHO+OH=C2H3+H2O+CO                         3.43E+09    1.2     -447.0
 325. C3H6+H=C2H4+CH3                                8.00E+21   -2.4    11180.0
 326. C3H6+H=aC3H5+H2                                1.70E+05    2.5     2490.0
 327. C3H6+H=CH3CCH2+H2                              4.00E+05    2.5     9790.0
 328. C3H6+O=CH2CO+CH3+H                             1.20E+08    1.6      327.0
 329. C3H6+O=C2H5+HCO                                3.50E+07    1.6     -972.0
 330. C3H6+O=aC3H5+OH                                1.80E+11    0.7     5880.0
 331. C3H6+O=CH3CCH2+OH                              6.00E+10    0.7     7630.0
 332. C3H6+OH=aC3H5+H2O                              3.10E+06    2.0     -298.0
 333. C3H6+OH=CH3CCH2+H2O                            1.10E+06    2.0     1450.0
 334. C3H6+HO2=aC3H5+H2O2                            9.60E+03    2.6    13910.0
 335. C3H6+CH3=aC3H5+CH4                             2.20E+00    3.5     5675.0
 336. C3H6+CH3=CH3CCH2+CH4                           8.40E-01    3.5    11660.0
 337. C4H+H(+M)=C4H2(+M)                             1.00E+17   -1.0        0.0
      Low pressure limit:  0.37500E+34 -0.48000E+01  0.19000E+04
      TROE centering:      0.64640E+00  0.13200E+03  0.13150E+04  0.55660E+04
```

* Rate parameters are only applicable to a pressure of 1 atm.

* Rate parameters are only applicable to a pressure of 1 atm.

```
         H2               Enhanced by    2.000E+00
         H2O              Enhanced by    6.000E+00
         CH4              Enhanced by    2.000E+00
         CO               Enhanced by    1.500E+00
         CO2              Enhanced by    2.000E+00
         C2H6             Enhanced by    3.000E+00
         AR               Enhanced by    7.000E-01
         C2H2             Enhanced by    3.000E+00
         C2H4             Enhanced by    3.000E+00
 338. C4H+O=C2H+C2O                                 5.00E+13    0.0        0.0
 339. C4H+O2=HCCO+C2O                               5.00E+13    0.0     1500.0
 340. C4H+H2=H+C4H2                                 4.90E+05    2.5      560.0
 341. C4H2+H(+M)=n-C4H3(+M)                         1.55E+10    0.9      954.0
      Low pressure limit:  0.47000E+48 -0.93690E+01  0.40900E+04
      TROE centering:      0.20200E+00  0.44700E+03  0.11620E+04  0.26350E+04
         H2               Enhanced by    2.000E+00
         H2O              Enhanced by    6.000E+00
         CH4              Enhanced by    2.000E+00
         CO               Enhanced by    1.500E+00
         CO2              Enhanced by    2.000E+00
         C2H6             Enhanced by    3.000E+00
         C2H2             Enhanced by    3.000E+00
         C2H4             Enhanced by    3.000E+00
 342. C4H2+H(+M)=i-C4H3(+M)                         2.20E+10    0.9      164.0
      Low pressure limit:  0.11000E+53 -0.10251E+02  0.46000E+04
      TROE centering:      0.10000E+01  0.51500E+03  0.51500E+03  0.25500E+04
         H2               Enhanced by    2.000E+00
         H2O              Enhanced by    6.000E+00
         CH4              Enhanced by    2.000E+00
         CO               Enhanced by    1.500E+00
         CO2              Enhanced by    2.000E+00
         C2H6             Enhanced by    3.000E+00
         C2H2             Enhanced by    3.000E+00
         C2H4             Enhanced by    3.000E+00
 343. C4H2+O=C3H2+CO                                2.70E+13    0.0     1720.0
 344. C4H2+OH=H2C4O+H                               6.60E+12    0.0     -410.0
 345. C4H2+OH=C4H+H2O                               3.37E+07    2.0    14000.0
 346. H2C4O+H=C2H2+HCCO                             5.00E+13    0.0     3000.0
 347. H2C4O+OH=CH2CO+HCCO                           1.00E+07    2.0     2000.0
 348. H2C4O+O=CH2CO+C2O                             2.00E+07    1.9      200.0
*349. n-C4H3=i-C4H3                                 2.46E+45  -10.5    50149.5
 350. n-C4H3+H(+M)=C4H4(+M)                         1.00E+14    0.0        0.0
      Low pressure limit:  0.17000E+49 -0.94370E+01  0.74800E+04
      TROE centering:      0.62000E+00  0.65900E+04  0.27520E+04
         H2               Enhanced by    2.000E+00
         H2O              Enhanced by    6.000E+00
         CH4              Enhanced by    2.000E+00
         CO               Enhanced by    1.500E+00
         CO2              Enhanced by    2.000E+00
         C2H6             Enhanced by    3.000E+00
         C2H2             Enhanced by    3.000E+00
         C2H4             Enhanced by    3.000E+00
*351. n-C4H3+H=i-C4H3+H                             9.30E+17   -1.0     6672.7
*352. n-C4H3+H=C2H2+H2CC                            7.45E+26   -3.8     8405.2
*353. i-C4H3+H=C2H2+H2CC                            2.60E+33   -5.5    14785.7
 354. i-C4H3+H(+M)=C4H4(+M)                         1.00E+14    0.0        0.0
      Low pressure limit:  0.11000E+54 -0.10703E+02  0.91000E+04
      TROE centering:      0.40000E+00  0.56000E+04  0.14340E+04  0.87280E+04
```

* Rate parameters are only applicable to a pressure of 1 atm.
* Rate parameters are only applicable to a pressure of 1 atm.
* Rate parameters are only applicable to a pressure of 1 atm.
* Rate parameters are only applicable to a pressure of 1 atm.

	H2	Enhanced by	2.000E+00		
	H2O	Enhanced by	6.000E+00		
	CH4	Enhanced by	2.000E+00		
	CO	Enhanced by	1.500E+00		
	CO2	Enhanced by	2.000E+00		
	C2H6	Enhanced by	3.000E+00		
	C2H2	Enhanced by	3.000E+00		
	C2H4	Enhanced by	3.000E+00		
355.	n-C4H3+H=C4H2+H2			3.00E+13	0.0	0.0
356.	i-C4H3+H=C4H2+H2			6.00E+13	0.0	0.0
357.	n-C4H3+OH=C4H2+H2O			2.00E+12	0.0	0.0
358.	i-C4H3+OH=C4H2+H2O			4.00E+12	0.0	0.0
359.	i-C4H3+O2=HCCO+CH2CO			7.86E+16	-1.8	0.0
360.	C4H4+H=n-C4H3+H2			6.65E+05	2.5	12240.0
361.	C4H4+H=i-C4H3+H2			3.33E+05	2.5	9240.0
362.	C4H4+OH=n-C4H3+H2O			3.10E+07	2.0	3430.0
363.	C4H4+OH=i-C4H3+H2O			1.55E+07	2.0	430.0
364.	C4H4+CH3=n-C4H3+CH4			3.98E+11	0.0	4972.0
365.	C4H4+CH3=i-C4H3+CH4			3.98E+11	0.0	4972.0
366.	C4H4+C2H=n-C4H3+C2H2			3.90E+13	0.0	0.0
367.	C4H4+C2H=i-C4H3+C2H2			3.90E+13	0.0	0.0